Sec22b Knockout Mice Offer Novel Insights Into Embryonic Development And Antigen Cross-Presentation

by

Shin-Rong Julia Wu

A dissertation submitted in partial fulfillment
of the requirements for the degree of
Doctor of Philosophy
(Immunology)
in the University of Michigan
2017

Doctoral Committee:

Professor Pavan R Reddy, Chair
Professor David Ginsburg
Professor Nicholas W Lukacs
Professor Malini Raghavan
Professor Michele S Swanson

srjwu@med.umich.edu
ORCID: 0000-0002-6671-2217

DEDICATION

To my family: Mom, Dad, Clara and Chaucer

ACKNOWLEDGMENTS

First and foremost, thank you to Pavan Reddy who made this work possible. Thanks for the freedom to do the experiment, the conversations discussing wild ideas and planning controls, and the lessons on flexibility, openness, and positivity. I'd also like to thank the Reddy lab members, past and present, who've been there for the whole journey and who pitched in to make Chapter 3 happen. In particular, Nathan, who got me set up in lab and showed me how to remotely access my work computer and run FlowJo on rickety RAM; Cynthia, for helping maintain my many colonies; Kay, for all the ASAP orders; Yaping and Tomomi, for their technical expertise; and Steph, for her insightful questions, boundless willingness to help, and consistently good music recommendations.

I also need to acknowledge others at the University of Michigan: my thesis committee, David Ginsburg, Nick Luckacs, Malini Raghavan, and Michele Swanson, for their thoughtful questions, feedback on manuscripts, introductions to colleagues, and belief in me; my honorary committee member Rami Khoriaty, for reading my manuscripts, helping with Chapter 2, and being a constant source of optimism and laughs; Guojing Zhu for setting up all the timed matings; Sue O'Shea without whom Chapter 2 would never have been completed; Beth Moore and Zarinah Aquil of the Immunology Program and Ron Koenig and Ellen

Elkin of the MSTP for crucial administrative and emotional support; Herman and Dorothy Miller for finding my research sufficiently interesting to fund. It was an honor to be selected. Finally, to my MSTP cohort: Amanda, Talha, Caroline, Heather, David, Ravi, Kirsten, Kevin, Yashar. You've taught me so much about being a scientist, a student, and a friend. I'm regularly inspired by your accomplishments in and out of lab. Thanks for helping make this fun!

Thanks as well to the mentors of my past: Nancy Brady, who taught me to write and to argue on the spot, and who helped me apply to my first research experience in high school even though the deadline had passed; Elizabeth Repasky, in whose lab I first cultured BMDCs and flow stained; Adrian Black for his instruction on cell culture technique; and Patrick Sung for the opportunity to work alongside Youngho Kwon for 2 years. Any skill I have with protein and molecular biology is entirely due to Youngho's instruction. The last half of Figure 3.10 was made possible by what I learned from him.

Finally, a huge thank you to my family, to whom this is dedicated: Mom, Dad, and Clara. The love, support, and advice you've provided has kept me sane, helped me be brave, and allowed me to strive for more. Mom, Dad, thanks for inspiring me to pursue research and Clara, thanks for reminding me I'm only human and for sharing your Netflix account. And, last but not least, thank you Chaucer, my favorite photography subject, writing partner, and reluctant receiver of big hugs, you are the sweetest and best dog.

PREFACE

The initial goal of this work was to study the role of cross-presentation in allogeneic bone marrow transplantation by generating a *Sec22b* knockout mouse, which was anticipated to exhibit severe cross-presentation defects given the data seen from *in vitro* silencing of the gene. In Chapter I, I review the current literature on SNARE protein SEC22B and introduce what is known about direct antigen presentation antigen cross-presentation, and summarize methods used to study cross-presentation.

It soon became clear that the project would not proceed as expected. From the observations we made using the *Sec22b* knockout mouse models we generated, two studies emerged. First, no whole body *Sec22b* knockout mice were ever observed at weaning, a discovery I investigate in Chapter II. Second, DC-specific *Sec22b* knockout mice did not exhibit any defects in cross-presentation, the implications of which I explore in Chapter III. While studying DCs, known to contribute to immune activation and immune tolerance, we began to wonder if alternative methods of tolerance exist. We consider this in the Appendix, delineating the evidence for tissue tolerance where tissue cells are active regulators of their own tolerance to immune-mediated damage as opposed to passive bystanders to immune cell activity.

TABLE OF CONTENTS

DEDICATION……..ii

ACKNOWLEDGMENTS……..…….iii

PREFACE…….……..……..……..……..…… v

LIST OF TABLES……..……..……..……..……ix

LIST OF FIGURES……..……..……..……..……x

LIST OF ABBREVIATIONS……..……..……..……..……xii

ABSTRACT……..……..……..……..……..…….. xvi

CHAPTER I

INTRODUCTION……..……..……..……..……...1

Sec22b: a multi-functional SNARE protein……..…… 1

Antigen presentation: a primer……..……..……..... 5

MHC I antigen presentation……..……..……..…. 6

MHC II antigen presentation……..……..……..… 8

Antigen cross-presentation……..……..……..….10

Cross-presenting cell populations……..……..……...19

Methods for detecting antigen presentation……..……20

CHAPTER II

SNARE PROTEIN SEC22B REGULATES EARLY EMBRYONIC DEVELOPMENT AND HEMATOPOIESIS……..……..……...24

Abstract……..……..……..……..……...24

Introduction……..……..……..……..…….26

Results……..……..……..……..……28

Discussion……..……..……..……..……...36

Materials and Methods……..……..……..……... 39

CHAPTER III

A CRITICAL ANALYSIS OF THE ROLE OF SNARE PROTEIN SEC22B IN ANTIGEN CROSS-PRESENTATION……..……..……...42

Abstract……..……..……..……..……...42

Introduction……..……..……..……..…….44

Results……..……..……..……..……47

Discussion……..……..……..……..……...66

Materials and Methods……..……..……..……... 70

CHAPTER IV

CONCLUSION...……..……..……..……..…….81

CHAPTER V

FUTURE DIRECTIONS……..……..……..…… 84

APPENDIX

REGULATING DAMAGE FROM STERILE INFLAMMATION……88

REFERENCES……..……..……..……..……..…110

LIST OF TABLES

Tables

Table 2.1 – Genotypic distribution of offspring from *Sec22b*$^{cgt/+}$ and *Sec22b*$^{+/-}$ mating schemes……..……..……..……...30

Table 2.2 – Genotypic distribution of offspring from *Vav1-Cre Sec22b*$^{fl/+}$ x *Vav1-WT Sec22b*$^{fl/fl}$ mating pairs……..……..……...32

Table 2.3 – Genotypic distribution of offspring from *CD11c-Cre Sec22b*$^{fl/+}$ x *Sec22b*$^{fl/fl}$ mating pairs……..……..……..……...35

Table 2.4 – Primers used for *Sec22b* and *Cre* genotyping……..…...40

Table A.1 – Terms used to describe concepts of tolerance……95

LIST OF FIGURES

Figures

Figure 1.1 – Human SEC22B bound to SEC23/24……..……....3

Figure 2.1 – Generation of gene targeted *Sec22b* alleles……..……. 29

Figure 2.2 – Characterization of *Sec22b*$^{+/-}$ and *Sec22b*$^{-/-}$ mice……..31

Figure 2.3 – *Vav1-Cre* mediated excision incomplete in *Vav1-Cre* *Sec22b*$^{fl/fl}$ adult mice……..……..……..……..33

Figure 2.4 – Survival in mice with *Sec22b* deletion in hematopoietic subsets……..……..……..……..……...33

Figure 2.5 – Complete blood counts on *Sec22b* haplodeficient mice…...34

Figure 3.1 – Generation and characterization of a DC-specific SEC22B knockout mouse……..……..……..……..…...48

Figure 3.2 – Purity of DCs used in assays……..……..……. 49

Figure 3.3 – Myeloid cell populations and lymphocyte development remain unchanged in *CD11c-Cre Sec22b*$^{fl/fl}$ mice……..……. 50

Figure 3.4 – DC-specific SEC22B knockout mice efficiently cross-present antigen *in vivo*……..……..……..……..…….. 53

Figure 3.5 – *Sec22b*$^{-/-}$ DCs show no *in vitro* defect in cross-presentation of soluble or particulate antigen……..……..……. 55

Figure 3.6 – *Sec22b*$^{-/-}$ DCs demonstrate no defect in induction of antigen-specific T cell cytokine production……..……..……56

Figure 3.7 – OVA source does not mask cross-presentation defect in *Sec22b*$^{-/-}$ BMDCs……..……..……..……..… 57

Figure 3.8 – Cross-presentation by BMDCs reduced by *Sec22b* knockdown……..……..……..……..……... 59

Figure 3.9 – *Sec22a* and *Sec22c* expression are unchanged in *Sec22b*$^{-/-}$ BMDCs, Related to Figure 4……..……..……..…… 61

Figure 3.10 – *Sec22b*-targeting shRNA treatment induces cross-presentation defect in KO BMDCs……..……..……62

Figure A.1. Tolerance is the relationship between immune stimulus and health of the tissue being studied.……..……..……..……..89

Figure A.2. Mechanisms of tissue tolerance.……..……..……..93

Figure A.3. Tissue tolerance interacts with immune tolerance to mediate immunopathology……..……..……..……..…….. 99

Figure A.4. Differential organ tissue-specific responses to allogeneic immune attack.……..……..……..……..……..….100

Figure A.5. Tissue tolerance is context dependent.……..……..…...108

LIST OF ABBREVIATIONS

AIRE	Autoimmune regulator
AKT	Protein kinase B
APC	Antigen presenting cell
ATG	Autophagy-related protein
β2-m	β2-microglobulin
BFA	Brefeldin A
BMDC	Bone marrow derived dendritic cell
BrdU	Bromodeoxyuridine
BSA	Bovine serum albumin
cDC	Conventional dendritic cell
CFSE	Carboxyfluorescein succinimidyl ester
CMV	Cytomegalovirus
CRT	Calreticulin
CTL	Cytotoxic T lymphocyte
CXN	Calnexin
DC	Dendritic cell
DNA-PKcs	DNA-dependent protein kinase catalytic subunit
DSS	Dextran sodium sulfate
EBV	Epstein-Barr virus

ELISA	Enzyme-linked immunosorbent assay
ER	Endoplasmic reticulum
ERAP	ER aminopeptidase
ERGIC	ER-Golgi intermediate compartment
ERS24	ER-Golgi SNARE of 24 kDa
FL	Floxed
GI	Gastrointestinal
GILT	Gamma-interferon-inducible lysosomal thiol reductase
GM-CSF	Granulocyte macrophage-colony stimulating factor
GVHD	Graft versus host disease
GVL	Graft versus leukemia/lymphoma
HSCT	Hematopoietic stem cell transplant
Hsp	Heat shock protein
I chain	Invariant chain
IEC	Intestinal epithelial cell
Igtp	Interferon gamma-induced GTPase
IRAP	Insulin-regulated aminopeptidase
ISC	Intestinal stem cell
KGF	Keratinocyte growth factor
KO	Knockout
LCMV	Lymphocytic choriomeningitis virus
MHC	Major histocompatibility complex
MHC I	MHC class I

MHC II	MHC class II
MIIC	MHC class II compartment
mTECs	Medullary thymic epithelial cells
NOX2	NADPH oxidase 2
Nrf2	Nuclear factor erythroid 2-related factor
OVA	Ovalbumin
PCR	Polymerase chain reaction
PERK	Protein kinase-like endoplasmic reticulum kinase
PI3K	Phosphoinositide 3-kinase
PLC	Peptide loading complex
PM	Plasma membrane
qPCR	Quantitative PCR
qRT-PCR	Quantitative reverse transcription PCR
RNAseq	RNA sequencing
ROS	Reactive oxygen species
shRNA	Small hairpin RNA
SIINFEKL	$OVA_{257-264}$ peptide amino acid sequence
SNARE	Soluble N-ethylmaleimide sensitive factor attachment protein receptor
TAP	Transporter associated with antigen processing
TCR	T cell receptor
UPR	Unfolded protein response
VLDL	Very low density lipoprotein
VPS33B	Vacuolar protein sorting-associated protein 33b

WT	Wildtype
XBP1	X-box binding protein 1

ABSTRACT

The SNARE protein SEC22B contributes to a number of critical biological processes in a variety of cells. However, its functions have previously only been studied *in vitro*. We investigated SEC22B *in vivo* using four types of *Sec22b* transgenic mice: a *Sec22b* conditional gene-trap containing mouse, a *Sec22b* null allele containing mouse, and mice with *Vav1-Cre* and *CD11c-Cre* mediated *Sec22b* deletion. In deleting *Sec22b* from the whole organism using gene-trapped and null allele mice and from the hematopoietic system using *Vav1-Cre*, we uncover a previously undescribed function for *Sec22b* in mediating embryonic development before E8.5 and after E11.5. This was not explained by deletion of *Sec22b* in CD11c+ cells. Previously, SEC22B had been implicated as an essential mediator of antigen cross-presentation. Using *CD11c-Cre Sec22b*$^{fl/fl}$ mice with DC-specific deletion of *Sec22b*, we tested this function *in vivo*. We discovered that not only is *Sec22b* not necessary for cross-presentation *in vivo* or *in vitro*, but that previous cross-presentation phenotypes were due to off-target effects from the *Sec22b* shRNAs used. Collectively, these studies offer novel insights into the function of *Sec22b in vivo,* demonstrating that SEC22B is essential for embryogenesis but not for cross-presentation. Moreover, we show the limitations of drawing conclusions from *in vitro* work and shRNA silencing studies alone.

CHAPTER I

INTRODUCTION

Sec22b: a multi-functional SNARE protein

SEC22B, also known as ERS24 (ER-Golgi SNARE of 24 KDa) belongs to the family of proteins known as soluble N-ethylmaleimide-sensitive factor attachment protein receptor (SNARE) proteins[1]. SNARE proteins contain unique coiled-coil SNARE domains that form hydrophobic interactions with SNARE domains in other SNARE proteins[1,2]. When these interacting SNARE protein partners are located on different membranes, a trans-SNARE complex, composed of four such SNARE domains, forms[1,2]. Trans-SNAREs zip together, physically moving membranes into close proximity while releasing the energy necessary to fuse the cellular membranes[2].

Intrinsic pairing limitations mediate partner SNARE interactions; while hundreds of trans-SNARE complexes are theoretically possible, only a fraction promote membrane fusion[2]. Fusion events are additionally regulated by SNARE localization, where v-SNAREs are found on vesicles and t-SNARES on target membranes, such as the plasma membrane[2,3]. Because what is a target membrane is loosely defined, another biochemically-based categorization

system exists based on SNARE domain contributions to a conserved interaction between one arginine (R) and three glutamine (Q) residues at the center of the trans-SNARE complex[2,3]. Whether the SNARE supplies the R or the Q residue thus denotes whether it is an R-SNARE or a Q-SNARE[2,3]. Generally, Q-SNARES are t-SNARES and R-SNARES are v-SNARES[2,3].

Defying this generalization, SEC22B is a t-SNARE and R-SNARE[3] that localizes to the endoplasmic reticulum (ER) and, through the assistance of COPII-mediated transport[4], to the ER-Golgi intermediate compartment (ERGIC)[5]. It also belongs to a subgroup of SNAREs termed longin SNAREs, which are characterized by a long N (longin)-terminal domain with regulatory properties[1]. SEC22B's longin domain assists in its intracellular sorting; its folding into SEC22B's SNARE motif creates a conformational change that is recognized and bound by COPII inner coat proteins SEC23 and SEC24A/B for transport to the ERGIC[4] (Figure 1.1). SEC22B's known binding partners are primarily plasma membrane (PM)-SNARES, including longin SNARE syntaxin 1[6] as well as syntaxins 4[5] and 5[7]. SEC22B also interacts with ER-SNARE syntaxin 18[8] and with golgin-family tether protein, p115, which may assist with SEC22B localization[9]. In rats, SEC22B forms a salt bridge with rbet1[10], a small SNARE that rapidly cycles between the ER and Golgi and is localized to the ERGIC and early Golgi[11].

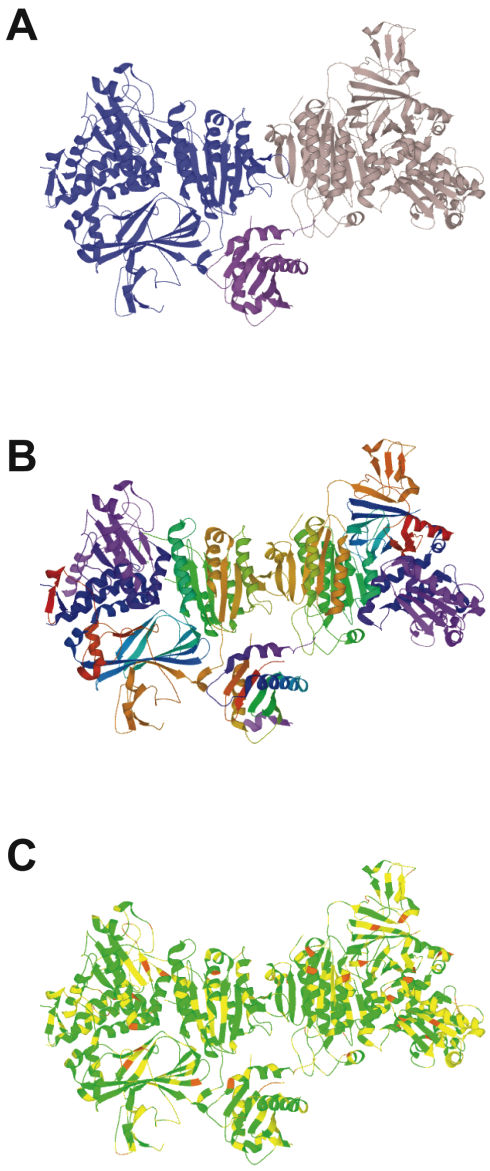

Figure 1.1. Human SEC22B bound to SEC23/24[4]. (A) SEC24 in blue, SEC23 in pink, and SEC22B in purple. **(B)** SEC22b complexed with SEC23 and SEC24 with each secondary structure highlighted by color. **(C)** Worldwide Protein Data Bank structural validation. Green indicates no validation issue. Yellow indicates potential hydrogen atom clashes. Orange indicates potential hydrogen atom clashes and unusual sidechain conformations.

SEC22B's functions are varied. The yeast homolog of murine SEC22B, Sec22p, contributes to macroautophagy[12] whereas in flies, Sec22 modulates ER morphology[13]. In vertebrates, SEC22B is necessary for certain specialized cell functions, such as secretion of very-low-density-lipoproteins (VLDL) in rat hepatocytes[14] and axonal growth in cultured neurons through a novel, nonfusogenic interaction with syntaxin 1, which creates a permissive environment for lipid transfer as opposed to inducing membrane

fusion[6]. In a HeLa cell line, SEC22B suppresses the release of infectious coronavirus particles[15].

Even within the hematopoietic compartment, SEC22B has diverse functions, contributing to secretory autophagy[16] and ROS accumulation during *S. aureus* infection in macrophages[17]. SEC22B also mediates membrane expansion during *Legionella*[18,19] and *Leishmania*[20,21] infection in macrophages. In dendritic cells, SEC22B was reported to be a critical regulator of cross-presentation[5]. Through shRNA-mediated knockdown in BMDCs, SEC22B was silenced. This appeared to reduce cross-presentation while direct antigen presentation on MHC I and MHC II was unaffected[5]. The evidence suggested that this was mediated through a number of cell biological changes, including decreased access of antigen to the cytosol, slowed phagosomal maturation, and transport of ER-localized proteins necessary for cross-presentation to the phagosome through its interaction with PM-SNARE syntaxin 4[5]. The role of SEC22B in the hematopoietic compartment of mice is further examined in Chapter 2, and its role in cross-presentation is further explored in Chapter 3.

SEC22B has also been implicated in specific disease processes. It forms a fusion protein with NOTCH2 in some breast cancers[22], and it may also serve as a biomarker for Alzheimer's disease[23]. Whether SEC22B plays a role in the pathophysiology of these diseases, however, remains open to investigation. In addition to its partner SNARES, SEC22B co-immunoprecipitates with vacuolar

protein sorting-associated protein 33b (VPS33B). Mutations in VPS33B cause a number of disease phenotypes in patients, including a lack of platelet α-granules. Interestingly, in megakaryocytes lacking VPS33B, SEC22B localization is perturbed, suggesting that SEC22B may be necessary for α-granule production[24]. Finally, in an *in vitro* model of Parkinson's disease, SEC22B moderately promotes the secretion of α-synuclein, suggeting a potential neuroprotective role in the brain[25].

In mammals, two SEC22B homologs exist, SEC22A and SEC22C[26]. Although both localize to the ER, neither possess the coiled-coil domain necessary for SNARE activity[1]. Their roles remain undefined, and we test their contribution to antigen cross-presentation in Chapter 3.

Antigen presentation: a primer

The immune system employs several information dissemination strategies to coordinate its activity, one of which is antigen presentation. During antigen presentation, a peptide segment is bound to a specialized molecule, known as a major histocompatibility complex (MHC), and presented to a T cell expressing a T cell receptor (TCR). If the TCR recognizes the MHC:peptide complex, that T cell's activity state will change: if antigen is presented on the surface of the antigen presenting cell (APC) along with costimulatory molecules, naïve T cells with cognate TCRs are stimulated into a state of heightened immune responsiveness, known as activation. However, if MHC:peptide is presented in

the absence of costimulatory molecules, naïve T cells are induced into a tolerogenic state where they become unresponsive to further immune stimulation[27]. This can be protective where tolerance is advantageous, such as during homeostasis or in the context of specific pathological states such as graft-versus-host disease or autoimmune disease. Other factors that may protect against immunopathology are explored in the Appendix.

Two MHC protein classes have been discovered in vertebrates, MHC class I (MHC I) and MHC class II (MHC II)[28]. The proteins are distinct in structure, expression pattern, and function and possess unique polymorphisms between individual humans and between mouse strains[28]. MHC molecule polymorphism is believed to mediate autoimmune disease[29], graft versus host disease[30], and solid organ transplantation[31]. Other factors that may regulate the degree of tissue damage during such sterile inflammation is discussed in the Appendix.

MHC I antigen presentation

The MHC I molecule consists of three immunoglobulin domains that form the α chain[28]. For stability, this α chain must associate with β2-microglobulin (β2-m) to form the MHC I complex[28]. Three subclasses of MHC I exist in mice: H2-K, H2-D, and H2-L[28]. In C57/BL6 mice, all MHC I molecules are of the b haplotype and thus can be denoted as H2-K^b, etc.

During direct presentation, MHC I molecules present peptides derived from endogenously expressed proteins. As part of regular cellular catabolism, these endogenous antigens are ubiquitinated and degraded by cytosolic proteasomes[32]. Cytosolic proteases may also trim antigen further[33] before the transporter associated with antigen processing (TAP) transfers antigenic peptide into the ER[34]. In the ER, ER aminopeptidase (ERAP) 1 and/or 2 may further trim peptides[35,36] to achieve a final length of about 8-9 amino acids, optimal for MHC I binding[37].

MHC I itself is manufactured in the ER and is initially stabilized by the chaperone protein calnexin (CXN)[28]. Even after β2-m binds MHC I, the complex remains unstable without peptide. Thus, besides mediating peptide loading, the peptide loading complex (PLC)—composed of TAP, calreticulin (CRT), ERp57, tapasin, and MHC I—serves to further stabilize MHC I[28,37]. TAP is recruited to this complex by tapasin, which is believed to help increase the efficiency of peptide loading[37]. CRT, a chaperone and lectin, binds *N*-glycosylated MHC I and stabilizes the interaction between MHC I and tapasin[38]. ERp57, recruited to the PLC by CXN and CRT, regulates disulfide bond isomerization, and thus promotes proper MHC I folding[39]. After the PLC successfully loads peptide onto MHC I, the MHC I:peptide complex is transported to the surface of the cell for presentation to naïve CD8 T cells.

All cells express this machinery and present endogenously expressed peptide under physiologic conditions[32], signaling to circulating immune cells that they have not undergone transformation or infection. If a cell becomes infected or begins expressing mutated proteins, immune effector cells can detect and respond to the concomitant changes in the presented peptides.

The primary effector cell for MHC I antigen presentation is the CD8 T cell. When activated, CD8 T cells become cytotoxic T lymphocytes (CTLs), which specifically detect and kill infected or transformed cells. Activation occurs when a specialized APC expresses MHC I:peptide along with costimulatory molecules, such as CD80 and CD86, and a CD8 T cell is able to recognize these molecules through a cognate TCR and costimulatory receptors, such as CD28[40]. This APC is typically a dendritic cell (DC), unique amongst APCs in its ability to activate naïve T cells.

MHC II antigen presentation

Two subunits, the α and β subunits[28], make up the MHC II molecule. In most mouse strains, there are two MHC II molecules, I-A and I-E[28]. While MHC I typically binds shorter peptides, MHC II accommodates longer ones, varying from 11-30 amino acids in length[41], due to peptide interaction occurring in the center of the MHC II binding groove as opposed to at the ends[42,43].

MHC II antigen presentation, distinct from MHC I antigen presentation, is performed only by APCs and presents exogenously derived peptides, ingested via endo- or phagocytosis. As endosomes and phagosomes mature, their pH drops, enhancing the activity of pH-sensitive lysosomal proteases called cathepsins[37,44], responsible for digesting antigen into presentable peptides. Gamma-interferon-inducible lysosomal thiol reductase (GILT) also contributes to peptide processing for MHC II presentation[45,46].

MHC II molecules themselves are trafficked to the antigen-containing vacuole from the ER, where they are initially synthesized and associate with the invariant chain (I chain; also referred to as Ii and CD74)[47]. Two dileucine sorting motifs on the I chain[48] are recognized by adaptor proteins AP1 and AP2, guiding trafficking to the late endosome[49], also known as the MHC II compartment (MIIC)[37]. In the MIIC, Cathepsins S and L degrade the I chain into the CLIP peptide[50], which remains in the MHC II peptide binding groove until antigenic peptide is loaded, an exchange facilitated by H2-DM in mice or HLA-DM in humans[37].

In DCs, the final MHC II:peptide complex is trafficked to the surface of the cell by actin-based myosin motors[51,52]. Once at the surface, cognate CD4 T cells, as opposed to CD8 T cells with MHC I antigen presentation, can be activated and can differentiate, depending on the cytokine milieu generated by DCs and other cells, into a helper T cell subset. Helper T cells propagate the immune response

through cytokine production which promotes antibody class-switching and supports the differentiation and maturation of other T cells[53].

Antigen cross-presentation

General principles

Cross-presentation describes the process by which extracellular antigen is taken up, processed, and presented on MHC I. This process is most efficiently performed by DCs, as described in more detail below. The stimulation of a cognate CD8 T cell through cross-presentation is called cross-priming. Cross-presentation helps activate the immune response against tumors[54-56] and viruses both with and without DC specificity[57-60]. It also contributes to disease processes such as graft versus host disease (GVHD)[61-64] and various autoimmune diseases[65-67]. It may also promote oral tolerance, though other antigen presentation pathways assist in this as well[68]. Furthermore, if antigen is cross-presented in the absence of costimulatory molecules, responding CD8 T cells may become tolerogenic in a phenomenon known as cross-tolerance[67,69-71]. Other tissue-specific factors that may contribute to tolerance are explored in the Appendix.

In general, while there is substantial data demonstrating cross-presentation occurs, the intracellular mechanisms governing cross-presentation remain poorly described and, at times, a source of controversy. While a number of variables have been shown to up- or downregulate cross-presentation, no

targetable factor has yet been identified which can specifically and completely eliminate cross-presentation. Furthermore, as discussed below, the tools to detect cross-presentation are limited, leading to the popular use of a non-pathogenic, physiologically irrelevant model antigen: ovalbumin (OVA). Finally, the use of a wide variety of antigenic forms—model[5,58,72-845755,57] and physiologic antigen[54,56,57,59,63,65,66,85,86]; soluble[5,74-77,80,81,87-89], insoluble[5,58,72,75,76,82,835757], and cell-associated[5,54,56,59,63,65,66,73,77-79,84-86,90]—to identify a variety of phenotypes, necessarily limits the formation of generalized conclusions from individual experiments.

With these limitations in mind, the current evidence supports a hypothesis where there are two primary cross-presentation pathways, the vacuolar pathway and the cytosolic pathway (or the phagosome-to-cytosol pathway[91,92]), both named in reference to the anticipated location of antigen degradation. Whether these two pathways are mutually exclusive is unknown, as is how each might be regulated in relation to the other.

In the vacuolar pathway, cross-presented antigen appears to be processed by endosomal vacuolar proteases[91,92], explaining why deletion of TAP and treatment with proteasome inhibitors does not completely eliminate cross-presentation[60,93-95]. Other work has shown that loss of vacuolar proteases[60,96,97], such as Cathepsin S in mice[60,76] and Cathepsin D in human DCs[98], impairs cross-presentation.

While vacuolar cross-presentation does cross-prime CD8 T cells, its contribution *in vivo* seems smaller than that from the cytosolic cross-presentation pathway[60], where antigen is exported from the phagosome to the cytosol and then proteasomally processed like endogenously expressed protein. Three sets of observations have demonstrated the existence of this pathway. The first measured cytosolic activity of exogenous protein to assay transport of whole protein from the phagosome to the cytosol, such as cytochrome *c*[87] or gelonin, a ribosomal inactivating protein[88,89]. The second visualized phagocytosed antigen in the cytosol through staining and cell fractionation studies[99,100]. The last assayed activation of exogenous peptide by cytosolic enzymes[5].

While the vacuolar and cytosolic pathways are the best described cross-presentation pathways, limited evidence does exist for a TAP-independent and proteasome-dependent cross-presentation pathway, the mechanisms of which remain unclear[101,102].

Notably, the evolutionary argument best supports the dominance of the cytosolic pathway. To be effective, activated T cells must recognize target cells with cognate MHC I:peptide complexes, where the peptides are generated through proteasomal degradation[89]. Thus, cross-presenting APCs are thought to use proteasomal degradation as well to produce the same MHC I:peptide cross-presenting complexes to activate naïve CD8 T cells.

Internalization, transport, and processing of cross-presented antigen

Antigen can be internalized for cross-presentation through a variety of mechanisms. Fluid-phase pinocytosis of soluble antigen is the least efficient; high concentrations of antigen are necessary for detectable cross-presentation[103,104]. However, if soluble antigen is taken up by receptor-mediated endocytosis, cross-presentation is more efficient[105-107]. Cross-presentation is most efficient when particulate antigen is taken up by phagocytosis and macropinocytosis[88,104,108]. Finally, in a phenomenon known as cross-dressing, DCs can capture MHC I:peptide complexes from other cells, using these complexes to cross-prime a naïve T cell[109-111].

When processed by the vacuolar pathway, antigens need not undergo further transport to be degraded. However, if processed via the cytosolic pathway, antigen must next exit the endocytic vacuole. How this happens is poorly understood. Some clues have come from studying endoplasmic-reticulum-associated-degradation (ERAD), the mechanism most cells use to transport misfolded proteins from the ER lumen to the cytosol for proteasomal degradation[112,113]. Cross-presentation does seem to partially rely on ERAD components[99,114-117], though whether manipulating ERAD causes cross-presentation-specific defects or defects in normal protein synthesis and quality control with downstream effects on cross-presentation remains undetermined. Further obfuscating the role of ERAD in cross-presentation, while ERAD transport proteins Sec61, Derlins, and Hrd1 assist in trafficking misfolded

proteins into the cytosol[112,118-120], Derlin-1 is not necessary for cross-presentation[116]. Moreover, there is some controversy over whether Sec61 plays this role during cross-presentation[91,116]. The role of Hrd1 has not yet been explored.

Another possible mechanism for antigen transport to the cytosol is phagosomal disruption. Particles such as silica crystals and aluminum salts can destabilize phagosomes, leading to membrane rupture and release of phagosomal contents into the cytosol[121]. However, though this theory proves a more elegant explanation for the transfer of non-protein products such as dextrans[88] and whole, functional protein to the cytosol[87-89] than one relying on protein transporters, it remains challenging to study due to a poor mechanistic understanding of how phagosomal disruption occurs. Theoretically, oxidative bursts might modify membrane lipids, leading to phagosomal destabilization[122] and, interestingly, NOX2 (NADPH oxidase 2), a generator of reactive oxygen species (ROS), has been shown to promote cross-presentation[80]. However, phagosome integrity was not assessed in this system[80].

ROS promotion of cross-presentation[80,81,123-126] appears to be mediated, at least in part, through its effects on phagosomal pH, a known modulator of cross-presentation efficiency. ROS elevates pH, neutralizing the phagosome, and protecting antigen against excessive degradation prior to export to the cytosol. Conversely, a lower pH promotes cross-presentation through the vacuolar

pathway[60,96] as acidic environments activate cathepsins. Transcription factor EB (TFEB) may be a master regulator for this process, reducing cytosolic cross-presentation by promoting lysosomal acidification[74]. Indeed, its expression is reduced in CD11c+ CD8+ splenic DCs, a specialized cross-presenting subset of DCs (see below) as compared to CD11c+ CD4+ splenic DCs[74]. Lipid body formation, mediated by immune-related GTPase Irgm3 (Igtp), which promotes cross-presentation, may also regulate vacuolar pH[127]. Overall, these pH-dependent effects appear to be mediated through protease activity, not through the pH change itself as protease inhibitor treatment reverses the effects of vacuolar acidification on cross-presentation[124]. Additionally, physiologic protease inhibitors such as serpinb9[128] may counteract the effects of an acidifying endosome on cross-presentation.

For many years, whether antigen transport to the cytosol and phagosomal acidification might be regulated together was a mystery. Intriguingly, SEC22B has been posited to unify these elements, as its shRNA-mediated knockdown in bone marrow derived DCs (BMDCs) slowed phagosomal acifidication and decreased antigen transport from the phagosome to the cytosol while simultaneously reducing cross-presentation[5]. SEC22B and its specific role in cross-presentation is further explored in Chapter 3.

The cross-presenting compartment

Where cross-presentation occurs within the cell is still a subject of active debate. A large body of evidence suggests that cross-presentation occurs in endosomes/phagosomes. MHC I localizes to these structures,[129,130] and disruption of this process interrupts cross-presentation[129,131]. Additionally, when OVA antigen is used, H2-K^b molecules complexed with $OVA_{257-264}$ peptide (SIINFEKL) have been identified in phagosomes[82,100,114,129,132]. However, whether this complex is newly generated or recycled from the surface is unclear.

Of the endocytic compartments, early endosomes seem best-suited to cross-present through the cytosolic pathway due to their more neutral pH compared to late endosomes[91]. This model is supported by evidence showing that targeting TAP inhibitors to the early endosome reduces cross-presentation[100] and that targeting antigen to early endosomes enhances cross-presentation[133,134]. Furthermore, TAP1 and IRAP (insulin-regulated aminopeptidase), both necessary for cross-presentation, are present in early endosomes[82,100,135]. In fact, IRAP traffics specifically to endosomes[91]. Moreover, Sec61 colocalizes with antigen in Rab5+ early endosomes[117], further suggesting that this is the cross-presenting compartment.

Some evidence, however, also suggests that cross-presentation may occur in the late endosome. Antigen targeted to late endosomes, through DEC205-mediated uptake[136] or association with a TLR (toll-like receptor) ligand[78], is still cross-presented. Furthermore, H2-K^b:SIINFEKL complexes have been detected

in both early and late endosomes[129], though whether this localization is through uptake of surface H2-K^b:SIINFEKL is unknown. It might be that the vacuolar pathway uses late endosomes to cross-present what antigen has not yet been exported to the cytosol, though this idea has never been specifically studied.

Since the ER is the site of peptide loading during MHC I antigen presentation, it is an attractive candidate for the cross-presenting compartment. Indeed, combined ERAP1 and IRAP deficiency demonstrates an additive reduction in cross-presentation[135]. However, the evidence supporting endosomes as the cross-presenting compartment suggests that the ER makes, at most, a minor contribution to the final pool of MHC I:peptide complexes. Additionally, the ERGIC has been implicated in the cytosolic cross-presentation pathway[5], though its specific contributions remain undefined.

MHC I and antigen colocalization

How antigen reaches MHC I, particularly in the cytosolic pathway, remains a subject of debate. Three forms of antigen trafficking into putative cross-presentation compartments have been observed: (1) TAP-dependent transport into the ER, as occurs during direct MHC I antigen presentation[82,89], (2) TAP-dependent transport into the phagosome[83,137], and (3) TAP-independent transport into the phagosome[100]. Which method is dominant and the conditions that might select one over another have not been investigated.

While MHC I, TAP, Sec61, CXN, CRT, and tapasin, normally found in the ER, have all been observed in the phagosome[5], how they arrive there is poorly understood. Though some MHC I may enter the phagosome through incidental reuptake or regulated recycling, there is still a role for newly synthesized MHC I molecules from the ER in cross-presentation[93]. Furthermore, because brefeldin A (BFA) treatment inhibits cross-presentation, ER to Golgi transport may be responsible for trafficking of other PLC components to the phagosome[89,98]. Possible mediators for this trafficking include SEC22B[5] (discussed in further detail in Chapter 3) and the I chain[138,139]. However, some evidence suggests that these proteins are not necessary for cross-presentation[60,93] (see Chapter 3).

As mentioned above, unlike other ER-localized PLC proteins, MHC I can be recycled from the plasma membrane[129,131]. This trafficking may be especially critical during vacuolar cross-presentation because neither BFA treatment[102,108,140] nor inhibition of protein synthesis[103,108] fully suppresses cross-presentation. Finally, G-proteins involved in endosomal recycling, specifically Rab3b, c[141], Rab22a[142,143], and Rab11a[78], also impact crosspresentation, suggesting that surface MHC I are reused for cross-presentation. These MHC I might be internalized alongside antigen, bringing the two to the same intracellular location.

Contributions from other cellular processes

In addition to the cellular factors described above, other pathways may also be involved in cross-presentation. Autophagy, the process by which cells break down and recycle organelles and proteins, may regulate cross-presentation under specific circumstances. While ATG5 (autophagy-related protein 5) knockout mice do not exhibit a cross-presentation defect[144], ATG7 deficiency does reduce cross-presentation of soluble but not cell-associated or DEC205-associated antigen[145]. In addition, autophagy-associated proteins may promote cross-presentation through autophagy-independent means, such as LC3 stabilization of NOX2 and regulation of phagosome-lysosome fusion[144,146,147].

While it is clear that TLR activation alters cross-presentation efficiency, how it does so is not. In some instances, TLR stimulation inhibits cross-presentation[148,149], but in others, TLR agonists can promote cross-presentation[100,131,132,150], such as when antigen is bound to the agonist[151]. Downstream effects of TLR stimulation, such as Type I interferon production, can also promote cross-presentation[152].

Cross-presenting cell populations

Conventional dendritic cells (cDCs), which express CD11c and MHC II[153,154], are the primary cross-presenting population *in vivo*[90,155-158]. Within the cDC population, cells denoted cDC1s are the more efficient cross-presenters and can be distinguished from their cDC2 counterparts by surface marker expression. In the spleen and lymph nodes of mice, cDC1s express

CD8α[84,148,159,160], CD24, and the chemokine receptor XCR1[161]. In nonlymphoid tissues, cDC1s express XCR1 and CD103 and migratory cDC1s maintain the surface phenotype of their peripheral counterparts[161]. Although CD8α is commonly used to isolate cross-presenting cDCs, its isolated expression on lymphoid organ resident DCs reduces its utility[17]. XCR1, on the other hand, appears to be a universal marker for cDC1s[162,163]. Recent studies suggest that the most efficient strategy to identify cDC1s in any tissue is to select for CD11c+ MHC II+ CD26+ CD64– XCR1+ cells[164]. The human equivalent of murine XCR1+ DCs express XCR1 as well and can be identified as BDCA3+ XCR1+ CD141+ cells[165-167]. *Batf3* expression can also be used to identify cDC1s, as *Batf3* knockout mice lack CD8α+ and CD103+ DCs and exhibit cross-presentation defects[155,168].

In addition to these *in vivo* cell populations, cultured DC systems can also cross-present. JAWS II, a murine DC cell line, can cross-present antigen[5,142] as can BMDCs cultured in granulocyte-macrophage colony stimulating factor (GM-CSF)[56,92]. The studies on cross-presentation in Chapter 3 make use of both *ex vivo* CD8α+ splenic DCs as well as CD11c+ BMDCs.

Methods for detecting antigen cross-presentation

Antigen cross-presentation can be detected by directly assaying cross-presentation on the APC or by measuring cross-priming of CD8 T cells. Typical controls for cross-presentation assays include: using a peptide that does not

require processing for presentation, such as $OVA_{257-264}$ (SIINFEKL) if OVA antigen is being used; assaying for concomitant MHC II antigen presentation; or measuring MHC I surface expression.

Direct measurement of cross-presentation

Only one commercially available antibody is able to detect a specific peptide presented on MHC I: clone 25-D1.16, which detects H2-K^b bound to SIINFEKL[169]. However, it is a weak antibody, only detectable with high concentrations of substrate MHC I:peptide complex.

Measuring cross-priming

Several antigen-specific transgenic T cell receptor (TCR) mice and hybridoma cell lines exist. To measure the cross-presentation of OVA, OT-I mice, which are on a C57/BL6 background and restricted to haplotype *b*, can be used[170]. It is the mouse model employed in Chapter 3 to study cross-presentation. Due to the presence of a transgenic TCR that recognizes H2-K^b:SIINFEKL, all T cells within these mice express the same TCR and are virtually all CD8+[170]. An alternative to these mice is the B3Z hybridoma cell line, which also recognizes H2-K^b:SIINFEKL[171]. Cross-presentation of lymphocytic choriomeningitis virus (LCMV) antigen is assayable using T cells from P14 transgenic mice, which are also on a C57/BL6 background and express a transgenic TCR specific for H2-D^b presenting the $gp33_{33-41}$ peptide from LCMV[172]. Like OT-I mice, virtually all their T cells carry the same TCR and are CD8+[172].

Proliferation of activated T cells can be directly measured using intracellular dyes, such as CFSE (carboxyfluorescein succinimidyl ester), which covalently bind to cellular proteins, creating a stepwise drop in fluorescent intensity with each round of cell division that permits quantification of individual cell divisions[173]. This marker is used to detect cross-priming in Chapter 3. Proliferation can also be inferred by incorporation of tritium labeled thymidine (3H-thymidine) or thymidine analog BrdU[173] into the DNA of rapidly dividing cells. Ki67, expressed during all cell cycle stages except G_0 can also be used to measure proliferation[174]. Finally, quantifying T cells through counting or flow analysis of a specific marker, such as with congenic markers, with fluorescence expression or staining, or with a tetramer, can capture information on proliferation.

Flow cytometry can also be used to measure activation marker expression on or cytokine production from cross-primed T cells, a method used in Chapter 3 alongside CFSE staining. Western Blot can also be used to measure activation by detecting protein phosphorylation states and subcellular localization of transcription factors[175]. Cytokine production can also be measured in aggregate through ELISA (enzyme-linked immunosorbent assay) on cell culture media, another popular method for detection of cross-priming[74-76,78,93].

Finally, *in vivo*, the goal of antigen presentation is to induce an antigen-specific CTL response. Thus, demonstrating CTL function can be a powerful demonstration of antigen presentation.

CHAPTER II

SNARE PROTEIN SEC22B REGULATES EARLY EMBRYONIC DEVELOPMENT AND HEMATOPOIESIS

AUTHORS: S Julia Wu, Rami Khoriaty, Sue O'Shea, Guojing Zhu, Cynthia Zajac, Katherine Oravecz-Wilson, Tomomi Toubai, Yaping Sun, David Ginsburg, Pavan Reddy

ABSTRACT

The highly conserved SNARE protein SEC22B plays a vital role in cell biology, contributing to diverse functions, including intracellular infection, phagocytosis, cell growth, autophagy, and protein secretion. However, these cellular activities have thus far only been examined *in vitro*. Here, we expand our understanding of *Sec22b* by testing its contributions *in vivo* in mice by deleting *Sec22b* in three increasingly specific experimental models: the whole organism, the hematopoietic system, and CD11c-expressing cells. These knockout models reveal that hematopoietic expression of *Sec22b* is required for embryonic development, as mice with hematopoietic system-specific *Vav1-Cre*-driven deletion of *Sec22b* die *in utero*. However, embryonic survival does not require *Sec22b* expression in the CD11c-expressing cells of the hematopoietic system.

Germline deletion of *Sec22b* results in developmental delay at 7.5 days post conception (E7.5) and embryonic death at E8.5, before the onset of *Vav1-Cre* expression, suggesting a critical SEC22B function in a non-hematopoietic tissue(s).

INTRODUCTION

Intracellular trafficking plays a critical role in cellular biology, regulating the distribution and organization of secretory proteins. One protein class which helps mediate this complex choreography is the SNAREs (soluble N-ethylmaleimide-sensitive factor attachment protein receptor). Partner SNAREs bind and mediate the fusion of two membranes by physically bringing the membranes sufficiently close to fuse[176]. SEC22B is an endoplasmic reticulum (ER)-SNARE which localizes to the ER and the ER-Golgi intermediate compartment[5]. It functions as a vesicular-SNARE[7,177], and its known interacting partners include plasma membrane-SNAREs syntaxin 1[6], syntaxin 4[5] and syntaxin 5[7] as well as another ER-SNARE, syntaxin 18[8].

Functioning at the interface between the plasma membrane and the ER membrane, SEC22B appears to mediate membrane expansion under several conditions, including *Legionella* and *Leishmania* infection in macrophages[20,178,179] as well as during axonal growth from isolated cortical neurons[6]. Some evidence suggests that SEC22B contributes to cellular homeostasis as well. For example, in murine macrophages, SEC22B negatively regulates phagocytosis[8] but promotes reactive oxygen species accumulation during *S. aureus* infection[17]. In flies, Sec22 influences ER morphology[13], while in yeast, Sec22 contributes to autophagosome biogenesis[12]. In human cell lines, it has been implicated in the secretory autophagy pathway[16] as well as in

macroautophagy[180]. SEC22B has also been implicated in other secretory pathways, such as that in VLDL (very-low-density lipoprotein)-secreting rat hepatocytes. Thus, current evidence suggests that SEC22B plays a fundamental role in cell biology. However, its function *in vivo* remains untested.

We generated *Sec22b* deficient mice to explore *Sec22b*'s role *in vivo* in three targeted compartments: the whole organism, the hematopoietic system, and in a specific immune cell population. We observed that *Sec22b* is critical for embryonic development. Embryos with a global deficiency in *Sec22b* do not survive beyond 8.5 days post-conception (E8.5). Deletion of *Sec22b* from the hematopoietic compartment results in embryonic lethality. However, normal development was observed with deletion of *Sec22b* in CD11c-expressing hematopoietic cells.

RESULTS

Sec22b is necessary for embryonic development

To determine the role of SEC22B *in vivo*, we first intercrossed mice heterozygous for a FRT recombination site-flanked conditional gene-trapped *Sec22b* allele (*Sec22b*$^{cgt/+}$) (Figure 2.1A, B). Moreover, we did not detect any *Sec22b*$^{cgt/cgt}$ offspring at weaning (p<0.0001) (Table 2.1A). To exclude the possibility that an off target gene trap effect[181], as opposed to the loss of functional *Sec22b*, was responsible for this phenotype, we generated mice heterozygous for the *Sec22b* null allele (*Sec22b*$^{+/-}$). We next crossed the *Sec22b*^{cgt} allele to mice expressing FLP recombinase driven by the human β-actin promoter and excised the gene trap cassette, resulting in the *Sec22b*^{fl} allele (Figure 2.1C), where exon 3 is flanked by *LoxP* sites (Figure 2.1A). Subsequently, the *Sec22b*^{fl} allele was crossed to mice expressing Cre recombinase driven by the germline-expressed *Ella* promoter, producing the *Sec22b*$^{-}$ allele (Figure 2.1A, D). Haploinsufficient *Sec22b*$^{+/-}$ mice survived to term and exhibited normal survival (p=0.6473) (Table 2.1B). However, no *Sec22b*$^{-/-}$ pups were observed at weaning (p=0.0008) (Table 2.1C).

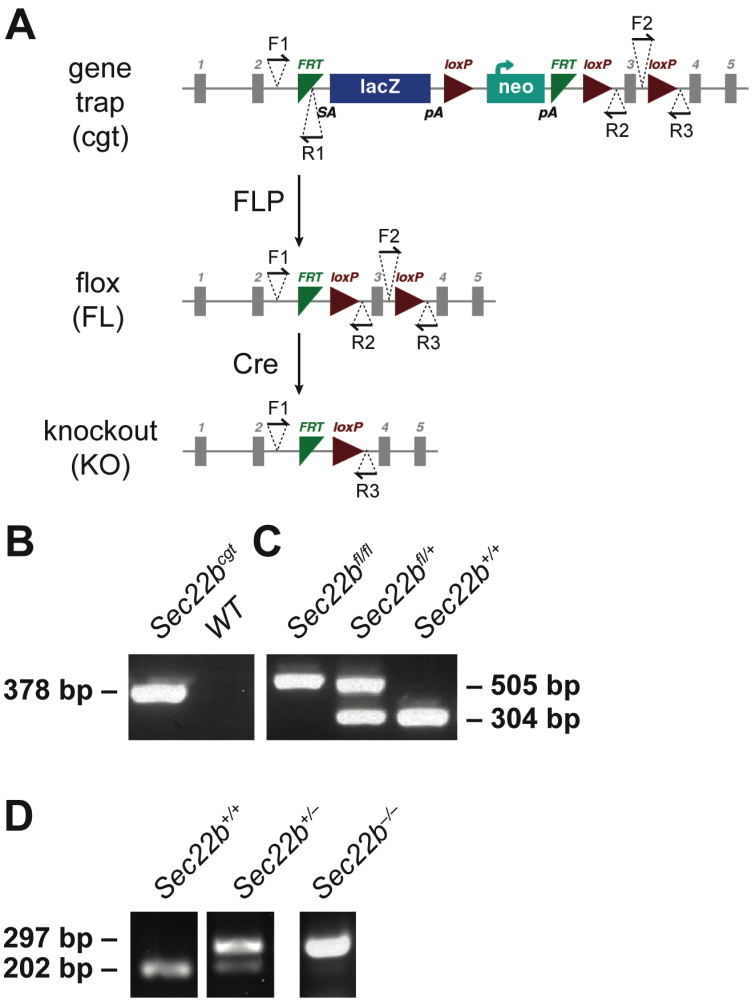

Figure 2.1. Generation of gene targeted *Sec22b* alleles. (A) *Sec22b*-conditional gene trapped mice, with FRT-flanked gene trap inserted between exons 2 and 3, on a C57BL/6 background were mated to FLP-recombinase transgenic mice to create floxed mice, with *LoxP* sites flanking exon 3. Floxed mice were mated to *Ella-Cre* to generate the germline null allele (Sec22b^{-}), or to *Vav1-Cre* or *CD11c-Cre* transgenic mice to generate tissue specific Sec22 deficiency. Binding sites for genotyping primers (F1, F2, R1, R2, R3) are indicated with half arrowheads. **(B)** PCR with primers F1 and R1 detect the insertion of the conditional gene trap in *Sec22b*. **(C)** PCR with primers F1 and R2 detect the excision of the conditional gene trap by FLP recombinase and distinguish between *Sec22b^{fl}* homozygous and heterozygous mice. **(D)** Competitive PCR with primers F1, F2, and R3 detect the excision of exon 3 of *Sec22b* and distinguish between *Sec22b^{-}* heterozygous and homozygous mice.

A. Genotype:	***Sec22b*$^{+/+}$**	***Sec22b*$^{+/cgt}$**	***Sec22b*$^{cgt/cgt}$**	***p*-value**
***Sec22b*$^{cgt/+}$ x *Sec22b*$^{cgt/+}$ Expected Ratios**	**25%**	**50%**	**25%**	
At weaning (n=73)	33% (24)	67% (49)	0% (0)	*<0.0001*
B. Genotype:	**Sec22b$^{+/+}$**	**Sec22b$^{+/-}$**		**p-value**
***Sec22b*$^{+/-}$ x *Sec22b*$^{+/+}$ Expected Ratios**	**50%**	**50%**		
Weaning (n=234)	48% (113)	52% (121)		0.6473
C. Genotype:	***Sec22b*$^{+/+}$**	***Sec22b*$^{+/-}$**	***Sec22b*$^{-/-}$**	***p*-value**
***Sec22b*$^{+/-}$ x *Sec22b*$^{+/-}$ Expected Ratios**	**25%**	**50%**	**25%**	
Weaning (n=34)	24% (8)	76% (26)	*0% (0)*	*0.0008*
E13.5 (n=9)	22% (2)	78% (7)	0% (0)	0.0833
E11.5 (n=17)	24% (5)	76% (16)	0% (0)	*0.0173*
E9.5 (n=12)	25% (5)	75% (15)	0% (0)	*0.0459*
E8.5 (n=35)	34% (12)	60% (21)	6% (2)	*0.0055*
E7.5 (n=9)	22% (2)	56% (5)	22% (2)	>0.9999
E3.5 (n=33)	27% (9)	52% (17)	21% (7)	0.6929

Table 2.1. Genotypic distribution of offspring from *Sec22b*$^{cgt/+}$ and *Sec22b*$^{+/-}$ mating schemes. (A) Genotypic distribution of offspring at weaning from *Sec22b*$^{cgt/+}$ intercrosses with expected Mendelian distribution. **(B)** Genotypic distribution of offspring at weaning from *Sec22b*$^{+/-}$ x *Sec22b*$^{+/+}$ crosses compared to expected Mendelian distribution. **(C)** Genotypic distribution of offspring at weaning and at indicated days post conception (e.g. E13.5) from *Sec22b*$^{+/-}$ intercrosses as compared to expected Mendelian distribution. *P*-values are calculated from a two-tailed chi-square test for *Sec22b*$^{-/-}$ versus all other genotypes.

Sec22b$^{-/-}$ mice do not survive beyond E8.5

To determine the stage at which germline loss of *Sec22b* results in embryonic death, we next performed timed matings on *Sec22b*$^{+/-}$ intercrosses. Offspring from this intercross exhibited Mendelian genotypic distribution at E3.5

(p=0.6929) and E7.5 (p>0.999) (Table 2.1C). However, at E8.5, *Sec22b*$^{-/-}$ mice were significantly underrepresented (p=0.0055) (Table 2.1C). Thereafter, at E9.5, E11.5, and E13.5, no *Sec22b*$^{-/-}$ embryos were observed (Table 2.1C).

Loss of *Sec22b* does not impact embryo size

Although many null embryos exhibited some degree of developmental delay compared with control littermates based on visual inspection and reduced *Sec22b* dose seemed to trend with reduced embryo length (Figure 2.2A, B), these differences were not statistically significant (Figure 2.2B). No differences in weight exist between *Sec22b*$^{+/-}$ and *Sec22b*$^{+/+}$ adult mice either (Figure 2.2C), suggesting that *Sec22b* does not impact embryo size.

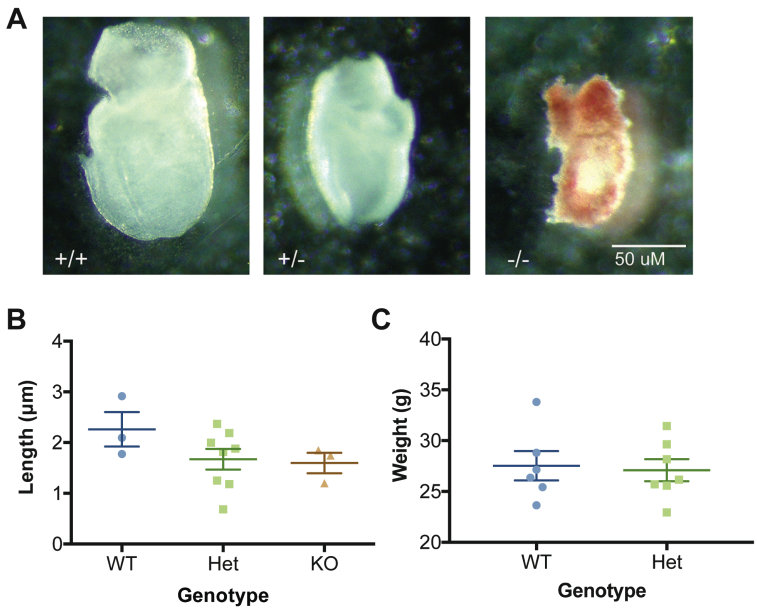

Figure 2.2. Characterization of *Sec22b*$^{+/-}$ and *Sec22b*$^{-/-}$ mice. **(A)** Ventrolateral view of early somite (*Sec22b*$^{+/+}$ (+/+), *Sec22b*$^{+/-}$ (+/–)) and egg cylinder (*Sec22b*$^{-/-}$ (–/–)) embryos immediately after dissection. **(B)** Length of *Sec22b*$^{+/+}$ (WT), *Sec22b*$^{+/-}$ (Het), *Sec22b*$^{-/-}$ (KO) embryos in µm. Error bars represent SEM. **(C)** Weight in grams of 4.5-5 month old *Sec22b*+/– (n=7) compared to littermate *Sec22b*$^{+/+}$ (n=6) mice. Error bars represent SEM.

Hematopoietic deficiency of *Sec22b* results in embryonic lethality

Because of the observed roles for SEC22B in immune cell function[5,8,16,17,20,178,179], we examined the role of *Sec22b* within the hematopoietic system using the *Vav1-Cre* transgene. We observed a significantly reduced number of *Vav1-Cre* *Sec22b*$^{fl/fl}$ mice at weaning (p<0.0001) (Table 2.2), suggesting that *Sec22b* expression in the hematopoietic compartment is necessary for embryonic survival.

Genotype:	***Vav1*$^{+/+}$ *Sec22b*$^{fl/fl}$**	***Vav1*$^{+/+}$ *Sec22b*$^{fl/+}$**	***Vav1*$^{Cre/+}$ *Sec22b*$^{fl/+}$**	***Vav1*$^{Cre/+}$ *Sec22b*$^{fl/fl}$**	***p*-value**
Expected Ratios	25%	25%	25%	25%	
Observed at weaning (n=125)	29% (52)	29% (52)	36% (64)	5% (9)	*<0.0001*

Table 2.2. Genotypic distribution of offspring from *Vav1-Cre* *Sec22b*$^{fl/+}$ x *Vav1-WT* *Sec22b*$^{fl/fl}$ mating pairs. *G*enotypic distribution of offspring at weaning from *Vav1-Cre* *Sec22b*$^{fl/+}$ x *Vav1-WT* *Sec22b*$^{fl/fl}$ crosses as compared to expected Mendelian distribution. *P*-values are calculated from a two-tailed chi-square test for *Vav1-Cre* *Sec22b*$^{fl/fl}$ versus all other genotypes.

Amplification of genomic DNA at the *Sec22b* locus in peripheral blood cells from the rare surviving *Vav1-Cre* *Sec22b*$^{fl/fl}$ mice (Figure 2.3) suggests that incomplete excision at exon 3 of *Sec22b* may explain this incompletely penetrant survival into adulthood (Figure 2.4A).

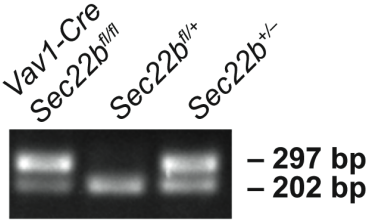

Figure 2.3. *Vav1-Cre* mediated excision incomplete in *Vav1-Cre Sec22b$^{fl/fl}$* adult mice. Products from PCR on genomic DNA from the peripheral blood of a surviving *Vav1-Cre Sec22b$^{fl/fl}$* mouse and a *Vav1-WT Sec22b$^{fl/fl}$* littermate control compared to DNA from *Sec22b$^{+/-}$* mice, which have equal quantities of excised and unexcised DNA.

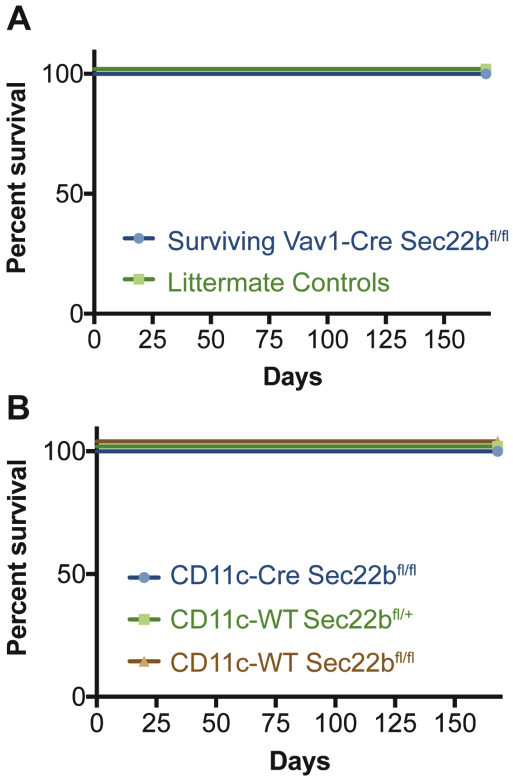

Figure 2.4. Survival in mice with *Sec22b* deletion in hematopoietic subsets. 6 month survival curves for **(A)** *Vav1-Cre Sec22b$^{fl/fl}$* mice (n=5) as compared to littermates (n=4) and for **(B)** *CD11c-Cre Sec22b$^{fl/fl}$* mice (n=53) as compared to *CD11c-WT Sec22b$^{fl/+}$* (n=52) and *CD11c-WT Sec22b$^{fl/fl}$* (n=38) littermates.

Sec22b$^{+/-}$ mice exhibit no hematopoietic phenotype under physiologic conditions

Because mice with hematopoietic loss of *Sec22b* exhibit embryonic lethality (Table 2.2), we wondered if partial loss of *Sec22b* might cause a hematopoietic phenotype. To test this possibility, we performed complete blood counts on peripheral blood collected from *Sec22b$^{+/-}$* mice. These profiles were indistinguishable from that obtained from littermate controls, including total white blood cells (Figure 2.5A), monocytes

(Figure 2.5B), lymphocytes (Figure 2.5C), neutrophils (Figure 2.5D), hemoglobin (Figure 2.5E) and platelet counts (Figure 2.5F).

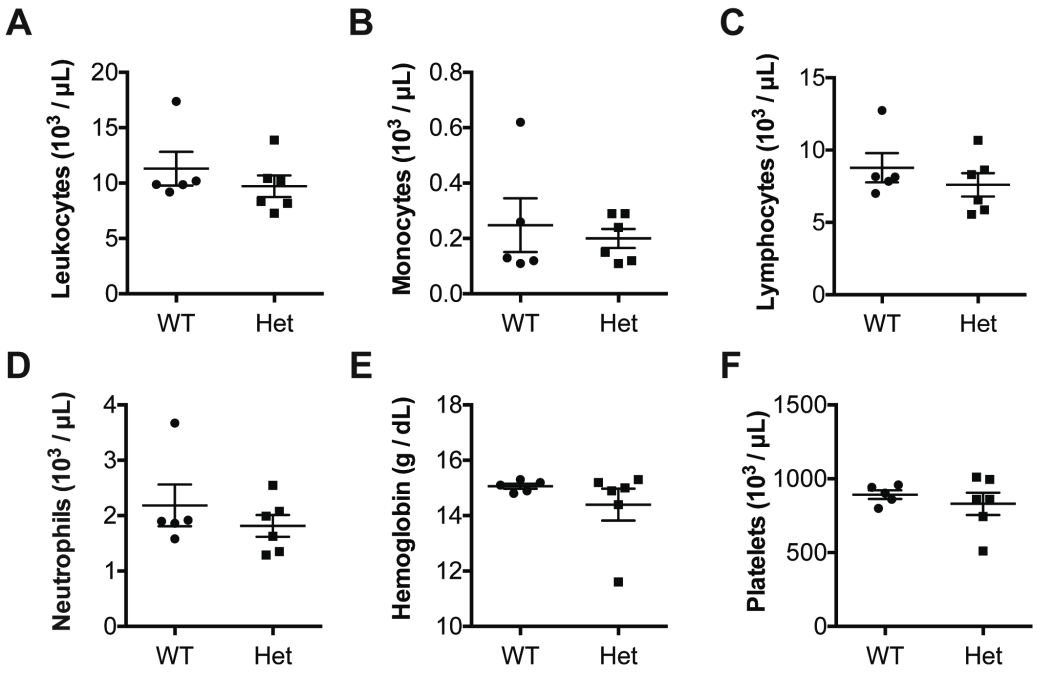

Figure 2.5. Complete blood counts on *Sec22b* haplodeficient mice. **(D)** Total leukocytes, **(E)** monocytes, **(F)** lymphocytes, **(G)** neutrophils, **(H)** hemoglobin, and **(I)** platelets from peripheral blood of 5 month old *Sec22b*$^{+/+}$ (n=5) and Sec22b$^{+/-}$ (n=6) littermates quantified as indicated on axes. Error bars represent SEM.

Mice with *Sec22b* deletion in CD11c^{+} cells survive to adulthood

Given the demonsrated role for SEC22B in macrophages *in vitro*[8,17,20,179] and dendritic cells (DCs[5], we used *Itgax-Cre* (*CD11c-Cre*) to delete *Sec22b* in CD11c-expressing macrophages and DCs (*CD11c-Cre Sec22b*$^{fl/fl}$). Offspring generated by crossing *CD11c-Cre Sec22b*$^{fl/+}$ and *Sec22b*$^{fl/fl}$ mice exhibited the expected Mendelian distribution (Table 2.3) as well as normal survival up to 6 months (168 days) (Figure 2.4B).

Genotype:	***CD11c*$^{+/+}$ *Sec22b*$^{fl/fl}$**	***CD11c*$^{+/+}$ *Sec22b*$^{fl/+}$**	***CD11c*$^{Cre/+}$ *Sec22b*$^{fl/+}$**	***CD11c*$^{Cre/+}$ *Sec22b*$^{fl/fl}$**	***p*-value**
Expected Ratios	25%	25%	25%	25%	
Observed at weaning (n=606)	28% (171)	25% (149)	22% (133)	25% (153)	0.8881

Table 2.3. Genotypic distribution of offspring from *CD11c-Cre Sec22b*$^{fl/+}$ x *Sec22b*$^{fl/fl}$ mating pairs. *G*enotypic distribution of offspring at weaning from *CD11c-Cre Sec22b*$^{fl/+}$ x *Sec22b*$^{fl/fl}$ mating pairs as compared to expected Mendelian distribution. *P*-values are calculated from a two-tailed chi-square test for *CD11c-Cre Sec22b*$^{fl/fl}$ versus all other genotypes.

DISCUSSION

Our studies demonstrate that mouse embryos require *Sec22b* to survive past E8.5. *Sec22b* haploinsufficient mice appear to grow normally, although we did observe some developmental delay in null embryos. Deletion of *Sec22b* from the hematopoietic compartment also results in partial embryonic lethality, though *Sec22b* haploinsufficient mice do not have a hematopoietic phenotype under physiologic conditions. Deletion of *Sec22b* within a specific hematopoietic subpopulation, CD11c-expressing cells, did not reproduce the embryonic lethality.

The exact mechanism by which *Sec22b* mediates survival of the early mouse embryo remains unclear. Our data suggests *Sec22b* regulates embryonic survival through activity in at least two distinct tissues. We have found that *Sec22b* is required early, before E8.5. However, at this point, *Vav1*, remains unexpressed[182]; it isn't until E11.5 that *Vav1* transcripts are first detectable[183,184]. This implies that *Sec22b* regulates survival later during embryogenesis as well, through activity within *Vav1*-expressing cells, supporting the hypothesis that *Sec22b* is necessary in at least two tissues to support embryonic development. *Sec22b* has previously been shown to be required *in vitro* for axonal growth in isolated mouse cortical neurons[6] and for VLDL secretion in rat hepatocytes[14], whereas in *D. melanogaster,* loss of *Sec22* results in defects in eye

development[13]. Future studies will explore how *Sec22b* expression in these tissues alters embryonic development and survival.

Our examination of *Sec22b*'s contribution to hematopoiesis raises interesting possibilities. While loss of *Sec22b* in the compartment leads to embryonic lethality, *Sec22b*$^{+/-}$ mice demonstrate no hematopoietic abnormalities. Further research will be necessary to determine how *Sec22b* causes this phenotype. How does *Sec22b*-mediated transport affect hematopoietic cell function? Must *Sec22b* be deleted from hematopoietic stem cells to induce embryonic lethality, or would loss of *Sec22b* in a terminally differentiated cell population be sufficient? Our data demonstrate that, at least with regard to the latter question, loss of *Sec22b* in CD11c-expressing cells also produces no survival defect. Interestingly, loss of *Sec22b* in this compartment does not seem to affect the development or function of CD11c^{+} cells (in press).

In summary, our data demonstrate a crucial role for *Sec22b* in embryogenesis. When deleted in all cells, embryos fail to survive past E8.5. When deleted in *Vav1*-expressing cells, embryonic lethality is still observed. This pattern suggests that *Sec22b* expression in at least two tissue types, including the hematopoietic system, is necessary for embryonic survival. Deleting *Sec22b* in CD11c-expressing cells demonstrated that loss of *Sec22b* in this cell population is not responsible for the embryonic lethality observed in the hematopoietic

system-specific knockout. Further investigation is necessary to determine the precise mechanism by which *Sec22b* mediates embryonic survival.

MATERIALS AND METHODS

Mice

Mice with FRT-flanked conditional gene trap between exons 2 and 3 of *Sec22b* were obtained from the European Conditional Mouse Mutagenesis Program (EUCOMM; $Sec22b^{tm1a(EUCOMM)Wtsi}$) and crossed to mice with *FLP* recombinase expressed under the control of human β-actin promoter (005703, The Jackson Laboratory) to create the $Sec22b^{fl}$ allele. *EIIa-Cre* (005703, The Jackson Laboratory), *Vav1-Cre (*003724, The Jackson Laboratory), and *CD11c-Cre* transgenic mice (008068, The Jackson Laboratory), were bred to $Sec22b^{fl/fl}$ mice to create *EIIa-Cre* $Sec22b^{fl/fl}$, *Vav1-Cre* $Sec22b^{fl/fl}$, *CD11c-Cre* $Sec22b^{fl/fl}$ mice.

Timed Matings

Breeders were co-housed in the evening and females examined for a vaginal plug the following morning (0.5 days post-conception; E0.5). Those with plugs were euthanized at the appropriate time point. Embryos were dissected from uteri and, where indicated, photographed prior to fixation.

DNA Isolation

Mice were genotyped by digesting tail clips in DirectPCR Lysis Reagent (Mouse Tail) (Viagen, 102-T) with Proteinase K (Sigma Aldrich, P4850) at 56°C overnight followed by 1 hour denaturation at 95°C. Genomic DNA from E7.5-13.5 embryos and from peripheral blood was obtained using the DNeasy Blood & Tissue Kit

(Qiagen, 69504), following manufacturer's instructions. E3.5 blastocysts were harvested into 1xPBS into PCR tubes (USA Scientific, 1402-2500) and frozen at -80°C, and then thawed. Thawed product was used for genotyping PCR.

Primers and Genotyping

Cre transgene and *Sec22b* allele genotyping primers are collected in Table 2.4. *Sec22b* primer binding sites are identified in Figure 2.1A. The *Sec22b* F1+R1 primers was used to identify gene-trapped mice and the *Sec22b* F1+R2 primers was used to identify floxed versus wildtype mice. *Sec22b* F1, F2, R3 were used in a competitive PCR to identify the null allele versus the floxed allele. Genotyping was performed via PCR reaction with GoTaq Green Master Mix (Promega, M7122) according to manufacturer's recommendations.

Primer Name	***Sequence (5'→3')***
Sec22b F1	AAGGGTGGATGGATTCTTCACAC
Sec22b F2	TCCTTTTGAATGGAGAAAGCTTC
Sec22b R1	TTGGTGGCCTGTCCCTCTCACCTT
Sec22b R2	GCAGCTCAGCAGTAAGAACACGTC
Sec22b R3	CCTGTGACAGTCTACAGATTGGA
Cre F	TTACCGGTCGATGCAACGAGT
Cre R	TTCCATGAGTGAACGAACCTGG
Vav1 F1	AGATGCCAGGACATCAGGAACCTG
Vav1 R1	ATCAGCCACACCAGACACAGAGATC
Vav1 F2	CTAGGCCACAGAATTGAAAGATCT
Vav1 R2	GTAGGTGGAAATTCTAGCATCATC

Table 2.4. Primers used for *Sec22b* and *Cre* genotyping. *Sec22b* primers include F1 and F2 forward primers and R1, R2, and R3 reverse primers. *Sec22b* primer binding positions are indicated in Figure 1A. *Cre* primers detect both *EIIa*- and *CD11c-Cre* transgenes. *Vav1* primers are used together to detect the *Vav1-Cre* transgene.

Imaging and Analysis

Embryos were dissected and imaged by light microscopy (Leica, DM IRB). ImageJ was used to calculate the surface area of photographed embryos.

Complete blood counts

Peripheral blood was collected into K2 EDTA-coated Microvette collection tubes (Sarstedt, 16.444.100). CBCs were performed with a HEMAVet950 (Drew Scientific, CT) at the University of Michigan In Vivo Animal Core.

CHAPTER III

A CRITICAL ANALYSIS OF THE ROLE OF SNARE PROTEIN SEC22B IN ANTIGEN CROSS-PRESENTATION

AUTHORS: S Julia Wu, Yashar S Niknafs, Stephanie H Kim, Katherine Oravecz-Wilson, Cynthia Zajac, Tomomi Toubai, Yaping Sun, Jayendra Prasad, Daniel Peltier, Hideaki Fujiwara, Israel Henig, Nathan D Mathewson, Rami Khoriaty, David Ginsburg, Pavan Reddy

ABSTRACT

Cross-presentation initiates immune responses against tumors and viral infections by presenting extracellular antigen on MHC I to activate $CD8^+$ T cell-mediated cytotoxicity. *In vitro* studies in dendritic cells (DCs) established SNARE protein SEC22B as a specific regulator of cross-presentation. However, the *in vivo* contribution of SEC22B to cross-presentation has not been tested. To address this, we generated DC-specific *Sec22b* knockout (*CD11c-Cre* $Sec22b^{fl/fl}$) mice. Contrary to paradigm, SEC22B-deficient DCs efficiently cross-present both *in vivo* and *in vitro*. Though *in vitro* shRNA-mediated *Sec22b* silencing in bone marrow-derived dendritic cells (BMDCs) reduced cross-presentation, treatment of SEC22B-deficient BMDCs with the same shRNA

produced a similar defect, suggesting the *Sec22b* shRNA modulates cross-presentation through off-target effects. RNAseq of *Sec22b* shRNA-treated SEC22B-deficient BMDCs demonstrated several changes in the transcriptome. Our data demonstrate, contrary to the accepted model, that SEC22B is not necessary for cross-presentation and caution against extrapolating phenotypes from knockdown studies alone.

INTRODUCTION

Antigen cross-presentation describes the process by which exogenous antigen is processed and presented on MHC I to $CD8^+$ T cells[92]. Cross-presentation drives antigen-specific cytotoxic $CD8^+$ T cell responses against tumors and viruses lacking tropism for hematopoietic cells. Of the known antigen presenting cells, dendritic cells (DCs) are the most efficient cross-presenters[92,185].

The process of cross-presentation involves key steps that include (a) uptake of extracellular antigen, (b) processing of the antigen into peptides that can be presented on MHC I and (c) peptide-loading onto MHC I followed by trafficking of the MHC I:peptide complex to the surface of the cell. Disrupting any of these steps can alter cross-presentation[92]. At the antigen uptake stage, manipulation of endo- and phagocytic receptors modulates cross-presentation[106,186,187]. Subsequent processing of internalized antigen is also highly regulated. For example, as endosomes and phagosomes mature, they acidify and proteolytic activity increases. Evidence suggests that delaying maturation and maintaining an elevated pH, a process mediated in part by NOX2 activity, regulated by Rac2[81,188] and Siglec-G-mediated signaling[126], promotes cross-presentation. The immunoproteasome has also been implicated at the antigen processing stage of cross-presentation[189]. Additionally, loss of ERAP1, involved in the final peptide processing steps for loading onto MHC I, has been shown to be necessary for cross-presentation of cell-associated antigen and immune-complexed antigen[190]. Finally, because cross-presenting MHC I may derive from

the endoplasmic reticulum (ER) or from the cell surface through the endocytic recycling compartment[191], trafficking of MHC I can impact cross-presentation efficiency as well[151].

Notably, the events necessary for cross-presentation require resources from a wide array of cell compartments. Thus, to unify these distinct cell biological observations into a centralized antigen cross-presentation pathway, much attention has been given to intracellular trafficking pathways. SNARE proteins, which mediate vesicle fusion events, are essential for nearly all intracellular trafficking pathways[176]. Recently, the ER-SNARE protein SEC22B was identified as a key mediator of cross-presentation[5]. SEC22B localizes to the ER-Golgi intermediate compartment (ERGIC)[5,177] and interacts with plasma membrane-SNARE syntaxin 4 and Golgi-SNARE syntaxin 5[5]. Cebrian *et al* and others used an *in vitro* shRNA-mediated knockdown (KD) approach to reduce *Sec22b* expression in DCs, which resulted in increased access of antigen to the cytosol, delayed phagosomal maturation, increased access of ER-associated proteins to the phagosome, and ultimately reduced cross-presentation without affecting conventional antigen presentation pathways[5,151]. While its central regulatory role has been incorporated into the current model of cytosolic cross-presentation[28,91,92,186,187,191-196], whether SEC22B is critical for antigen cross-presentation *in vivo* remains unknown.

Because DCs are the most efficient cross-presenting cells *in vivo*, we generated a DC-specific *Sec22b* knockout mouse (*CD11c-Cre Sec22b*$^{fl/fl}$) to address this outstanding question. Based on our understanding of SEC22B's function in DCs *in vitro*, we hypothesized SEC22B would be critical for cross-presentation *in vivo*. In contrast to the above reports, SEC22B did not regulate cross-presentation *in vivo*. Furthermore, analysis of *Sec22b*$^{-/-}$ DCs *in vitro* demonstrated no defect in cross-presentation across varying antigenic sources and lengths of incubation. However, treatment of *Sec22b*$^{-/-}$ BMDCs with the previously reported *Sec22b*-targeting shRNA recapitulated the cross-presentation defect. Furthermore, RNAseq analysis identified a reduction in mRNA transcripts for many off-target genes, demonstrating that the effect of KD on cross-presentation is independent of SEC22B. Taken together, our data demonstrate that, contrary to the current paradigm, SEC22B is not required for cross-presentation either *in vivo* or *in vitro*.

RESULTS

DC-specific *Sec22b* knockout mice demonstrate normal immune cell composition and DC functions

We generated DC-specific *Sec22b* knockout mice by first breeding *Sec22b* gene-trapped mice (*Sec22b*^{cgt}) to *FLP* recombinase expressing mice to create *Sec22b*$^{fl/fl}$ mice (Figure 3.1A). *Sec22b*$^{fl/fl}$ (FL) mice were then bred to *CD11c-Cre* (*Itgax-Cre*) mice to generate *CD11c-Cre Sec22b*$^{fl/fl}$ (KO) mice where exon 3 of *Sec22b* is deleted specifically in CD11c-expressing DCs (Figure 3.1A). This excision event was confirmed by PCR (Figure 3.1B, C) using genomic DNA from MACS-enriched CD11c^{+} BMDCs (Figure 3.2A) and FACS-enriched CD11c^{+} CD8^{+} and CD8^{-} splenic DCs (Figure 3.2B). Splenic DCs from *CD11c-Cre Sec22b*$^{fl/fl}$ mice exhibited virtually complete *Sec22b* knockout (Figure 3.1B, C) and a majority of BMDCs from these mice had also undergone Cre-mediated excision at exon 3 (Figure 3.1B, C). Loss of *Sec22b* expression was confirmed by qRT-PCR (Figure 3.1D) and Western Blot (Figure 3.1E, F) analysis with marked reduction of *Sec22b* in CD11c^{+} BMDCs (Figure 3.1D, E, F) and splenic DCs (Figure 3.1E, F).

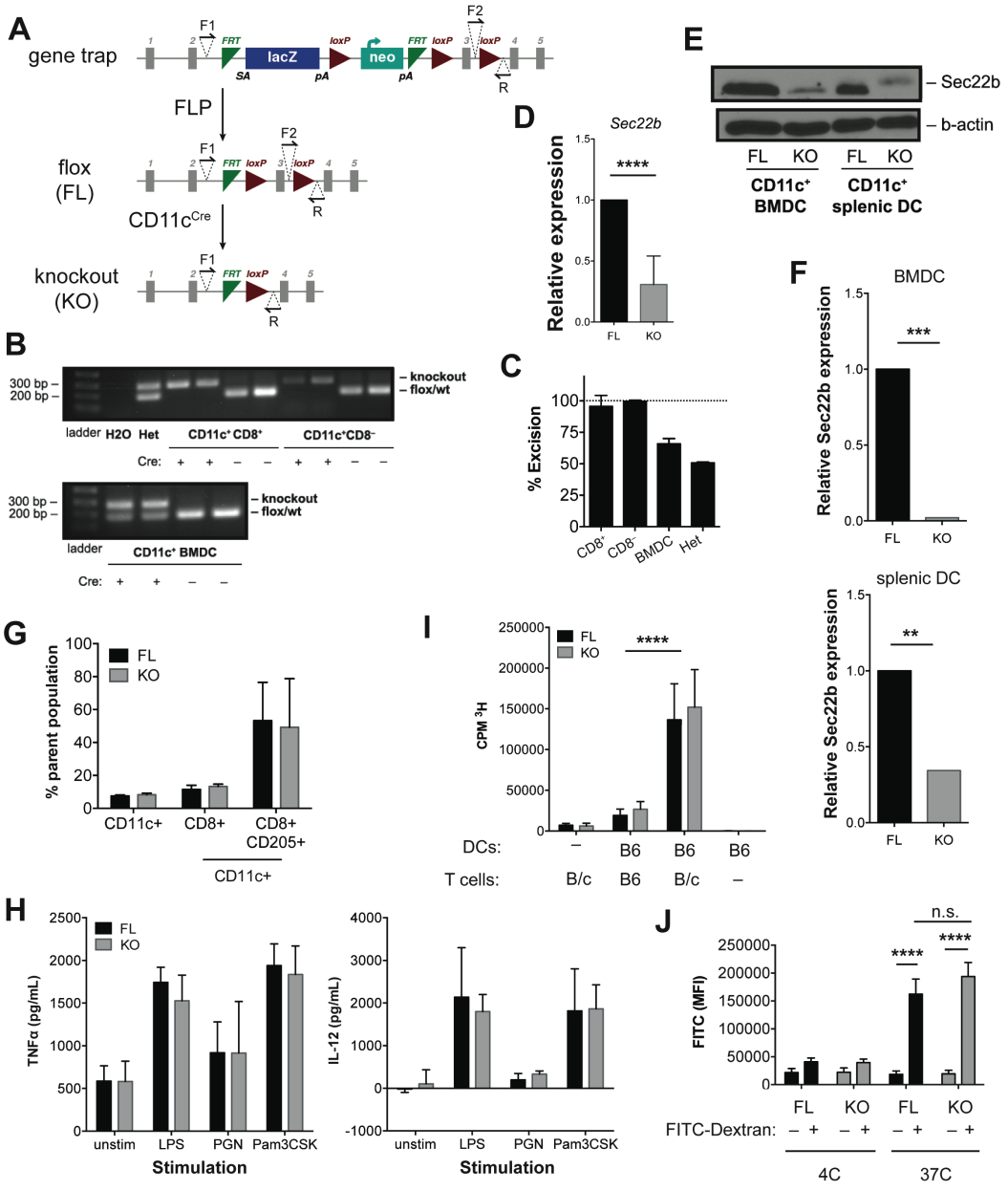

Figure 3.1. Generation and characterization of a DC-specific SEC22B knockout mouse. (A) DC-specific *Sec22b* knockout (KO) mice were bred from gene-trapped founders using FLP recombinase and *CD11c-Cre* transgenic mice. Half-arrowheads indicate binding sites for forward (F1, F2) and reverse (R) primers used for **(B)** PCR to measure excision of exon 3 in FACS-enriched CD11c^{+} CD8^{+} and CD8^{-} splenic DCs and MACS-enriched CD11c^{+} BMDCs, comparing *CD11c-Cre* (+) to *CD11c-wt* (–) populations. A *Sec22b*$^{+/-}$ mouse was used a heterozygous (het) control for 50% excision. **(C)** Quantification of *Sec22b* exon 3 excision rates in *CD11c-Cre* cell populations. **(D)** qRT-PCR (mean±SEM, *n*=11) measures *Sec22b* transcript levels in MACS-enriched CD11c^{+} BMDCs and **(E)** Western Blot measures SEC22B protein expression in MACS-enriched

CD11c^{+} BMDCs and splenic DCs from *CD11c-Cre Sec22*$^{fl/fl}$ mice (KO) compared to *CD11c-wt Sec22b*$^{fl/fl}$ mice (FL). **(F)** Bar graph quantifies SEC22B protein expression. **(G)** *Ex vivo* flow cytometric immunophenotyping of splenic DC populations plotted as mean proportion of singlets or indicated parent population±SD (*n*=3). See related data in Figure 3.3. **(H)** TNFα and IL-12 production by BMDCs stimulated overnight with TLR ligands lipopolysaccharide (LPS, 500 ng/mL), peptidoglycan (PGN, 5 ug/mL), and Pam3CSK (300 ng/mL) as measured by ELISA and plotted as mean±SEM (*n*=3). **(I)** Balb/c (B/c) and C57BL/6 (B6) CD90.2^{+} T cell ^{3}H-thymidine uptake plotted as mean±SD of triplicate repeats after 4 day stimulation by MACS-sorted CD11c^{+} splenic DCs from C57BL/6 KO and FL mice, at 40:1 T cell:DC cell ratios. Data is representative of 3 total experiments. **(J)** BMDCs were incubated with FITC-Dextran or 1xPBS vehicle for 30 min at 4C or 37C. Uptake was analyzed by flow cytometry and plotted as mean±SEM (*n*=4). n.s.= not significant, $^{**}p\leq0.01$, $^{***}p\leq0.001$, $^{****}p\leq0.0001$. Purity information on sorted DCs can be found in Figure 3.2.

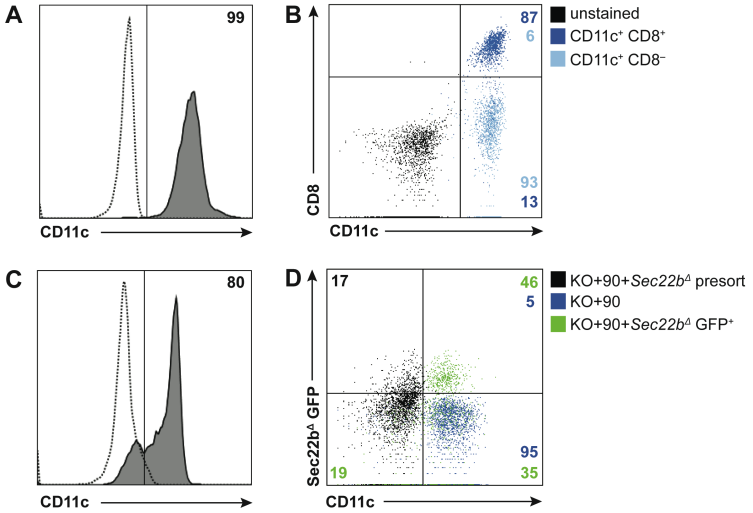

Figure 3.2. Purity of DCs used in assays.
(A) Representative histogram of MACS enrichment of CD11c^{+} BMDCs for experiments in Figure 3.1B-F, H, J; Figure 3.5C-E; and Figure 3.6, 3.7. **(B)** Dot plot representing enrichment of CD11c^{+} CD8^{+} and CD11c^{+} CD8^{-} splenic DCs after FACS for experiments in Figure 3.1B, C. **(C)** Representative histogram of MACS enrichment of CD11c^{+} splenic DCs for experiments in Figure 3.1E, F, I; Figure 3.5A, B. **(D)** Dot plot representing enrichment of CD11c^{+} KO BMDCs after *Sec22b* knockdown (KO+90) and rescue with *Sec22b*$^{\Delta}$ transgene (KO+90+*Sec22b*$^{\Delta}$), as reported by GFP expression, by FACS for crosspresentation assay in Figure 3.10H.

Next, we assessed the impact of SEC22B-deficiency in CD11c^{+} cells on DC development, phenotype, and the development of other immune cells. We immunophenotyped *CD11c-Cre Sec22b$^{fl/fl}$* mice and observed normal development of DC and myeloid cell populations (Figure 3.1G, 3.3A), T cell populations (Figure 3.3B), thymocyte differentiation (Figure 3.3C), T cell activation state (Figure 3.3D), and other lymphoid populations (Figure 3.3E).

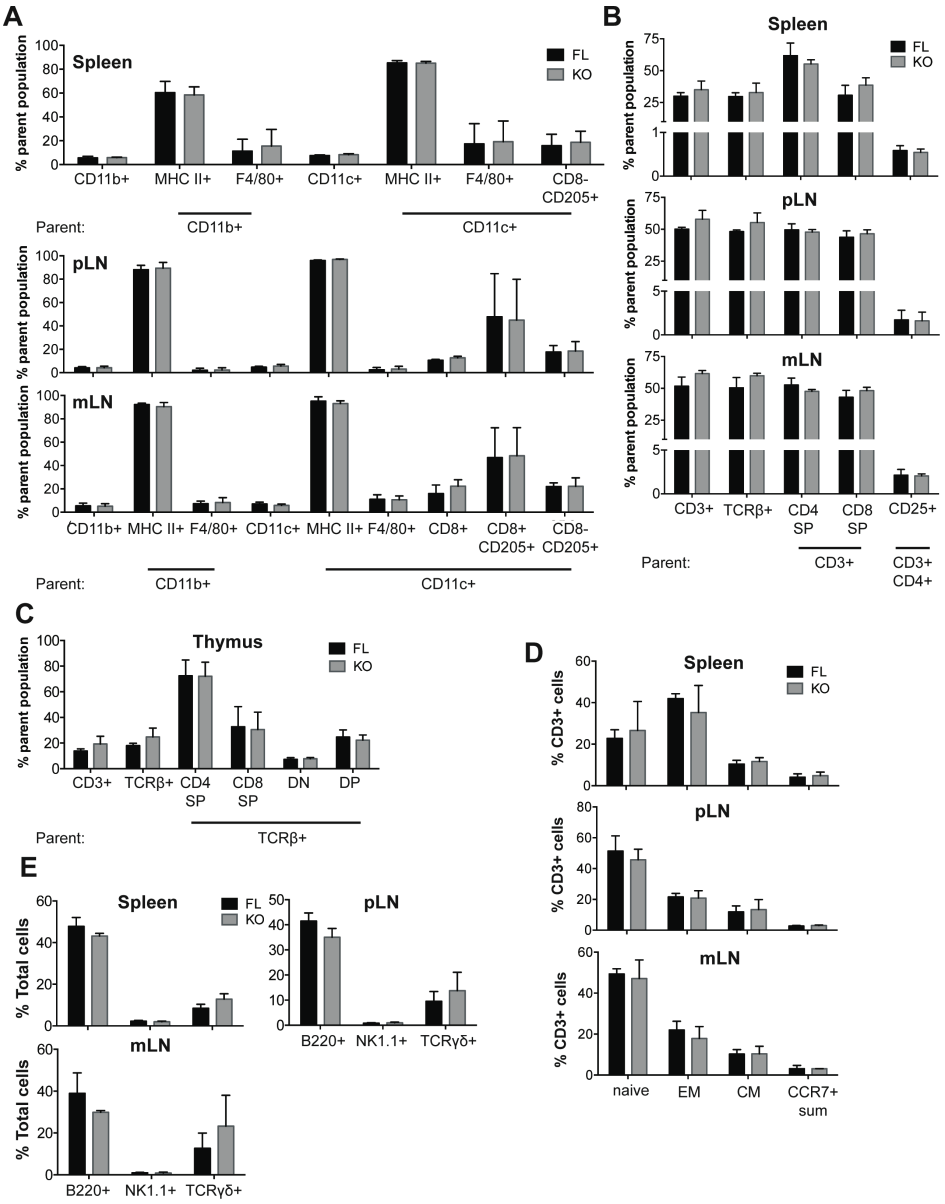

Figure 3.3. Myeloid cell populations and lymphocyte development remain unchanged in *CD11c-Cre Sec22b$^{fl/fl}$* mice. (A) CD11b^{+} and CD11c^{+} myeloid cells, along with MHC II^{+}, F4/80^{+}, CD8^{+}, and CD205^{+} subpopulations, plotted as mean proportion of total singlets or indicated parent populations, in spleen, peripheral lymph nodes (pLN), and mesenteric lymph nodes (mLN). Plotted as mean±SD (*n*=3). **(B)** CD3^{+} and TCRβ^{+} T cell populations along with CD4 SP (CD4^{+} CD8^{-}), CD8 SP (CD4^{-} CD8^{+}), and CD25^{+} subpopulations, measured as proportion of total singlets or indicated parent populations, in spleen, pLN, and mLN±SD (*n*=3). **(C)** CD3^{+} and TCRβ^{+} thymocyte populations and CD4 SP, CD8 SP, DN (CD4^{-} CD8^{-}), and DP (CD4^{+} CD8^{+}) subpopulations, plotted as mean proportion of singlets or indicated parent population±SD (*n*=3). **(D)** CCR7 expression on CD3^{+} cells measured along with CD62L and CD44 expression on CD3^{+} cells to characterize naïve (CD62L^{+} CD44^{-}), effector memory cells (EM, CD62L^{-} CD44^{+}), central memory (CM, CD62L^{+} CD44^{+}) from spleen, pLN, and mLN. Plotted as mean±SD (*n*=3). **(E)** B220^{+}, NK1.1^{+}, and TCRγδ^{+} cells measured as proportion of total singlets from spleen, pLN, and mLN. Plotted as mean±SD (*n*=3).

We then determined whether absence of SEC22B affects DC functions. We first tested *Sec22b*$^{-/-}$ BMDC responses to innate immune stimuli by overnight culture of MACS-enriched CD11c^{+} BMDCs (Figure 3.2A) with TLR 1/2, 2, and 4 ligands Pam3CSK, peptidoglycan, and LPS, respectively. Supernatants were tested by ELISA for production of TNFα and IL-12, which did not differ between *CD11c-Cre Sec22b$^{fl/fl}$* and *CD11c-WT Sec22b$^{fl/fl}$* samples (Figure 3.1H). To determine direct antigen presentation capability, we assessed MHC surface expression on MACS-enriched CD11c^{+} splenic DCs (Figure 3.2C) from *CD11c-Cre Sec22b$^{fl/fl}$* or *CD11c-WT Sec22b$^{fl/fl}$* animals, using them as stimulators in an allogeneic mixed lymphocyte reaction. After 4 days of incubation, allogeneic BALB/c T cell proliferation was measured by ^{3}H-thymidine uptake and found to be similar between stimulation groups (Figure 3.1I). Finally, we tested the impact of SEC22B on antigen uptake. We incubated MACS-enriched CD11c^{+} *Sec22b*$^{-/-}$

BMDCs (Figure 3.2A) with FITC-dextran for 30 minutes at either 4°C or 37°C. BMDCs that had taken up antigen ($CD11c^+$ $FITC^+$ cells) were identified by flow cytometry. We observed no dependence on SEC22B expression for antigen uptake (Figure 3.1J). Taken together, these data suggest SEC22B is dispensable for DC development, cytokine response to TLR stimulation, direct antigen presentation, and endocytic antigen uptake.

Cross-presentation *in vivo* does not rely on SEC22B expression in dendritic cells

We next analyzed whether SEC22B expression in DCs is required for *in vivo* cross-presentation. In light of previous data[5,151], we hypothesized that the absence of SEC22B would reduce cross-presentation. We performed an *in vivo* cross-presentation assay as described previously[197]. Briefly, we intraperitoneally (i.p.) injected ovalbumin (OVA) antigen or bovine serum albumin (BSA), then adoptively transferred CFSE-stained OT-I T cells. After 7 days, spleen, mesenteric lymph nodes (mLN), and the superficial inguinal lymph nodes from the side ipsilateral to antigen administration (siLN) were harvested and analyzed by flow cytometry for proliferation of SIINFEKL ($OVA_{257-264}$)-restricted $CD8^+$ T cells (OT-I T cells) (Figure 3.4A, B). Surprisingly, animals lacking SEC22B in $CD11c^+$ cells induced robust proliferation of OT-I T cells (Figure 3.4B, C). Indeed, comparing *CD11c-Cre Sec22b*$^{fl/fl}$ or *CD11c-WT Sec22b*$^{fl/fl}$ mice, we observed no differences in the proliferation of OVA-specific T cells. These data

demonstrate that SEC22B is not required for *in vivo* cross-presentation of soluble antigens.

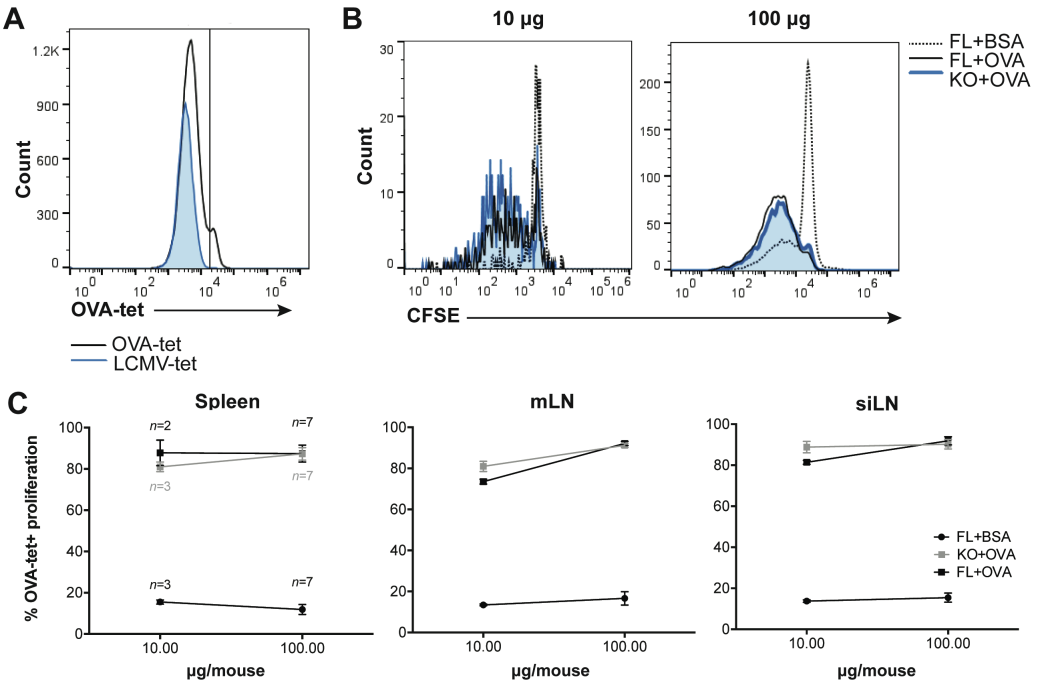

Figure 3.4. DC-specific SEC22B knockout mice efficiently cross-present antigen *in vivo*. OVA or BSA was delivered *i.p.* and CFSE-stained OT-I T cells (10^6/mouse) were delivered *i.v.* to FL or KO mice on day 0. On day 7, mice were euthanized and spleen (spl), mesenteric LN (mLN), and superficial inguinal lymph nodes ipsilateral to injection site (siLN) were harvested and flow stained to identify proliferating antigen-specific T cells. **(A)** Representative histogram demonstrating OVA tetramer (OVA-tet; H2-K^b bound to SIINFEKL ($OVA_{257-264}$) peptide) identification of SIINFEKL-restricted $CD3^+$ $CD8^+$ T cells. LCMV tetramer (LCMV-tet; H2-K^b bound to gp_{34-43}) used to control for nonspecific binding. **(B)** Representative histograms plotting $CFSE^-$ fraction of OVA-tet^+ cells from spleens of FL or KO mice given either 10 or 100 µg OVA or BSA per mouse. **(C)** Line graphs quantify $CFSE^-$ OVA-tet^+ cells as mean±SD.

SEC22B is not necessary for cross-presentation of soluble or particulate antigen *in vitro*

Because our *in vivo* results appeared to contradict previous observations on the role of SEC22B in cross-presentation[5,151], we wanted to test the possibility that SEC22B regulation of cross-presentation may only be germane to *in vitro* studies. To do this, we used MACS-enriched $CD11c^+$ splenic DCs (Figure 3.2C) to cross-present soluble OVA to OT-I T cells under the same conditions used in the cited reports. However, *Sec22b*$^{-/-}$ splenic DCs induced similar OT-I T cell proliferation and expression of activation markers as compared to control DCs (Figure 3.5A, B). The use of the SIINFEKL control peptide, which can be presented by the MHC I molecule H2-K^b without further processing, verified that MHC I expression on the BMDCs was not perturbed (Figure 3.5A, B). Similar results were obtained with MACS-enriched $CD11c^+$ *Sec22b*$^{-/-}$ BMDCs (Figure 3.2A), demonstrating that SEC22B does not have a unique regulatory function in BMDCs compared to splenic DCs (Figure 3.5C, Figure 3.6).

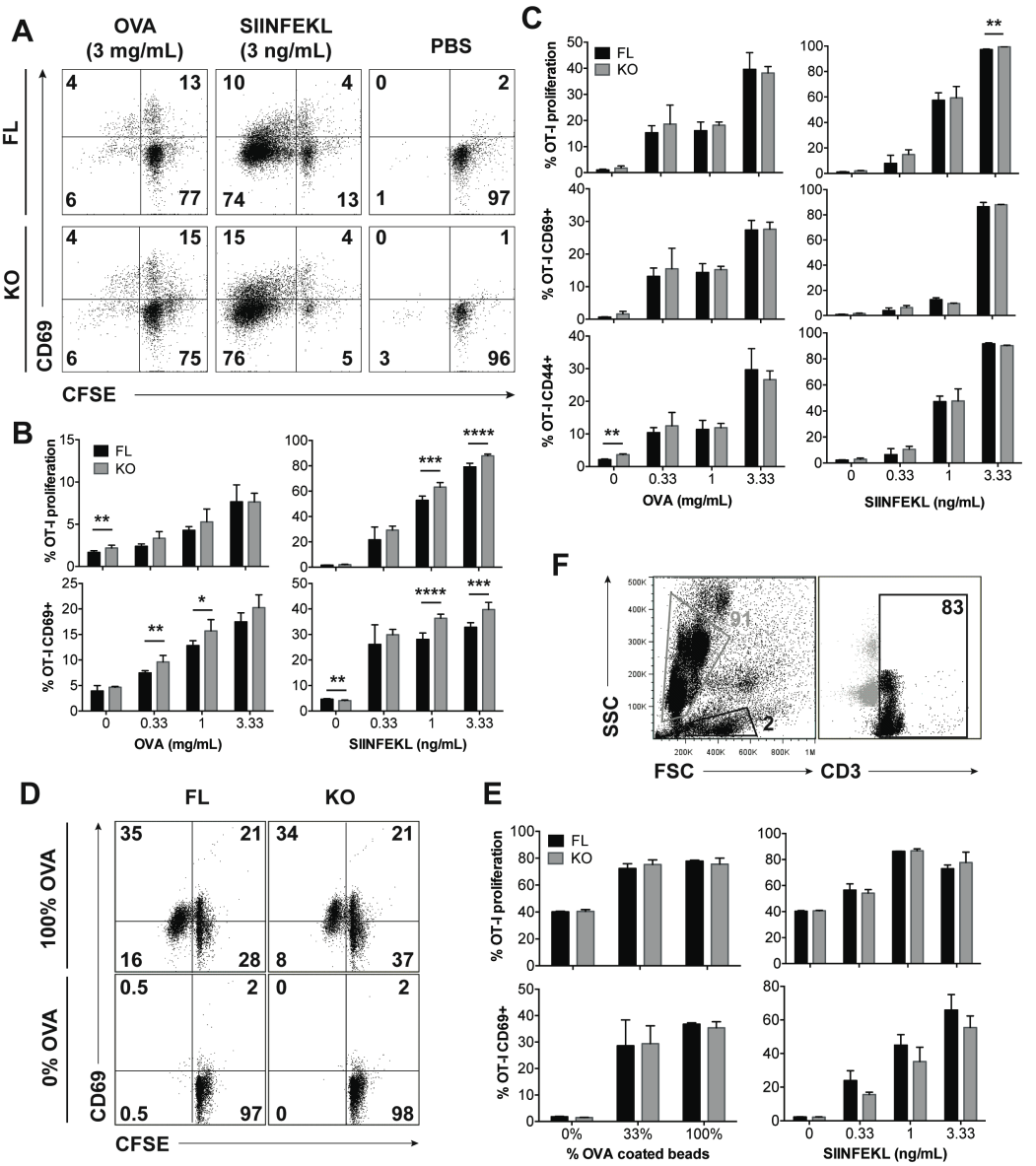

Figure 3.5. *Sec22b*$^{-/-}$ DCs show no *in vitro* defect in cross-presentation of soluble or particulate antigen. (A, B) CD11c^{+} splenic DCs or **(C)** CD11c^{+} BMDCs loaded with OVA or SIINFEKL peptide were washed, fixed, and cultured with CFSE-stained OT-I T cells. After 3 days, OT-I T cells were harvested and analyzed as shown in the **(A)** representative dot plots. Bar graphs quantify mean±SD **(B, C)** CFSE^{-}, CD69^{+} and **(C)** CD44^{+} populations from triplicate repeats. Panel **(B)** presents data representative of 4 experiments and panel **(C)** presents data representative of 7 experiments. **(D)** CD11c^{+} BMDCs incubated with latex beads coated with varying proportions of OVA to BSA (0% OVA/100% BSA, 33% OVA/66% BSA, or 100% OVA/0% BSA) were washed, fixed, and cultured with CFSE-stained OT-I T cells. After 3 days, OT-I T cells were harvested and analyzed for proliferation and CD69

expression as shown in the representative dot plots. **(E)** Bar graphs quantify mean±SD $CFSE^{-}$ and $CD69^{+}$ populations from triplicate repeats from a representative experiment out of 3. **(F)** Beads were excluded from analysis by size and CD3 expression. *$p \leq 0.05$, **$p \leq 0.01$, ***$p \leq 0.001$, ****$p \leq 0.0001$. Purity information on sorted DCs can be found in Figure 3.2. Related experiments can be found in Figures 3.6 and 3.7.

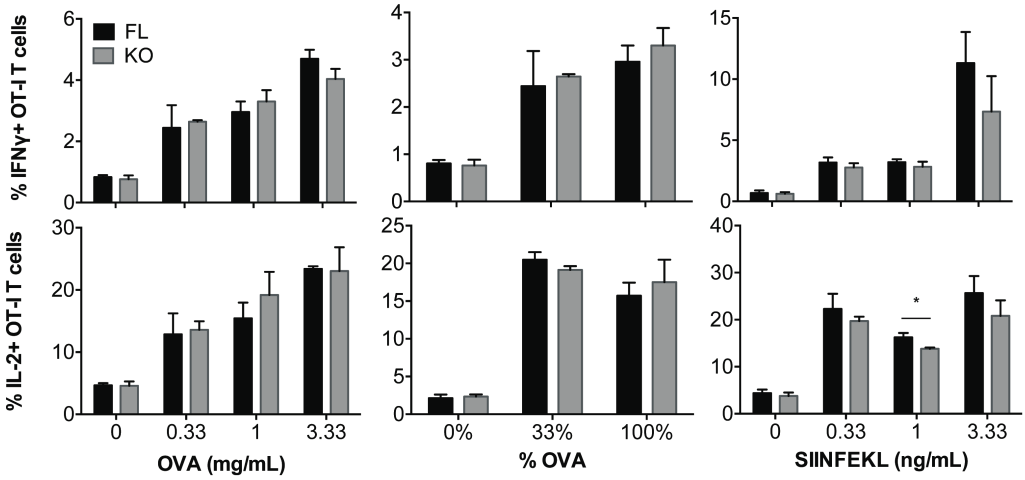

Figure 3.6. *Sec22b*$^{-/-}$ DCs demonstrate no defect in induction of antigen-specific T cell cytokine production. $CD11c^{+}$ FL and KO BMDCs loaded with soluble or particulate OVA were washed, fixed, and cultured with CFSE-stained OT-I T cells. After 3 days, OT-I T cells were stimulated with PMA/ionomycin and IFNγ and IL-2 production were measured by intracellular staining. Bar graphs quantify mean±SD $IFN\gamma^{+}$ and $IL\text{-}2^{+}$ populations from triplicate repeats from a representative experiment out of 2. *$p \leq 0.05$.

To confirm that antigen type is not a critical determinant for SEC22B regulation of cross-presentation in DCs, we analyzed the ability of *Sec22b*$^{-/-}$ BMDCs to cross-present particulate antigen. Using OVA-coated latex beads, we found cross-presentation of particulate antigen to be independent of SEC22B expression (Figure 3.5D, E, 3.6). Beads were efficiently excluded by their scatter plot distribution (Figure 3.5F) and thus did not confound analysis. We excluded the possibility that OVA source or endotoxin contamination was confounding our

data by testing *Sec22b*$^{-/-}$ BMDCs with endotoxin-free OVA from a different supplier, which failed to produce a cross-presentation defect (Figure 3.7). We therefore conclude that SEC22B is not required for cross-presentation of soluble or particulate antigen.

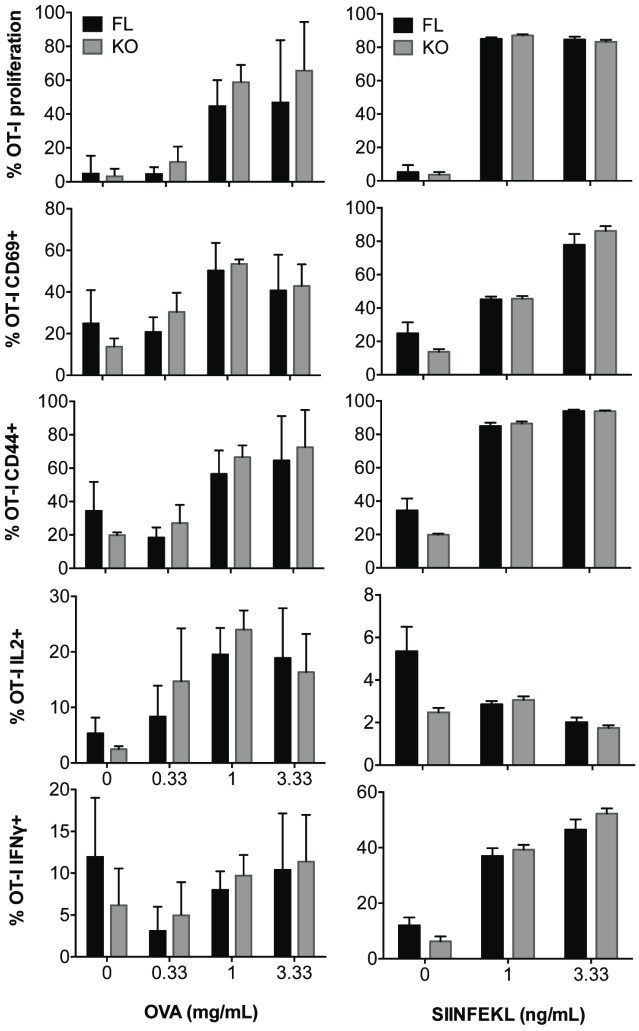

Figure 3.7. OVA source does not mask cross-presentation defect in *Sec22b*$^{-/-}$ BMDCs. MACS-enriched CD11c^{+} *Sec22b* FL and KO BMDCs incubated overnight with soluble endotoxin-free OVA from Worthington Bio-chemical Corporation (LS003059) were washed, fixed, and cultured with CFSE-stained OT-I T cells. After 3 days, OT-I T cells were harvested and stained for flow cytometric analysis. For intracellular staining, cells were stimulated with PMA/ionomycin for the final 5 hours of culture. Bar graphs quantify mean±SEM populations from two experiments, each performed in triplicate.

shRNA-mediated knockdown of *Sec22b* reduces cross-presentation in BMDCs

SEC22B was previously identified as a cross-presentation mediator using shRNA to silence its expression in BMDCs[5,151]. Our discrepant observations might then be secondary to methodology, i.e. potential differences between a genetic knockout approach versus a molecular silencing approach. To corroborate this, we obtained a previously validated shRNA sequence [5], shRNA 90, to silence *Sec22b in vitro* in BMDCs generated from C57/BL6 (WT) mice (Figure 3.8A). Using previously reported conditions[5,151], we administered soluble OVA to shRNA-treated BMDCs and measured cross-presentation with CFSE-stained OT-I T cells. Consistent with previous observations[5,151], we observed that *Sec22b* KD BMDCs showed reduced cross-presentation of OVA when compared with BMDCs treated with an empty vector (EV) control (Figure 3.8B, C). Thus, shRNA-mediated KD of Sec22b reduces cross-presentation, as previously demonstrated[5,151].

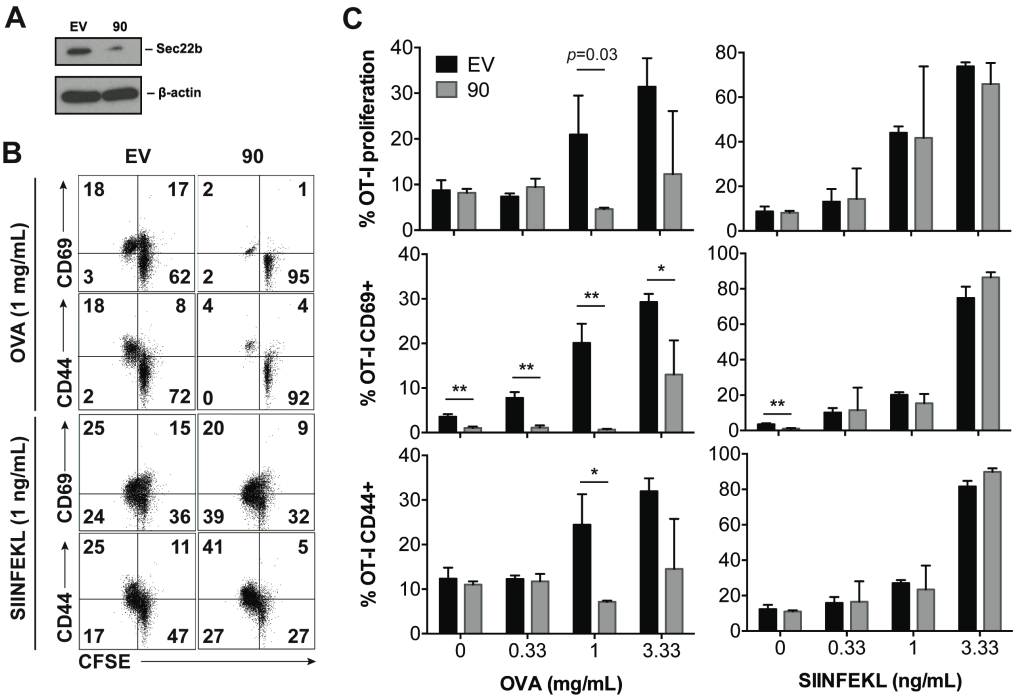

Figure 3.8. Cross-presentation by BMDCs reduced by *Sec22b* knockdown. (A) Western Blot evaluating reduction in SEC22B expression in C57/BL6 BMDCs after treatment with Sec22b-specific shRNA 90 as compared to empty vector (EV)-treated controls. **(B)** Representative dot plots of CFSE intensity and CD69 and CD44 expression from OT-I T cells after 3 days of co-culture with fixed BMDCs preincubated with OVA or $OVA_{257-264}$ control peptide (SIINFEKL). **(C)** Bar graphs quantify mean±SD of $CFSE^{-}$, $CD69^{+}$, and $CD44^{+}$ populations from triplicate repeats. Data is representative of 3 total experiments. *$p \leq 0.05$, **$p \leq 0.01$.

Sec22b-targeting shRNAs 89 and 90 mediate cross-presentation through effects on off-target genes

Collectively, our observations demonstrate when *Sec22b* is knocked out, it is not necessary for cross-presentation (Figures 3.4B, C, 3.5, 3.6, 3,7), but when knocked down in BMDCs, it seems to be essential[5,151] (Figure 3.8B, C).

To resolve the discrepancy between the knockout and KD results, we systematically analyzed three potentially mutually exclusive hypotheses: (1) there is compensation by other *Sec22* paralogs for the loss of SEC22B only in the total absence of *Sec22b* (in *CD11c-Cre Sec22b*$^{fl/fl}$ mice or *Sec22b*$^{-/-}$ DCs), but not in an acute deficiency state (in *Sec22b* KD BMDCs), a confounding possibility observed in another model system[198]; (2) viral stimulation and silenced *Sec22b* expression together reduce cross-presentation, suggesting that viral infection might have uniquely induced predominant use of a SEC22B-dependent cross-presentation system; or (3) the observed effects of the shRNA on cross-presentation may be a consequence of off-target effects of the shRNA.

In mammals, there are two *Sec22b* paralogs, *Sec22a* and *Sec22c*[177]. While little is known about the functions of SEC22A and C, they have been shown to localize to the ER[26,177], and so might plausibly compensate for loss of SEC22B. To test this, we quantified *Sec22a* and *Sec22c* transcripts in MACS-enriched CD11c^{+} *Sec22b*$^{-/-}$ and *Sec22b*$^{fl/fl}$ BMDCs. If SEC22A and/or SEC22C were functionally compensating for loss of SEC22B, we hypothesized we would see an increase in expression of these genes in *Sec22b*$^{-/-}$ DCs. Using qRT-PCR, we observed no difference in the level of *Sec22a* or *Sec22c* expression relative to housekeeping gene *Gapdh* in *Sec22b*$^{-/-}$ BMDCs compared to *Sec22b*$^{fl/fl}$ controls (Figure 3.9). These data suggest that the absence of a cross-presentation defect in *Sec22b*$^{-/-}$ DCs is not likely due to compensation by paralogs.

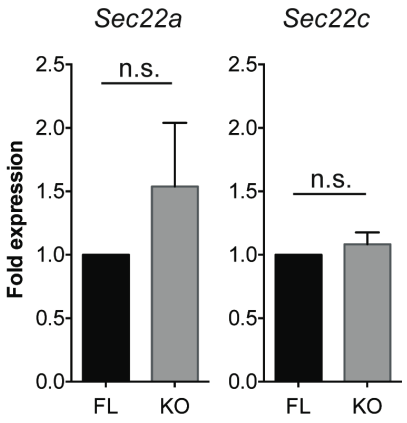

Figure 3.9. *Sec22a* and *Sec22c* expression are unchanged in *Sec22b*$^{-/-}$ BMDCs, Related to Figure 3.8. qRT-PCR was preformed on cDNA from CD11c^{+} FL and KO BMDCs to measure *Sec22a* and *Sec22c* transcript levels relative to *Gapdh*, plotted as mean±SEM (*n*=11). *n.s.*= not significant.

Next, to clearly distinguish between the remaining two possibilities, we performed the following experiment. We transduced *Sec22b*$^{-/-}$ and *Sec22b*$^{fl/fl}$ BMDCs with shRNA 90 or EV control (Figure 3.10A, B). After each BMDC group was incubated with soluble OVA, washed, fixed, and cultured with CFSE-stained OT-I T cells, we observed deficient cross-presentation in all groups treated with shRNA 90, independent of *Sec22b* genotype (Figure 3.10C). These data suggested that shRNA 90 mediates its effects on cross-presentation not through its activity on *Sec22b* but through off-target effects (hypothesis 3). Additionally, these data further invalidate the idea that there may be functional compensation for the loss of SEC22B (hypothesis 1), because, were that the case, cross-presentation would have been reduced only in the shRNA 90-treated *Sec22b*$^{fl/fl}$ BMDC (FL+90) condition. Furthermore, this data also invalidates the hypothesis that viral stimulation uniquely activates a Sec22b-dependent cross-presentation pathway (hypothesis 2). Such a phenomenon would have resulted in reduced cross-presentation in all conditions where there

was loss of Sec22b expression (FL+90, KO+EV, KO+90). Collectively, these data strongly suggest that shRNA 90 reduces cross-presentation in BMDCs through its off-target effects.

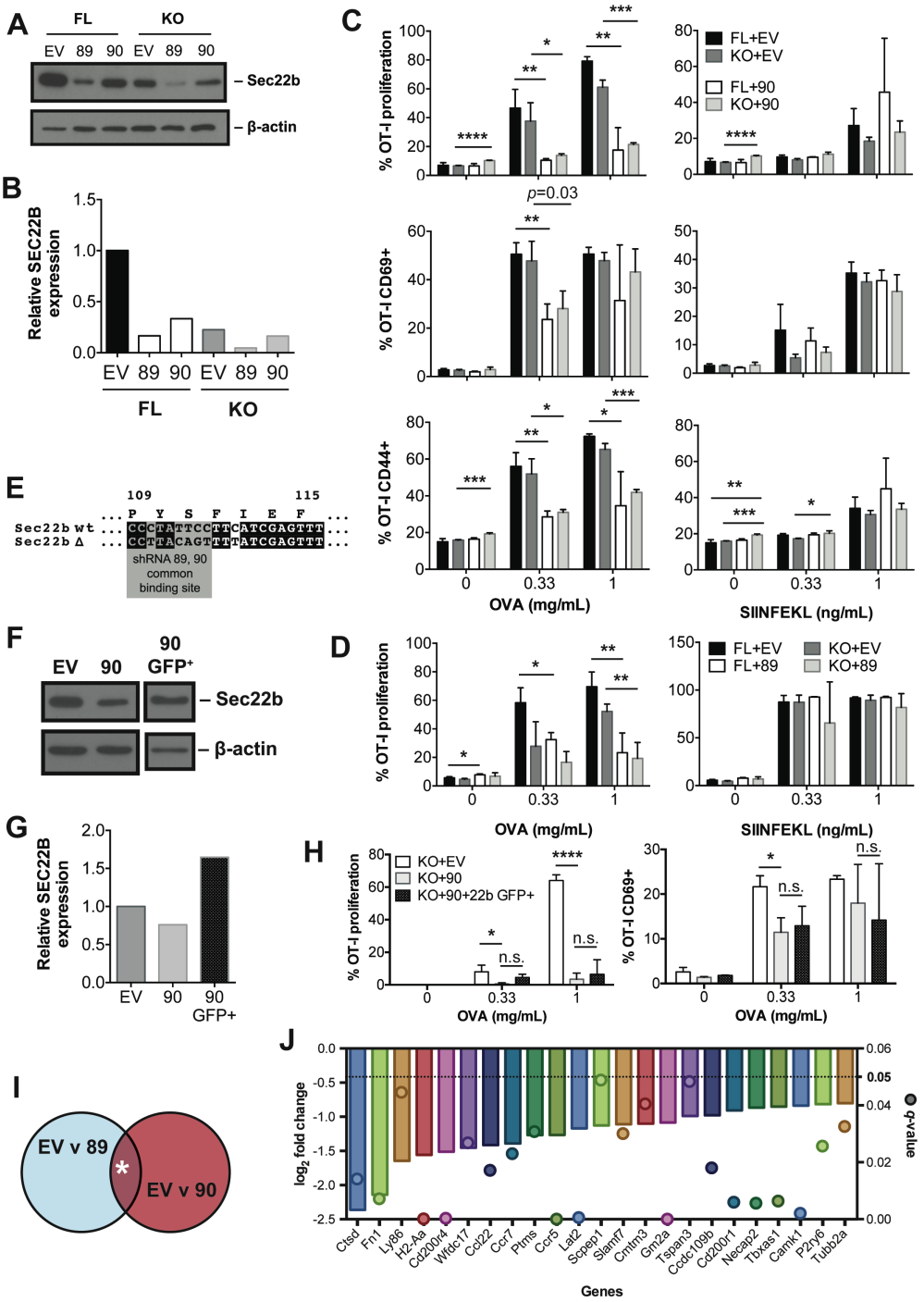

Figure 3.10. *Sec22b*-targeting shRNA treatment induces cross-presentation defect in KO BMDCs. (A) Western Blot and **(B)** quantification measuring SEC22B expression in FL and KO BMDCs treated with either shRNA 89, 90 or EV. After loading with OVA or SIINFEKL peptide, these BMDCs were washed, fixed, and cultured with CFSE-stained OT-I T cells. After 3 days, T cells were harvested and analyzed for **(C, D)** proliferation and **(C)** expression of CD69 and CD44, quantified in the bar graphs as mean±SD. Panel **(C)** is representative of 3 experiments; panel **(D)** is representative of 2 experiments. Data is plotted as mean±SD of triplicate repeats. **(E)** Sequence alignment of $Sec22b^{\Delta}$ transgene to $Sec22b^{wt}$ gene, with amino acid sequence indicated above the corresponding codons and the common binding site for shRNA 89 and 90 highlighted in gray. **(F)** Western Blot and **(G)** quantification evaluating SEC22B expression in FACS sorted $CD11c^{+}$ KO BMDCs after treatment with EV control, shRNA 90, or 90 and $Sec22b^{\Delta}$ transgene (GFP^{+}). **(H)** KO BMDCs treated with EV, 90, or 90 and $Sec22b^{\Delta}$ transgene were incubated with OVA peptide overnight, washed, fixed, and cultured with CFSE-stained OT-I T cells. After 3 days, T cells were harvested and analyzed for proliferation and CD69 expression. Data is plotted as mean±SD of triplicate repeats and is representative of 1 experiment **(I)** Ribosomal RNA-depleted RNA from KO BMDCs treated with EV, shRNA 89, or shRNA 90 were sequenced. Highly expressed transcripts, that showed statistically significant downregulation in both shRNA-treatment groups compared to EV groups (*) are **(J)** plotted, with bars representing $\log_2$-fold change compared to EV treatment and dots plotting the associated *q*-values (n=2). n.s.= not significant, *$p \leq 0.05$, **$p \leq 0.01$, ***$p \leq 0.001$, ****$p \leq 0.0001$. Purity information on DC sorting can be found in Figure S1.

Although our data demonstrate shRNA 90 alters cross-presentation through secondary effects on non-*Sec22b* genes, others have published observations on SEC22B and cross-presentation using a different shRNA sequence, shRNA 89[151]. Examining shRNAs 89 and 90, we noted an 8 nucleotide overlap in the gene-targeting regions of both shRNAs (5'-CCCTATTC-3'). In fact, these two shRNA sequences target the same segment of *Sec22b* exon 3. We wondered if shRNA 89 also mediates its effects on cross-presentation by silencing off-target

genes. To address this, we treated *Sec22b*$^{-/-}$ BMDCs with shRNA 89 (Figure 3.10A, B) and again observed a reduction in cross-presentation (Figure 3.10D), similar to shRNA 90.

Based on these data, we reasoned that the cross-presentation defect previously attributed to *Sec22b* silencing by shRNA-mediated knockdown (KD) was likely due to silencing of at least one off-target gene by shRNA 89 and 90. To test this, we rescued SEC22B expression in *Sec22b*$^{-/-}$ BMDCs treated with shRNA 90 using an overexpression vector to express a *Sec22b* transgene with silent mutations at the shRNA 89 and 90 binding site (*Sec22b*$^{\Delta}$) (Figure 3.10E-G). Viable, CD11c^{+} GFP+ cells (*Sec22b*$^{\Delta}$-expressing, shRNA 90-transduced, BMDCs) were enriched by FACS (Figure 3.2D). The rescue of SEC22B expression by *Sec22b*$^{\Delta}$ had no effect on cross-presentation (Figure 3.10H). This further demonstrates cross-presentation is independent of SEC22B and that the impact of shRNA 89 and 90 treatment on cross-presentation is mediated through off-target effects.

To formally test for evidence of off-target effects on gene expression, we used RNAseq to determine whether the utilization of these shRNAs altered RNA transcript levels of genes other than *Sec22b*. We assessed differential gene expression in *Sec22b*$^{-/-}$ BMDCs in response to shRNA 89 and 90 treatment compared to EV treatment (Figure 3.10I). We identified over 20 genes that were highly expressed in EV controls but whose expression was significantly

downregulated (q-value<0.05) under both shRNA 89 and 90 treatment conditions (Figure 3.10J). Taken together, these data confirm that shRNA 89 and 90 target an overlapping set of off-target genes and suggest these off-target effects reduce cross-presentation by BMDCs.

DISCUSSION

Part of the current cross-presentation paradigm includes a critical regulatory role for SEC22B[28,91,92,186,187,191-196]. However, this understanding was based primarily on *in vitro* studies[5,151] and had never been confirmed *in vivo*. Thus, we began this study seeking to answer this outstanding question: does SEC22B play a crucial role in cross-presentation *in vivo*? Utilizing a *CD11c-Cre Sec22b*$^{fl/fl}$ mouse to specifically delete *Sec22b* in DCs, we discovered that SEC22B is dispensable for *in vivo* antigen cross-presentation (Figure 3.4B, C). Furthermore, challenging the current paradigm, using soluble (Figure 3.5A, B, C, 3.6, 3.7) and particulate (Figure 3.5D, E, 3.6, 3.7) OVA model antigen, we also found that Sec22b was not necessary for cross-presentation *in vitro*. We observed no distinction between DC sources; both CD11c^{+} *Sec22b*$^{-/-}$ splenic DCs (Figure 3.5A, B) and CD11c^{+} *Sec22b*$^{-/-}$ BMDCs (Figure 3.5C, D, E, Figure 3.6) were fully competent cross-presenters thus ruling out tissue- and culture-specific artifacts as potential confounders.

Genetic deletion of *Sec22b* thus produced data that posed a seeming contradiction to data obtained from BMDCs with shRNA-mediated *Sec22b* KD[5,151]. Notably, treatment of BMDCs with the same shRNA sequences reduced cross-presentation in both *Sec22b*$^{-/-}$ and *Sec22b*$^{fl/fl}$ BMDCs (Figure 3.10C, D). This data demonstrate the cross-presentation defect previously associated with *Sec22b* silencing is instead linked to treatment with shRNA containing the nucleotide sequence 5'-CCCTATTC-3', targeting the 3rd exon of *Sec22b*. These

data were further bolstered by rescue of SEC22B expression in KD BMDCs (Figure 3.10E-G), which failed to rescue the shRNA-induced cross-presentation defect (Figure 3.10H), and by RNA sequencing of EV- and shRNA-treated KO BMDCs, which identified over 20 other unique targets of the *Sec22b*-"specific" shRNAs used (Figure 3.10J).

These collective findings serve to clarify the common understanding that SEC22B is essential for cross-presentation[28,91,92,186,187,191-196]. While our data confirms Cebrian et al's finding that KD with shRNA 90 does indeed reduce cross-presentation, it also suggests the cross-presentation phenotype was misattributed to *Sec22b* silencing.

A potential caveat to our studies might be found in the residual SEC22B expression seen in the *CD11c-Cre Sec22b*$^{fl/fl}$ BMDCs (Figure 3.1B-F). Cre-mediated excision of exon 3 in this population was 66% efficient (Figure 3.1C), which might be due to either mosaic Cre expression amongst DCs or inefficient Cre activity. It is thus theoretically possible that a fraction of SEC22B-producing DCs in the KO condition are capable of cross-presenting to T cells as efficiently as the entire population of DCs in the FL condition. However, the uniform response to antigen dose, almost complete loss of SEC22B protein in CD11c^{+} BMDCs obtained from *CD11c-Cre Sec22b*$^{fl/fl}$ mice (Figure 3.1E, F), and the inability of *Sec22b*$^{\Delta}$ rescue (Figure 3.10E-G) to mitigate the shRNA 90-induced cross-presentation defect (Figure 3.10H) suggest that this is an unlikely event.

Additional investigation will be needed to explore what impacts SEC22B overexpression in wildtype cells may have on cross-presentation, as our data do not address this.

In summary, our data do not exclude a role for SEC22B in cross-presentation but do demonstrate that SEC22B cannot be considered to be required for cross-presentation of soluble or particulate antigens. Further work will be necessary to determine the role of SEC22B in the cross-presentation of cell-associated antigens.

Our findings, moreover, offer an opportunity to identify which factor(s) is/are truly responsible for the cross-presentation defect induced by *Sec22b* shRNAs 89 and 90. Many of the off-target genes identified (Figure 3.10J) have no known association with antigen presentation pathways, though several do. Several protein products of the many genes that were altered are involved in phagosomal biology[72], cell-trafficking and immune-regulation. Notably, our inability to identify a single obvious off-target gene leaves open the possibility that shRNAs 89 and 90 mediate their effects on cross-presentation through the knockdown of several genes, which may function in an integrative fashion to promote cross-presentation.

For the wider community of experimental biologists using molecular techniques to manipulate gene expression, our data offers a cautionary tale. RNAi

technology carries the risk of off-target effects[199-202]. The off-target problem is not exclusive to KD technologies as the same concerns have been noted with endonuclease-mediated genome editing techniques[203-207]. Nor is this limited to mammalian systems. An elegant study in zebrafish found that 80% of phenotypes observed using morpholino-mediated silencing could not be replicated in knockout models[208]. Thus, our data support validation of gene targets with multiple methodologies as any one approach carries significant limitations.

Our findings correct the field's understanding of SEC22B's role in cross-presentation using a DC-specific *Sec22b* knockout mouse to demonstrate that there is no dependence on SEC22B expression for efficient cross-presentation. While this appears to contradict the observation that shRNA-mediated knockdown of *Sec22b* reduces cross-presentation efficiency, our data show the observed cross-presentation defect is likely due to the shRNA sequences acting on off-target genes. Taken together, our findings also point to the possibility of other potentially novel critical mediator(s) of cross-presentation.

MATERIALS AND METHODS

Reagents

RPMI, penicillin and streptomycin, and sodium pyruvate were purchased from Gibco; FCS from GemCell and Gemini, 2-ME from Sigma-Aldrich. Lipopolysaccharide (tlrl-smlps), Pam3CSK4 (tlrl-pms), and peptidoglycan (tlrl-pgns2) were obtained from Invivogen. Ovalbumin (OVA, A5503) and SIINFEKL/$OVA_{257-264}$ (S7951) antigen were purchased from Sigma-Aldrich unless otherwise noted. Bovine serum albumin (BSA, BP1600) was purchased from FisherScientific.

Mice

C57BL/6 (027) and Balb/c (028) wildtype mice were obtained from Charles River Laboratories. Two OT-I mouse models were used based on availability of reagents. OT-I transgenic TCR mice were obtained from Jackson Laboratory (003831) and *Rag2* KO OT-I mice were obtained from Taconic (2334). *Sec22b* gene-trapped founder mice were obtained from the European Conditional Mouse Mutagenesis Program (EUCOMM; $Sec22b^{tm1a(EUCOMM)Wtsi}$) and bred to *FLP* recombinase mice (005703, The Jackson Laboratory) to excise the *FRT*-flanked region between exons 2 and 3 (Figure 3.1A) and generate $Sec22b^{fl/fl}$ mice (Figure 3.1A). *CD11c-Cre* transgenic mice (008068, The Jackson Laboratory) were then bred to $Sec22b^{fl/fl}$ mice to create *CD11c-Cre* $Sec22b^{fl/fl}$ mice. Mice used for experiments ranged between 8 weeks and 1 year old and included both males and females. All animals were cared for under regulations reviewed and

approved by the University Committee on Use and Care of Animals of the University of Michigan, based on University Laboratory Animal Medicine guidelines.

Genotyping

The following primers were used to genotype the *Sec22b* allele: 5'-AAGGGTGGATGGATTCTTCACAC-3' (*Sec22b* F1), 5'-TTGGTGGCCTGTCCCTCTCACCTT-3' (*Sec22b* B1), 5'-GCAGCTCAGCAGTAAGAACACGTC-3' (*Sec22b* B2). The *Sec22b* F1+B1 primer pair was used to identify gene-trapped mice and the *Sec22b* F1+B2 primer pair was used to identify *floxed* mice. *Cre* primer sequences were: 5'-TTACCGGTCGATGCAACGAGT-3' (*Cre* F) and 5'-TTCCATGAGTGAACGAACCTGG-3' (*Cre* R).

Cells

Loosely adherent and nonadherent BMDCs were harvested after 7 days of bone marrow cell culture in GM-CSF (20 ng/mL, Peprotech, 315-03)-containing media. Where indicated, BMDCs were enriched with CD11c UltraPure MicroBeads (Miltenyi, 130-108-338) by MACS sorting. To obtain splenic DCs, spleens were cut into thirds, flushed with 1 mg/mL collagense D (Roche, 11088866001) and incubated for 1 hr at 37°C. Digested spleens were then homogenized between frosted slides, filtered through a 40 um cell strainer to achieve a single-cell suspension, and enriched with CD11c UltraPure

MicroBeads. T cells were isolated from single cell homogenates from spleen and lymph nodes and isolated using CD90.2 MicroBeads (Miltenyi, 130-049-101).

Flow cytometry

Antibodies

All antibodies were obtained from eBioscience and BioLegend: CD3 (145-2C11), CD4 (GK1.5), CD8α (53-6.7), CCR7 (4B12), CD62L (MEL-14), CD44 (IM7), CD69 (H1.2F3), CD25 (3C7), IL-2 (JES6-5H4), IFNγ (XMG1.2), CD11c (N418), CD11b (M1/70), CD205 (NLDC-145), F4/80 (BM8), B220/CD45R (RA3-6B2), NK1.1 (PK136), TCRβ (H57-597), TCRγδ (GL3), I-A/I-E (M5/114.15.2), Annexin V-APC (BioLegend, 640920), 7-AAD (BioLegend, 420404). H-2K^{b} OVA-APC (T03002) and H2-K^{b} LCMV-APC (T03019) tetramers were purchased from MBL International Corporation.

Cell staining

For immunophenotyping, single-cell suspensions were obtained by homogenizing tissues between frosted glass slides then filtering homogenates through a 40 um cell strainer. OT-I T cells were stained with 5 uM CFSE (Invitrogen, C34554) according to manufacturer's protocol. To control for nonspecific binding, cells were blocked with anti-CD16/CD32 antibody (BD Biosciences, 2.4G2) for 10 minutes at room temperature. Tetramer staining was performed according to manufacturer's protocol.

Surface staining for flow analysis was performed at 0.5 µL antibody/test for 15 minutes at 4°C, protected from light. For surface staining for flow sorting, cells were resuspended at $5x10^6$ cells/mL with 5 µL/mL antibody for 30 minutes at 4°C. Cells were fixed and any red blood cells lysed in Fix/Lyse solution (BD Biosciences, 349202) according to manufacturer's instructions.

For intracellular staining, cells were stimulated with PMA/ionomycin (eBioscience, 00-4975) and treated with brefeldin A (eBioscience, 00-4506-5) for 5 hours at 37°C. Permeabilization buffer (eBioscience, 00-8333) was used for intracellular cytokine staining which was performed at 0.5 uL antibody/test for 30 minutes at room temperature, protected from light.

Flow analysis

Cells were run on an Accuri C6, MACSQuant Analyzer, BioRad ZE5 Cell Analyzer, or Attune NxT. All analysis was performed using FlowJo v10.2.

Cell sorting

BMDCs were prepared for sorting by resuspending in FACS buffer containing 5 mM EDTA (Lonza, 51201) to prevent cell aggregation. Cells were sorted on a Beckman Coulter MoFlo Astrios EQ, Sony SY3200, or BD FACSAria II.

Western Blots

Whole cell lysates were obtained and protein concentrations determined by

BCA Protein Assay (Thermo Scientific, 23225). Protein was separated by SDS-PAGE gel electrophoresis and transferred to PVDF membrane (Millipore, IPVH00010) using a Bio-Rad semi-dry transfer cell (1703940) (20V, 1h). Blots were incubated with SEC22B (1:200, Santa Cruz, 29-F7) and B-ACTIN (1:1000, abcam, ab8226) primary antibodies overnight at 4°C. Incubation with secondary anti-mouse antibody conjugated to HRP (1:10,000, Santa Cruz, sc-2005) was performed for 1 hour at room temperature. Bound antibody was revealed using SuperSignal ECL substrate (Thermo Scientific). Densitometric analysis was performed using ImageJ.

Mixed lymphocyte reaction

5000 MACS-sorted $CD11c^+$ splenic cells were cultured with $2x10^5$ CD90.2+ T cells from Balb/c or C57BL/6 mice 96 well flat-bottom plates in 200 uL media for 96 hours. Incorporation of ^3H-thymidine (1 µCi/well) by proliferating T cells during the final 7 hours of culture was measured by a TopCount NXT (PerkinElmer, C9902).

ELISA

Supernatants from cell culture were harvested and analyzed for IL-12 (BD Biosciences, 555240) and TNFα (R&D Systems, MTA00B) following manufacturer's instructions.

Antigen Presentation Assays

In vitro cross-presentation of soluble OVA

DCs were plated at $0.05x10^6$ cells/well or $0.025x10^6$ cells/well for rescue assays in 96 well flat-bottom plates and incubated with OVA or SIINFEKL dissolved in 1xPBS for 2 hours at 37°C, unless otherwise noted. Cells were then washed with 1xPBS and fixed with 1% formaldehyde. Fixation was quenched by 0.2M glycine (Sigma-Aldrich, G5417) solution after which $0.2x10^6$/well CFSE-stained OT-I T cells were added. Assays were harvested 72 hours later.

In vitro cross-presentation of bead-bound OVA

Differing ratios of OVA and/or BSA was attached to 3 um carboxylate microspheres (Polysciences, 09850-5) using passive adsorption (100% OVA/0% BSA, 33% OVA/66% BSA, and 0% OVA/100% BSA). Beads were washed in MES buffer (Thermo Scientific, 28390) resuspended at 2% solids, then incubated with antigen (10 mg/mL total) overnight at room temperature with gentle rocking. Beads were washed 3x in MES buffer then stored at 1% solids in 1xPBS+0.1% glycine at 4°C until use. $1x10^6$ beads were incubated with $0.1x10^6$ MACS-sorted $CD11c^+$ BMDCs for 2 hours at 37°C. Subsequently, DCs were processed as in the soluble OVA cross-presentation assay.

In vivo cross-presentation assays

As previously described [197], on day 0, OVA or BSA was injected *i.p.* and $10x10^6$ CFSE-stained OT-I T cells were delivered *i.v*. On day 7, spleen, mesenteric

lymph nodes, and superficial inguinal lymph nodes ipsilateral to the side of antigen administration were harvested, processed, and analyzed by flow cytometry for SIINFEKL-restricted CD3+ CD8+ T cell proliferation.

Excision PCR

Genomic DNA was purified from MACS sorted BMDCs and FACS sorted splenic DCs using Trizol LS (Invitrogen, 10296028) according to manufacturer's instructions. The following primers and GoTaq Green Master Mix (Promega, M7122) were used to detect alleles: *Sec22b* F1, 5'-TCCTTTTGAATGGAGAAAGCTTC-3' (F2), and 5'-CCTGTGACAGTCTACAGATTGGA-3' (R). All reactions were performed according to manufacturer's instructions. 1 Kb Plus DNA Ladder (ThermoFisher, 10787018) was used for agarose gel analysis.

Quantitative RT-PCR

Cells were homogenized using a Qiagen QIAshredder (79654) and RNA purified using a Qiagen RNeasy Mini Kit (74104). Using SuperScript VILO (Invitrogen, 11754050), mRNA was reverse-transcribed into cDNA. The following primers and SYBR green (PowerUP SYBR Green Master Mix, Applied Biosystems, A25742) were used to detect transcripts: 5'-CAGGGCTCTAGACCCAAGTAGCA-3' and 5'-CCAGTGCTGTGCCACCATGAAA-3' (Sec22a), 5'-GCTCGGAGAAATCTAGGCTCC-3' and 5'-CCCCGCTGTAGGACTTCTTC-3' (Sec22b), 5'-GGGCGAGGTGTCCCCATGAC-3' and 5'-

AGGCTGAGAGGGGCAGTCCA-3' (Sec22c), 5'-TGACCTCAACTACATGGTCTACA-3' and 5'-CTTCCCATTCTCGGCCTTG-3' (GAPDH). All reactions were performed according to manufacturer's instructions and reaction specificity was verified by agarose gel analysis.

Lentiviral shRNA Knockdown and Overexpression of Sec22b

Generation of shRNA plasmids

RNA Consortium plasmids encoding shRNA-expressing lentivirus (TRCN0000115089 (89), TRCN0000115090 (90)) were obtained from ThermoFisher. Empty vector (EV, 10879) plasmid was obtained from Addgene. Plasmids were transformed into JM109 competent cells (P9751, Promega) following manufacturer's instructions. Preps were purified for lentiviral generation using the Qiagen Plasmid Plus Midi Kit (12943).

Generation of Sec22b$^{\Delta}$ *transgene overexpression vector*

Total RNA was prepared using Trizol LS according to manufacturer's instructions. SuperScript IV (Invitrogen, 18090010) was used to generate cDNA. *Sec22b* was amplified and adapted for TOPO cloning using AccuPrime Pfx Polymerase (Invitrogen, 12344024) and 5'-CACCATGGTGCTGCTGACGAT-3' and 5'-TCACAGCCACCAAAACCGCA-3' primers. Reaction products were analyzed by electrophoresis, then were gel purified (Qiagen Gel Extraction Kit, 28104), ligated to TOPO vector (Invitrogen, K2400-200) following manufacturer's instructions, and transformed into TOP10 chemically competent cells

(Invitrogen, C404010). Site-directed mutagenesis was performed using AccuPrime Pfx Polymerase and 5'-TACAGTTTTATTGAGTTTGATACCTTCATTCAGAAA-3' and 5'-TGGACGGCTAACAG TGGGCACCTTCTTC-3' primers in order to induce silent mutations at the site of shRNA 89 and 90 binding. Gateway™ recombination was used to insert the transgene into expression vector pLenti7.3/V5-DEST™ (Invitrogen, V53406). Clones were sequenced to verify sequences and in-frame insertion and plasmids from amplified preps were purified for lentiviral generation using the Qiagen Plasmid Plus Midi Kit (12943).

Generation of lentivirus

Plasmids were packaged using HEK293T cells by the University of Michigan Medical School Vector Core using a VSV-G envelope. Supernatants containing viral particles were concentrated 10X.

Dendritic cell infection

Bone marrow was plated in GM-CSF-containing media at $5x10^6$ cells per 100 mm dish on day 0. On day 2, cells were infected with 0.5 mL 10X shRNA-containing virus and, where indicated, 1 mL 10X *Sec22b*$^{\Delta}$-containing virus in a total of 5 mL GM-CSF-containing media with polybrene (8 ug/mL, Sigma-Aldrich, 107689). On day 4, cells treated with EV or shRNA 89 or 90 were selected with puromycin (5 ug/mL**,** Sigma-Aldrich, P8833) in 10 mL GM-CSF containing media. On day 7, BMDCs were harvested for assay use.

RNA-Seq

RNA preparation and sequencing

Total RNA was prepared using Trizol LS according to manufacturer's instructions and assessed for quality using a TapeStation (Agilent, Santa Clara, CA) following manufacturer's recommendations. Samples with RNA integrity numbers of ≥8 were prepped using the Illumina TruSeq Stranded mRNA Library Prep kit (RS-122-2101, RS-122-2102) (Illumina, San Diego, CA) using manufacturer's recommended protocols, where 1ug of total RNA was ribo-depleted with Epicentre Ribo-Zero protocol. Depleted RNA was fragmented and copied into first strand cDNA using random primers. The 3' ends of the cDNA were adenylated for ligation of adapters, one of which contained a 6-nucleotide barcode unique to each sample for sample pooling. Products were purified and enriched by PCR to create the final cDNA library. Final libraries were checked for quality and quantity by a TapeStation (Agilent) and qPCR using Kapa's library quantification kit for Illumina Sequencing platforms (KK4835) (Kapa Biosystems,Wilmington MA) using manufacturer's recommended protocols. Libraries were clustered on the cBot (Illumina) and sequenced 3 samples per lane on a 50 cycle paired end on a HiSeq 2500 (Illumina) in High Output mode using version 4 reagents according to manufacturer's recommended protocols.

Data Processing

RNA-sequencing reads were quantified to the mouse transcriptome (GENCODE vM4) using Kallisto (v0.43.0)[209]. GENCODE vM4 GTF was obtained from

GENCODE (https://www.gencodegenes.org/mouse_releases/4.html), and transcriptome fasta file was produced using the *rsem-prepare-reference* function of RSEM (version 1.2.26)[210]. Kallisto index was generated using the *kallisto index* function. Transcript level quantification obtained using the *kallisto quant* function. Gene level expression was obtained by summing the TPM values for all transcripts within each gene.

RNA-Seq Differential Expression Testing

Differentially expressed genes were obtained by comparing shRNA 89 condition to empty vector (EV) and the shRNA 90 condition to empty vector using DESeq2 [211]. In order to detect the most robust loss of expression, only genes with mean expression of 20 TPM or greater in the EV condition were considered for analysis. Significantly downregulated genes were defined a q-value<0.05 cutoff.

Statistics

Unless otherwise noted, all statistical comparisons were performed using a 2-tailed unpaired t-test. Statistical significance was determined using the Holm-Sidak method, with alpha=0.05. Each condition was analyzed individually, without assuming a consistent SD. Further information on statistical analyses can be found in the figure legends for each experiment.

CHAPTER IV

CONCLUSION

In summary, we have used novel *Sec22b* knockout mouse models to interrogate the role of *Sec22b in vivo*. In doing so, we discovered that, at minimum, *Sec22b* is essential for embryonic development at two time points, before E8.5 (Table 2.1C) and after E11.5, and in at least two distinct tissues, one being the *Vav1*-expressing cell population (Table 2.2). While a small minority of *Vav1-Cre Sec22b*$^{fl/fl}$ embryos survive to adulthood (Figure 2.4A), examination of the *Sec22b* allele from peripheral blood cells in these mice suggested this may be due to incomplete excision of exon 3 by *Vav1-Cre* (Figure 2.3). Loss of *Sec22b* in the *Itgax* (CD11c)-expressing sub-population was insufficient to explain this early lethality (Table 2.3, Figure 2.4B). While *Sec22b* null embryos appeared to have a developmental delay, mice with *Sec22b* haplodeficiency aged and grew normally (Figure 2.2C), with no detectable phenotype in size or in hematopoiesis in adults (Figure 2.5).

CD11c-Cre Sec22b$^{fl/fl}$ mice also allowed us to test the role of *Sec22b* in cross-presentation. In these studies, we demonstrated that SEC22B is dispensable for antigen cross-presentation by dendritic cells, *in vivo* and *in vitro* (Figure 3.4,

3.5, 3.6, 3.7), challenging the current paradigm of SEC22B's role in cross-presentation. Interestingly, WT and SEC22B KO BMDCs treated with a *Sec22b*-targeting shRNA exhibited reduced cross-presentation (Figure 3.8, 3.10C, D) which was not rescued by SEC22B overexpression (Figure 3.10E-H), suggesting that an off-target effect of the shRNAs used, not changes in SEC22B expression, are responsible for the previously reported cross-presentation phenotype[5,78]. RNAseq confirmed downregulation of off-target genes by two *Sec22b*-targeting shRNAs in KO BMDCs.

Whether these findings have implications for studies investigating the roles of SEC22B in cross-presentation remains to be determined. In a study of human peripheral blood monocyte-derived DCs, *Sec22b* was silenced by a pool of siRNAs and was found to be unnecessary for cross-presentation of tumor-derived long peptides through a protease-independent pathway relying on nascent MHC I molecules[93]. Because pooled siRNAs were used, the *Sec22b*-targeting specificity is unclear. Additionally, SEC22B was hypothesized to participate in the cytosolic cross-presentation pathway, not the vacuolar[5] pathway. Taken together, our data do not invalidate the findings presented in this particular study. Another set of experiments using shRNA 89 demonstrated that knockdown of *Sec22b* affected OVA cross-presentation on H2-K^b, which had been previously described[5], but not cross-presentation of an immunodominant *Toxoplasma gondii*-derived epitope from GRA6 on H2-L^{d212}. However, considering that the data in Chapter 3 demonstrates that shRNA 89

mediates cross-presentation through off-target activity, the gene or protein responsible for mediating this phenotype ought to be considered undefined.

Our data not only call into question the role for SEC22B in antigen cross-presentation, they also potentially challenge other phenotypes associated with SEC22B. Until now, all manipulations of SEC22B in mammalian cells have been carried out *in vitro* using siRNA or shRNA. In fact shRNAs 89 and 90 have been used to explore phenotypes such as axonal growth in cortical neurons[6] and ROS accumulation in macrophage phagosomes[17]. There is currently insufficient evidence to determine if these observations are truly SEC22B-dependent or if they too are due to off target effects of the shRNAs.

Altogether, these data suggest that *Sec22b* plays a central biological role given its requirement during early embryonic development, though its deletion does not appear to affect CD11c+ DC development, survival, activation, endocytosis, or antigen presentation. Additionally, these data highlight the importance of interpreting *in vitro* data with caution. Finally, they emphasize the risk of drawing conclusions from a single approach like shRNA-mediated silencing, particularly when the method used is known to have off-target effects[199-202].

CHAPTER V

FUTURE DIRECTIONS

While our work uncovers a novel role for SEC22B in embryonic development, the mechanism by which it mediates embryogenesis remains undefined. In yeast, Sec22p contributes to macroautophagy[12], a process employed during murine embryogenesis[213]. Further work will examine whether it is through its contribution to autophagy or through another pathway that SEC22B is necessary for embryonic survival.

Interestingly, SEC22B is highly expressed in T cells (data not shown). Our lab has observed that manipulating autophagy in T cells by deleting ATG5 perturbs T cell functionality, reducing proliferation and increasing cytokine production. Whether SEC22B might mediate T cell functionality in a similar way remains open to investigation. Because our data demonstrate that *Vav1-Cre Sec22b*$^{fl/fl}$ mice die *in utero*, a T cell-specific *Cre*, such as *Lck-Cre* or *CD4-Cre*, will need to be utilized to study the role of SEC22B in T cell activation.

The role of SEC22B in autophagy in DCs is also unknown. While we failed to elicit a phenotype in SEC22B KO DCs in response to allogenic or TLR stimulation and did not observe a dependence on SEC22B for antigen cross-

presentation, we did so without activating autophagy. Future experiments might attempt to stimulate autophagy in SEC22B KO DCs and examine the impact on DC activation and all varieties of antigen presentation.

The data presented also indicate that, although SEC22B is not important for cross-presentation, there may be one or more novel cross-presentation mediators that are targeted by the *Sec22b*-targeting shRNAs used. Some candidates identified by RNAseq have been associated with antigen presentation pathways or endosomal/phagosomal homeostasis. These include MHC II molecule H2-Aa as well as Cathepsin D[98], Scpep1[72], Gm2a[72], and Necap2[214]. If one of these candidates is responsible for the cross-presentation phenotype observed in KD BMDCs, overexpression of the gene in 89 or 90-treated BMDCs ought to restore the cells' ability to cross-present.

An alternative, unbiased approach to identifying which other cross-presentation gene(s) may have been targeted by the *Sec22b* shRNA sequences might use a CRISPR library screen. A recent study used the GeCKO v2 library to screen for genes mediating LPS stimulation of TNFα production in BMDCs[215]. By modifying their protocol to include an OVA antigen feeding step and utilizing the 25-D1.16 antibody to detect antigen cross-presentation, specific gene mutations that cause reduced or enhanced cross-presentation could be identified. Comparing targets identified in this screen to the candidates discovered using RNAseq, would help eliminate false positives, allowing for

more focused validation studies. Validation could be accomplished through a number of techniques, but, if biologically possible, final validation ought to occur using a knockout model given our findings that off target effects of shRNAs can elicit biologically significant phenotypes.

What also remains unexplored is whether the ERGIC, where *Sec22b* localizes[5], contributes to the cross-presentation pathway. While ERGIC biogenesis and homeostasis remain active areas of investigation, possible avenues of research might include disrupting COPI or COPII transport pathways, which connect the ERGIC to distal (Golgi) and proximal (ER) organelles, respectively[216].

Although cross-presentation is known to activate the immune response against tumors and viral infection and is the target of research into vaccines against such diseases[91,92], significant obstacles to furthering our understanding of this process remain, the largest of which is the lack of a mouse model where cross-presentation is specifically inhibited. Though our DC-specific *Sec22b* knockout cannot serve that purpose, the ultimate goal of validating candidates identified in the RNAseq study and by a CRISPR screen would be to identify a gene whose deletion *in vivo* reduces cross-presentation. This knockout mouse could then be used to study cross-presentation *in vivo* and measure its contributions to immune responses in disease models. Furthermore, identification of such a critical regulatory protein for cross-presentation would allow for studies to address the outstanding questions in the field regarding the molecular control of

cross-presentation that causes some cells to cross-present more efficiently than others.

Finally, much remains to be learned about *Sec22b* itself. How its activity is regulated, whether it has cargo specificity, and how its homologs *Sec22a* and *Sec22c* function are currently unknown. As a prototypical longin SNARE[1], furthering our understanding of the biology of SEC22B may offer insight into the functions of other SNARE proteins as well.

APPENDIX

REGULATING DAMAGE FROM STERILE INFLAMMATION

AUTHORS: S Julia Wu, Pavan Reddy

INTRODUCTION

The immune system has evolved to protect the organism from infectious non-self through mechanisms that mediate host 'resistance' against infections to reduce pathogen burden[217,218]. Additionally, 'disease tolerance' describes the pathogen-independent response to infection, functionally serving to mediate tissue damage caused either by pathogens or by the immune response against them[217,218]. Disease tolerance improves host fitness in the presence of similar pathogen burdens, and is distinct from resistance to an infection, that aims at reducing the pathogen burden[217,218]. This is illustrated in Figure A.1 where arrow AB demonstrates the contribution of resistance to health whereas arrow AC demonstrates the contribution of tolerance to health. Arrow AD models how both resistance and tolerance can cooperatively improve health. In the context of sterile, non-infectious inflammation such as in autoimmunity, another form of tolerance, 'immune tolerance' regulates the immune response to self. Efforts to

understand and mitigate tissue damage caused by sterile and infectious inflammation have primarily focused on the modulation of immune responses, inflammatory and tolerogenic.

In other words, current therapeutic approaches largely focus on moving along from point A to B in Figure A.1 by enforcing 'immune tolerance' to reduce the burden caused by autoimmune cells. Enhancing 'disease tolerance' in the context of infections in plants and more recently in mammals has shown impact in mitigating tissue damage[217,218]. How target tissues defend themselves in the context of autoimmunity, allergic reactions, allo-graft rejection and graft-versus-host disease (GVHD) has been considered under different terminology during discussions of disease tolerance[219]. However, whether target tissues play a role in mitigating damage from sterile or non-infectious immunopathology has not been systematically explored and remains poorly understood.

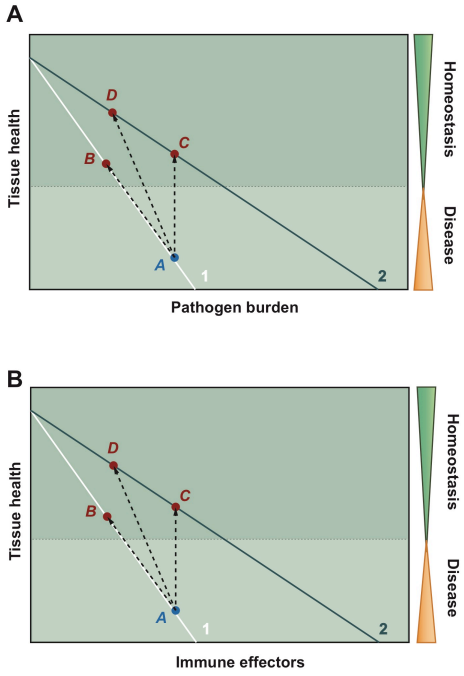

Figure A.1. Tolerance is the relationship between immune stimulus and health of the tissue being studied. (A) In disease tolerance, immune stimulus is measured by pathogen burden. Line 1 represents a tissue with low tolerance whereas Line 2 represents a tissue with high tolerance. Point A is used as a reference state. Moving from A to B results from increased resistance, reducing the pathogen burden alone. Moving from A to C results from increased tolerance; pathogen burden is unaffected but tissue health is

improved. Moving from A to D represents a scenario where both resistance and tolerance are employed. Homeostatic stability and disease severity are represented by the width of the appropriate cross-section of each respective wedge. **(B)** In tissue tolerance, immune stimulus is measured through the activity of immune effectors. Like in **(A)**, Lines 1 and 2 represent low and high tolerance tissues, respectively. With Point A as a reference state, moving from A to B results from immune tolerance mechanisms modifying immune effector function alone. Moving from A to C represents a case where immune effector activity remains the same but tissue health improves. Moving from A to D plots how both immune tolerance and tissue tolerance might work to improve tissue health. Homeostatic stability and disease severity are represented as in **(A)**.

Several disparate lines of experimental observations nonetheless do suggest that target tissue intrinsic features and responses contribute to disease severity during sterile immunopathology. Dampening the immune activation response may not always be sufficient to protect against immunopathology from autoimmune or allogeneic reactions. For example despite massive immunosuppression, we may be unable to completely mitigate immunopathology such as those illustrated by end-stage or steroid refractory GVHD[220]. Furthermore, patients with a genetic immunodeficiency can also show autoimmune symptomology[221]. Specifically, patients with mutations in *PRKDC* that encodes for DNA-dependent protein kinase catalytic subunit (DNA-PKcs), a kinase that is crucial for DNA double-strand break repair and that forms part of a protein complex required for AIRE (autoimmune regulator)-dependent expression of peripheral antigens in mTECs (medullary thymec epithelial cells), present with reduced T and B cells (Combined Immune Deficiency) yet demonstrate features of autoimmunity[221]. The mutation is present in all cells and whether this makes tissues in specific organs uniquely susceptible to damage

despite the reducing autoimmune T/B cell load is not known. However, it does offer an illustration of how tissue pathology can present as a movement from point D to A (Figure A.1), suggesting factor(s) other than immune effector cell number may contribute to health.

Experimental data also show that TLR signaling by the intestinal epithelial cells (IECs) protects them from non-infectious, DSS (dextran sulfate sodium)-induced colitis without reducing the leukocyte burden[222]. The protection was associated with increase in cytoprotective growth factors such as IL-6, hsp (heat shock protein) 25 and hsp72, demonstrating that tissue intrinsic signaling and generation of cytoprotective factors control target organ damage[222]. Recent observations showed that enhanced uptake and metabolism of butyrate by the IECs increased their survival and expression of junctional proteins and mitigated gastrointestinal (GI) GVHD without significantly altering the burden of alloreactive T cells[223]. Similarly, restoration of IL-22 or R-spondin in the intestinal tract mitigated GVHD damage by protecting intestinal stem cells (ISCs) and promoting intestinal regeneration without directly affecting alloreactive T cells[224,225].

In pathways responding to protein stress, UPR (unfolded-protein response)-associated PERK (protein kinase RNA-like ER kinase) in target cells seem to prove protective in models of multiple sclerosis[219] and XBP1 (X-box binding protein 1) protects against diabetic disease progression[219]. In accommodated

allo-graft organs, rejection is mitigated without unique pharmaceutical manipulation of immune cell activity[226].

Accommodation has been defined as a process wherein transplanted allo-graft do not succumb to humoral injury with no change in antigen or the antibody load or functions[226]. In Figure A.1, an accommodated organ might be represented by line 2 as compared to unaccommodated grafts, which might be represented by line 1.

Additionally, graft-intrinsic factors, may contribute to graft survival while leaving immune elicitor and response unchanged, shifting the graft from point A in Figure A.1 to point C. For example, in liver transplant, A20, through its protection against ischemic reperfusion injury and promotion of hepatocyte proliferation, contributes to liver graft survival[227]. In each of these models, the immune effector burden remained the same, but the ability of the target organs to 'tolerate' the immune effector burden appears to be critical for disease severity. Collectively these data point to tissue intrinsic resilience (Figure A.2A) and regeneration pathways (Figure A.2B) that protect against disease severity without altering the burden of reactive effector immune cells[219,221-226].

In light of these studies and the work on resistance and tolerance during infection, we define 'tissue tolerance' as properties that shift a tissue's response to inflammatory immune attack from line 1 to line 2 in Figure A.1. The

manifestation of various tissues' intrinsic, ability to 'tolerate' or withstand damage from inflammatory immune activity could include mechanisms that facilitate their regeneration, repair, or expand their homeostatic range (Figure A.1).

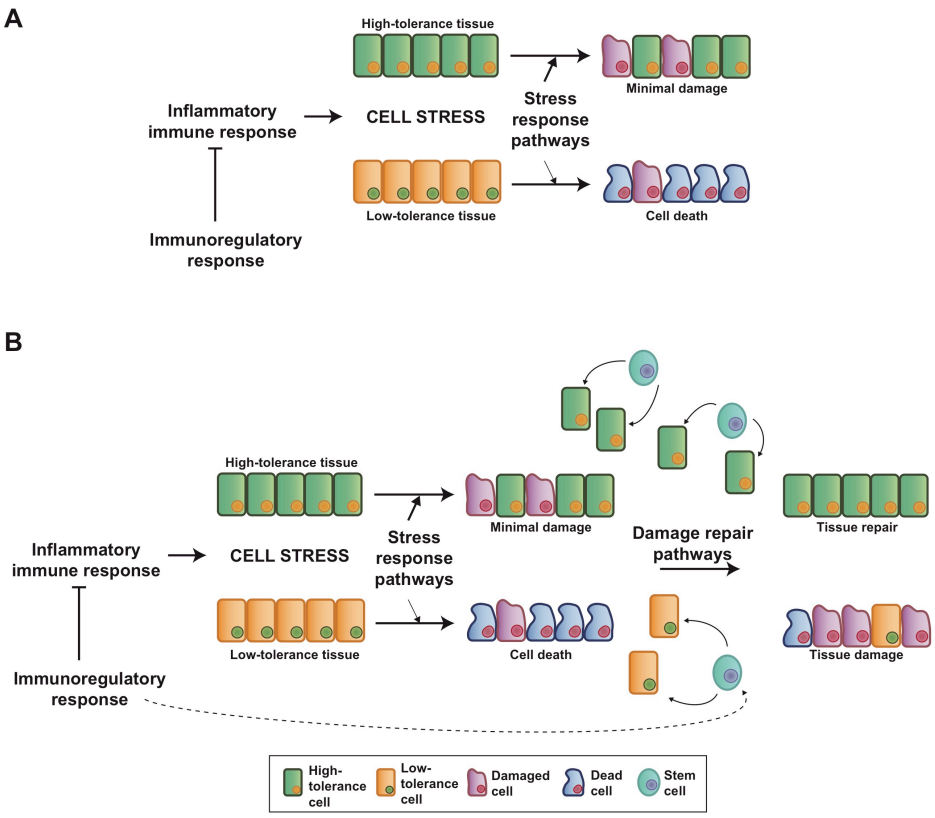

Figure A.2. Mechanisms of tissue tolerance. (A) Tissue-intrinsic pathways serve to protect parenchymal tissue from inflammatory immune attack by tissue cell-autonomous methods. **(B)** Tissue-extrinsic pathways protect parenchymal tissue from inflammatory immune attack by repairing damage, either in parallel with immune insult or after inflammation terminates.

Tissue tolerance mechanisms could include features that overlap or in some cases indistinguishable from cellular stress responses, tissue regeneration and repair[219]. Thus could include, but not be limited to metabolic, apoptotic,

autophagic, redox, or cell renewal pathways. Importantly, as damage inducing mechanisms vary in different pathologies, tissues and disease stages, the mechanisms of 'tissue tolerance' are likely to be context specific. The involved pathways may conversely be broadly conserved or uniquely developed and might share overlap with disease tolerance pathways[219]. For instance, like disease tolerance, tissue tolerance pathways may manifest as mechanisms to counteract these stressors[218]. Direct experimental evidence linking tissue tolerance and disease tolerance is currently lacking. However, accommodated organs were found to show increased expression of PI3K (phosphoinositide 3-kinase)/AKT (protein kinase B) and Nrf2 (nuclear factor erythroid 2-related factor)[228], two proteins which have been implicated in disease tolerance[217,219].

Thus considering tolerance(s) as involving both tissues as well as immune cells may lead to novel ways of not only understanding sterile immune-pathologies but may also allow for development of more effective therapies, just has been with the consideration of disease tolerance for infectious immunopathology[217,218]. Specifically, it becomes possible to consider therapies that may increase tissue tolerance to protect against organ damage. Thus this also has potential for broadening the development of potential treatment repertoire that could be adjuncts to strategies aimed at promoting immune tolerance or suppression. Therefore we propose that including 'tissue tolerance' along with immune tolerance in the conceptual repertoire for mitigating tissue damage will allow for better understanding and treatment of non-infectious immunopathology. The

terms we use in this section to describe resistance and tolerance are defined in Table A.1.

Term	Definition
Immune resistance	Immune cell-mediated inflammatory effector response. Contributes to homeostasis by clearing infections and tumor cells. Disturbs homeostasis by inducing immunopathology.
Immune tolerance	Immune cell-mediated regulatory mechanisms to inhibit immune resistance/inflammation. Contributes to homeostasis by protecting against immunopathology. Disturbs homeostasis by preventing immune resistance responses where it might be beneficial.
Disease tolerance	Parenchymal tissue-specific mechanisms to protect against immunopathology in the context of infectious inflammation.
Tissue tolerance	Parenchymal tissue-specific mechanisms to protect against immunopathology in the context of sterile/non-infectious inflammation.

Table A.1. Terms used to describe concepts of tolerance

TISSUE TOLERANCE IN GVHD

The immune system is a double-edged sword: while it protects from infection and malignancy, these same inflammatory effector responses can result in destructive immunopathology. This damage can be more than just a side effect; it can be the entire disease itself. A salient example occurs during allogeneic

hematopoietic stem cell transplantation (HSCT), a potentially curative therapy for many hematological diseases, whose utility is crucially limited by the coincident donor immune cell-mediated GVHD that occurs[229].

In order to mitigate its potential for harm, the immune system has evolved mechanisms to self-regulate its response, a concept called immune tolerance. However, limiting GVHD through intrinsic and extrinsic immunoregulatory mechanisms alone has not proven sufficient to mitigate disease. In the setting of infectious disease, a similar contradiction has been observed, where manipulating pathogen burden or immune responses alone are insufficient to maintain host health[219]. These observations led to the ceonceptualization of disease tolerance, a property that reduces the pathological impacts of an infection without direct effects on pathogen burden[217-219,230]. Disease tolerance, as seen in plants and animals, is a manifestation of various tissues' intrinsic, but variable, ability to tolerate damage from inflammatory immune activity during infection, implying both the immune system and tissues regulate homeostasis during inflammation. We propose that a similar tug of war for homeostatic maintenance also plays out in the setting of non-infectious inflammation, using GVHD as a model system. We posit that in the setting of GVHD, tissue tolerance, or the capacity of a parenchymal tissue to maintain homeostasis in the face of destructive inflammation, is a crucial player in disease outcome.

Tissue tolerance: an expanded model of tolerance

Our current understanding of the mechanisms driving the immunopathology seen in non-infectious settings such as autoimmune disease and alloimmune reactions is insufficient to fully explain clinical observations. Despite the ability to induce massive immunosuppression, we cannot completely mitigate the immunopathology seen in end-stage autoimmune diseases or steroid refractory GVHD and organ rejection. Furthermore, patients with a genetic immunodeficiency can also show autoimmune symptomology[221]. These data suggest the immune system may not be the sole factor regulating tissue homeostasis during non-infectious and sterile inflammation induced pathology. Therefore, we propose a new concept of tolerance: tissue tolerance. We define tissue tolerance as those immune cell-independent parenchymal tissue-specific mechanisms that maintain homeostasis in the face of pathologic non-infectious inflammation (Table A.1) and model it as the slope of host health plotted over immune stimulus (Figure A.1). Thus, tissue tolerance might be defined as an improvement in organism health and/or fitness for any given burden of immune elicitor. When interpreting the literature through this lens, we see evidence that host tissue factors contribute to disease in GVHD alongside immune tolerance and resistance. A recent publication has used the term tissue tolerance in the context of infection[231], but here we confine the use to the non-infectious setting, specifically GVHD. More work will need to be done to determine to what degree disease tolerance and tissue tolerance share mechanisms.

Tissue tolerance and allogeneic HSCT

Rejection

HSC rejection and GVHD, depending on the direction of immune reactivity, are the potential consequences of an allogeneic immune reaction following allogeneic HSCT. Are there HSC autonomous features that might explain why HSC rejection occurs in some patients despite stringent immunosuppression after allogeneic HSCT?

Some insight may be obtained by examining studies on allogeneic solid organ transplant rejection. Both clinical and experimental observations suggest a role for tissue tolerance in mediating the severity of allograft-rejection. For instance, in kidney transplantation, donor and recipient are typically matched by blood type to prevent hyperacute rejection. However, when ABO-mismatched transplants have been performed, not all grafts are universally rejected[226].

'Accommodation', a process that involves graft organ-specific factors and provides protection against immune-mediated rejection has been postulated in this context. Specifically, in 'accommodated' organs, complement and donor-reactive antibodies are able to bind but subsequent lysis is reduced[226,228]. The specific mechanisms mediating these protective phenotypes are not understood, but the observations can be viewed as target cell/tissue intrinsic adaptive mechanisms that mediate resistance to immune mediated attack of allogeneic organs. Viewed in this light, it could be seen as part of the tissue tolerance model. Experimental models have yet to evaluate such a notion in

HSC rejection following allogeneic HSCT but it is possible that better insight into the mechanisms governing accommodation will afford better insight into the mechanisms of HSC rejection. Prevention of allogeneic rejection, solid organ or HSC, is likely to be due to the net effect of both immune, and tissue tolerance (Figure A.3).

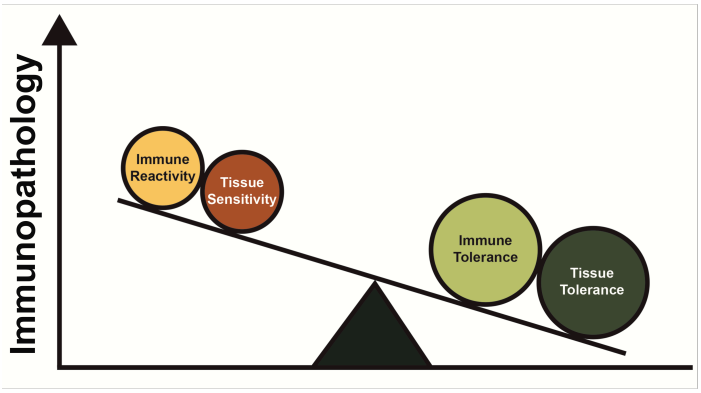

Figure A.3. Tissue tolerance interacts with immune tolerance to mediate immunopathology.

Acute GVHD

Several observations and emerging experimental data point to a potential role for target tissue autonomous features in determining the clinical severity and mortality of acute GVHD. These features seem predominantly independent of the quantity, intensity and magnitude of alloreactive T cells or inflammation.

Target organ specificity: Several clinical observations point towards the existence of immune cell and inflammation-independent determinants of GVHD severity. For instance, in most clinically significant GVHD mediated by alloreactive T cells, immune pathology is largely restricted to skin, liver, and GI tract. This is despite ubiquitous expression of alloantigens and the ability of

donor alloreactive T cells to gain access to many other tissues. The presence of a microfloral interface might be invoked to explain this target organ specificity, but fails to explain why genito-urinary and upper aero-digestive tracts are spared from acute GVHD, while the liver remains a bona fide target. Because the GI tract, skin and liver are large organs, the size of the allogeneic target tissue has been posited as a determinant. However, other large targets, such as skeletal muscle, are spared. Similarly, the fact that kidney, pancreas, heart, and lung allografts are rejected following solid organ transplant but are largely deemed not to be target organs of acute GVHD indicates that allo-antigen expression and allo-immune effector functions are not a predictor of disease organ specificity in GVHD (Figure A.4).

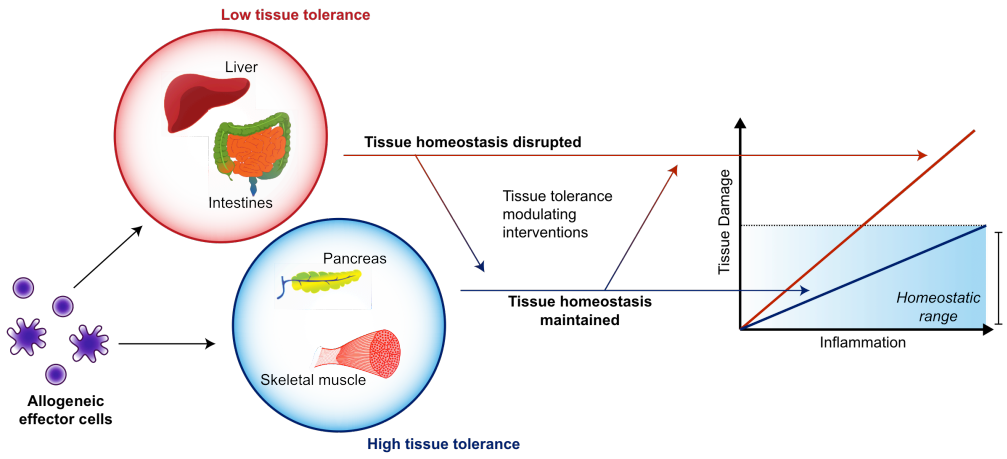

Figure A.4. Differential organ tissue-specific responses to allogeneic immune attack.

Therefore, while it is possible that many organs are targeted by a GVH reaction, but often only a subset will experience immune-pathological damage significant

enough to give rise to clinical signs and symptoms of disease. This suggests some other inherent property of parenchymal tissues, tissue tolerance, modulates tissue-susceptibility or tolerance to alloimmune damage (Figure 3). Thus disease severity may depend on how a tissue is able to protect itself i.e. 'tolerate' an immune-mediated attack by alloreactive T cells, an idea related to that proposed by Matzinger, who has hypothesized that tissues may actively modulate immune responses[232,233].

Immune suppression refractory GVHD: When viewed from the perspective of tissue tolerance, steroid (immune suppression) refractory acute GVHD may prove more explicable. Often understood and treated only as an immune tolerance/reactivity issue, patients who have developed steroid refractory GVHD are treated with a wide array of extremely potent immune-suppressants[234-243]. While the immune system appears massively suppressed from a 'clinical' standpoint (manifested by opportunistic infections, CMV (cytomegalovirus), EBV (Epstein-Barr virus) and other viral reactivations)[235-237,239,242,243], many steroid refractory patients seldom show 'clinical' response to such an intense immunosuppression strategy. This suggests suppressing immunity, at least to the point of clinical consequence of sever reactivations and opportunistic infections manifest, may not be sufficient to reduce mortality and morbidity from steroid refractory GVHD. However, besides the 'clinical' evidence of massive immune suppression, the exact amount of immune suppression, within the limits of ex-vivo assays, has not been studied. Thus it is nonetheless possible that

more immune suppression may still mitigate GVHD, but this will have severe clinical consequences from viral reactivations and opportunistic infections. We would like to suggest that in these cases, it is possible that, in addition to targeting the immune system, once tissue tolerance is better understood, enhancing target tissue intrinsic homeostatic and/or repair mechanisms that promote tissue tolerance may improve outcomes.

GVHD outcome improvement independent of direct immune system targeting: Recent improvements in clinical outcomes of acute GVHD despite similar immune-prophylaxis regimens have not only been attributed to better matching or immune-targeted treatment of GVHD, but also to better supportive care[244]. Some of the supportive care measures are due to improvements in antibiotics, antivirals and antifungals. Others are improvements in general supportive care that include better, more appropriate fluid, electrolyte and nutrition strategies. Many of these measures do not directly alter the load or function of allo-reactive T-cell or the magnitude of inflammation. Instead, these are likely enhancing the cellular and tissue adaptive/repair responses and thus limiting the deleterious effects of T cell- and inflammation-mediated stress and damage.

Experimental observations on tissue tolerance in acute GVHD

Emerging experimental data have begun to shed light on potential tissue tolerance mechanisms, elucidating tissue-specific pathways that support target organ tissue homeostasis and modulate GVHD severity with no direct effect on

allogeneic T cell populations and systemic inflammation. While the observations summarized below are all of intestinal epithelial tissue behavior, we have no reason to assume similar mechanisms are not used by other tissue types.

Microbiota and metabolites in GVHD

Previous observations have suggested a role for intestinal microbiota in the pathogenesis and severity of GVHD[245]. Recent studies have clearly demonstrated a strong correlation between shifts in the intestinal microbiome and GVHD severity both in experimental and human contexts[246-248]. Besides characterizing and enumerating the changes in intestinal microflora, recent work has also begun to explore the role of the intestinal metabolome in tissue homeostasis and GVHD severity. The microbiota perform key metabolic functions; they not only break down material directly ingested by the host but also produce their own metabolic byproducts[249,250]. The intestinal metabolome thus consists of products from discrete host metabolism, microbial metabolism, and mammalian-microbial cometabolism[251]. The impact of microbiota-derived metabolites is being increasingly appreciated, specifically in intestinal homeostasis[251].

A recent study explored the effects of metabolic by-products on GVHD after allogeneic HSCT in a major-MHC mismatch model of experimental bone marrow transplantation[223]. It made the surprising observation that amongst the short chain fatty acids, only butyrate, the primary energy source for intestinal cells, was reduced in IECs isolated from GVHD animals[223]. The study demonstrated

that butyrate supplementation promoted intestinal barrier function *in vivo* and, *ex vivo*, enhanced the ability of IECs to survive and withstand alloreactive T cell and inflammation induced damage[223]. This increased survival was associated with increased expression of junctional proteins promoting GI barrier integrity and increased expression of antiapoptotic proteins, promoting IEC survival[223]. Mice treated with butyrate or with butyrate-producing microbes exhibited reduced GVHD-associated morbidity and mortality[223]. Although Tregs are known to be induced by butyrate[252], the study demonstrated that donor Tregs were not critical for GVHD protection when butyrate was delivered locally, either directly or indirectly by shifting the microbiome towards high butyrate producing Clostridial species[223]. Furthermore, *ex vivo* analyses of donor T cells from the spleen showed no systemic effects of butyrate activity and no change in function when compared to control animals with active GVHD[223], indicating that the beneficial effects on GVHD severity were likely from local trophic effects on IECs, enhancing their ability to 'tolerate' immune mediated damage.

In another study, in hosts with host parenchymal target tissue-specific loss of NLRP6 signaling, GVHD severity was reduced, again with no significant effect on alloreactive T cell burden[253]. These data collectively show that it is possible to reduce GVHD severity without directly altering the load or function of immune cells but instead by altering target tissues ability to directly resist immunopathology (Figure A.4).

Regeneration of intestinal target tissue without altering allogeneic T cell function

Experimental evidence suggests regeneration of damaged tissue is another strategy used by tissues to increase tolerance against GVHD-associated inflammation, independent of alloreactive T cell burden. Administration of KGF (keratinocyte growth factor), a critical regulator of intestinal epithelial cell growth[254], can not only protect GI tissue from the harmful effects of the conditioning regimens for bone marrow transplant,[255] but also reduce morbidity and mortality from GI GVHD[256,257]. However, the studies did not directly explore effects on target tissues and inferred benefits from reshaping the donor immune response.

More recently, studies have directly explored how promoting ISC survival and repair mitigates GI GVHD. Specifically, treatment with Wnt-agonist R-spondin1 to stimulate the Wnt signaling pathway normally responsible for regulating IEC proliferation not only protects ISCs from damage due to conditioning therapy but also ameliorates GVHD pathology under otherwise identical transplant conditions[225]. Recent studies with IL-22, released by innate lymphoid cells, showed that IL-22 primarily affects ISCs to reduce GVHD severity[224]. This protection did not mitigate GVL (graft versus leukemia/lymphoma) responses or alter donor T cell responses. These results collectively suggest that enhancing tissues' ability to regenerate and repair allows them to tolerate alloreactive T cell mediated tissue damage and disease severity (Figure A.4).

Conclusion

Mechanisms of tissue tolerance

Exploring the mechanisms that promote tissue tolerance and exploiting them for therapeutic benefit in addition to continued understanding of immune tolerance could represent a novel area for research in GVHD. Mechanisms of immune and disease tolerance are complex. Similarly, tissue tolerance pathways are likely also complex, involving more than one mechanism of action. However, those pathways shown to regulate tissue tolerance could be classified into categories, much like those used to organize disease tolerance mechanisms. For example, experimental evidence[223-225,253,255-257] has demonstrated that involved pathways might be divided into parenchymal tissue cell-intrinsic and -extrinsic pathways. Furthermore, as reviewed by others, disease tolerance operates, in part, through adaptions to the unique stresses inflammatory attack will induce in parenchymal tissue cells. These stressors include increased protein production, elevated concentrations of reactive oxygen species which can lead to DNA damage, and altered nutrient resource pools[217-219,230]. Experimental evidence directly linking tissue tolerance and disease tolerance is lacking, but it is plausible they are intimately linked and similar tissue-specific adaptations function during GVHD to mediate tissue homeostasis.

It also remains unknown whether pathways of immune and tissue tolerance overlap or act antagonistically or synergistically. Evidence from the various salutary effects of butyrate and the overlapping role of TLR signaling in immune

and tissue functions point to potential overlap of at least some of the pathways for immune vs. tissue tolerance. Tissue tolerance could also include features indistinguishable from tissue damage control, adaptive responses to protect parenchyma from stress and damage. Further work will be necessary to dissect the specific contributions to tissue tolerance and to identify molecular targets for therapies.

Tissues may have variable tolerance capacities

Mechanisms of tissue tolerance may also be observed not just at the cellular level but also at the organ level. Specifically, the ability of an organ tissue to maintain function in spite of pathogenic immune effectors can vary compared to other organ tissues. Clinically, acute GVHD provides a dramatic illustration of this concept. As alluded to above, despite the fact that grafted bone marrow will generate blood cells that circulate through all organ tissues and the fact that allogeneic antigens are ubiquitous, acute GVHD affects only three organs: the skin, liver, and GI tract.

Interestingly, the liver, skin, and GI tract are seemingly amongst the most tolerogenic organ tissues given (1) that they can regenerate and repair injury and (2) that damage to one area of the organ does not necessarily compromise the entire organ. A paper cut does not prevent skin from regulating temperature and, within a certain range, liver and GI damage can be asymptomatic. This then presents an apparent contradiction with the fact that liver, skin, and GI tract are

most susceptible to alloimmune-mediated immunopathology. It also offers no resolution to the clinical observation that GI and skin involvement are seen at almost twice the rate of liver involvement[220].

A possible solution is offered by Little *et al*[258], who argue that in plotting a tolerance graph, a distinction needs to be made between slope and y-intercept. In considering two tissues, *a* and *b*, (Figure A.5, adapted[258]) health under low stress conditions may appear to be greater for *a*, but, under high stress conditions, the picture may change and *b* may show greater tolerance. Under this framework, a tissue's tolerogenic character cannot be fully described by studying its responses to only one category and intensity of stress. Furthermore, tissue tolerance may not be linear, such as in tissue *c* (Figure A.5). In this instance, the intensity of the GVH response, which may be impacted not just by load but also by time, will produce different pictures of tissue tolerance. Thus, even when studying tissue tolerance in the context of GVHD, the conclusions are likely to be context specific.

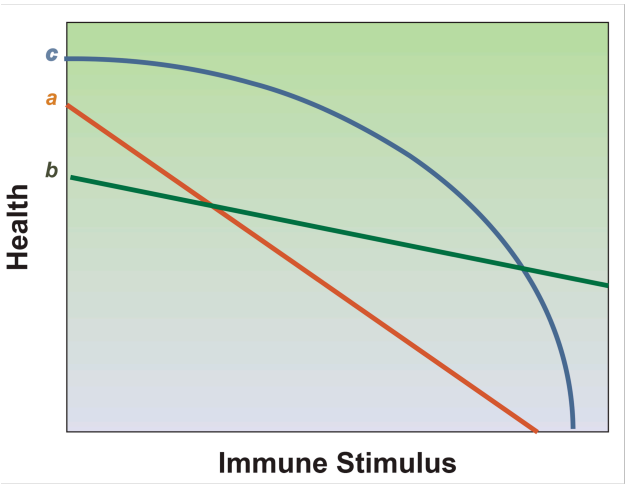

Figure A.5. Tissue tolerance is context dependent. (A) describes a linear relationship by health and immune burden regulated by tissue tolerance. (B) describes another linear relationship, but one where tissue tolerance may appear to be greater or less than (A)

depending on measurement conditions. (C) describes a non-linear mode of tissue tolerance-mediated regulation of health where tissue tolerance may appear relatively high or low depending on measurement conditions.

Future directions

In the prevention and treatment of allogeneic rejection and GVHD, it has become clear that, at least in some cases, immunosuppression or attempts at promoting immune tolerance, in patients, can be insufficient. Considering tolerance as involving both parenchymal/epithelial tissues as well as immune cells leads to novel and impactful ways of considering disease models. Specifically, it becomes possible to consider therapies that may increase tissue tolerance to protect against organ damage without severe global immunosuppression. With this potential for broadening the treatment repertoire, a future can be envisioned where we are able to deliver improved outcomes for patients with GVHD with reduced morbidity and mortality. However, to achieve this, experimentation intentionally directed towards measuring tissue tolerance will need to rigorously performed.

In conclusion, we posit that including ‘tissue tolerance’ in the conceptual tool kit of allogeneic HSCT patient care may allow for better understanding of organ damage from GVHD. If this concept is validated, novel clinical strategies can be developed to capitalize on this deepened understanding, allowing for development of approaches that promote tissue tolerance that complement immune suppression/tolerance strategies to prevent and treat GVHD.

REFERENCES

1 Daste, F., Galli, T. & Tareste, D. Structure and function of longin SNAREs. *J Cell Sci* **128**, 4263-4272, doi:10.1242/jcs.178574 (2015).

2 Sudhof, T. C. & Rothman, J. E. Membrane fusion: grappling with SNARE and SM proteins. *Science* **323**, 474-477, doi:10.1126/science.1161748 (2009).

3 Hong, W. & Lev, S. Tethering the assembly of SNARE complexes. *Trends Cell Biol* **24**, 35-43, doi:10.1016/j.tcb.2013.09.006 (2014).

4 Mancias, J. D. & Goldberg, J. The Transport Signal on Sec22 for Packaging into COPII-Coated Vesicles Is a Conformational Epitope. *Molecular cell* **26**, 403-414, doi:10.1016/j.molcel.2007.03.017 (2007).

5 Cebrian, I. *et al.* Sec22b regulates phagosomal maturation and antigen crosspresentation by dendritic cells. *Cell* **147**, 1355-1368, doi:10.1016/j.cell.2011.11.021 (2011).

6 Petkovic, M. *et al.* The SNARE Sec22b has a non-fusogenic function in plasma membrane expansion. *Nature cell biology* **advance on**, doi:10.1038/ncb2937 (2014).

7 Xu, D., Joglekar, A. P., Williams, A. L. & Hay, J. C. Subunit structure of a mammalian ER/Golgi SNARE complex. *J Biol Chem* **275**, 39631-39639, doi:10.1074/jbc.M007684200 (2000).

8 Hatsuzawa, K. *et al.* Sec22b is a negative regulator of phagocytosis in macrophages. *Mol Biol Cell* **20**, 4435-4443, doi:10.1091/mbc.E09-03-0241 (2009).

9 Wang, T., Grabski, R., Sztul, E. & Hay, J. C. p115-SNARE interactions: a dynamic cycle of p115 binding monomeric SNARE motifs and releasing assembled bundles. *Traffic* **16**, 148-171, doi:10.1111/tra.12242 (2015).

10 Joglekar, A. P., Xu, D., Rigotti, D. J., Fairman, R. & Hay, J. C. The SNARE motif contributes to rbet1 intracellular targeting and dynamics independently of SNARE interactions. *J Biol Chem* **278**, 14121-14133, doi:10.1074/jbc.M300659200 (2003).

11 Hay, J. C. Localization, Dynamics, and Protein Interactions Reveal Distinct Roles for ER and Golgi SNAREs. *The Journal of Cell Biology* **141**, 1489-1502, doi:10.1083/jcb.141.7.1489 (1998).

12 Nair, U. *et al.* SNARE proteins are required for macroautophagy. *Cell* **146**, 290-302, doi:10.1016/j.cell.2011.06.022 (2011).

13 Zhao, X. *et al.* Sec22 regulates endoplasmic reticulum morphology but not autophagy and is required for eye development in Drosophila. *J Biol Chem* **290**, 7943-7951, doi:10.1074/jbc.M115.640920 (2015).

14 Siddiqi, S., Mani, A. M. & Siddiqi, S. A. The identification of the SNARE complex required for the fusion of VLDL-transport vesicle with hepatic cis-Golgi. *Biochem J* **429**, 391-401, doi:10.1042/BJ20100336 (2010).
15 Vogels, M. W. *et al.* Identification of host factors involved in coronavirus replication by quantitative proteomics analysis. *Proteomics* **11**, 64-80, doi:10.1002/pmic.201000309 (2011).
16 Kimura, T. *et al.* Dedicated SNAREs and specialized TRIM cargo receptors mediate secretory autophagy. *EMBO J* **36**, 42-60, doi:10.15252/embj.201695081 (2017).
17 Abuaita, B. H., Burkholder, K. M., Boles, B. R. & O'Riordan, M. X. The Endoplasmic Reticulum Stress Sensor Inositol-Requiring Enzyme 1alpha Augments Bacterial Killing through Sustained Oxidant Production. *MBio* **6**, e00705, doi:10.1128/mBio.00705-15 (2015).
18 Wood, R. E., Newton, P., Latomanski, E. A. & Newton, H. J. Dot/Icm Effector Translocation by Legionella longbeachae Creates a Replicative Vacuole Similar to That of Legionella pneumophila despite Translocation of Distinct Effector Repertoires. *Infect Immun* **83**, 4081-4092, doi:10.1128/IAI.00461-15 (2015).
19 Kagan, J. C., Stein, M.-P., Pypaert, M. & Roy, C. R. Legionella subvert the functions of Rab1 and Sec22b to create a replicative organelle. *The Journal of experimental medicine* **199**, 1201-1211, doi:10.1084/jem.20031706 (2004).
20 Canton, J., Ndjamen, B., Hatsuzawa, K. & Kima, P. E. Disruption of the fusion of Leishmania parasitophorous vacuoles with ER vesicles results in the control of the infection. *Cell Microbiol* **14**, 937-948, doi:10.1111/j.1462-5822.2012.01767.x (2012).
21 Ndjamen, B., Kang, B.-H., Hatsuzawa, K. & Kima, P. E. Leishmania parasitophorous vacuoles interact continuously with the host cell's endoplasmic reticulum; parasitophorous vacuoles are hybrid compartments. *Cellular microbiology* **12**, 1480-1494, doi:10.1111/j.1462-5822.2010.01483.x (2010).
22 Veeraraghavan, J., Ma, J., Hu, Y. & Wang, X. S. Recurrent and pathological gene fusions in breast cancer: current advances in genomic discovery and clinical implications. *Breast Cancer Res Treat* **158**, 219-232, doi:10.1007/s10549-016-3876-y (2016).
23 Zhao, Y., Tan, W., Sheng, W. & Li, X. Identification of Biomarkers Associated With Alzheimer's Disease by Bioinformatics Analysis. *Am J Alzheimers Dis Other Demen* **31**, 163-168, doi:10.1177/1533317515588181 (2016).
24 Dai, J. *et al.* Vps33b regulates Vwf-positive vesicular trafficking in megakaryocytes. *J Pathol* **240**, 108-119, doi:10.1002/path.4762 (2016).
25 Thayanidhi, N. *et al.* Alpha-synuclein delays endoplasmic reticulum (ER)-to-Golgi transport in mammalian cells by antagonizing ER/Golgi SNAREs. *Mol Biol Cell* **21**, 1850-1863, doi:10.1091/mbc.E09-09-0801 (2010).

26 Tang, B. L., Low, D. Y. & Hong, W. Hsec22c: a homolog of yeast Sec22p and mammalian rsec22a and msec22b/ERS-24. *Biochem Biophys Res Commun* **243**, 885-891, doi:10.1006/bbrc.1998.8194 (1998).
27 Lenschow, D. J., Walunas, T. L. & Bluestone, J. A. CD28/B7 system of T cell costimulation. *Annu Rev Immunol* **14**, 233-258, doi:10.1146/annurev.immunol.14.1.233 (1996).
28 Blum, J. S., Wearsch, P. A. & Cresswell, P. Pathways of antigen processing. *Annu Rev Immunol* **31**, 443-473, doi:10.1146/annurev-immunol-032712-095910 (2013).
29 Vyse, T. J. & Todd, J. A. Genetic analysis of autoimmune disease. *Cell* **85**, 311-318 (1996).
30 Ferrara, J. L. & Deeg, H. J. Graft-versus-host disease. *N Engl J Med* **324**, 667-674, doi:10.1056/NEJM199103073241005 (1991).
31 McKenna, R. M., Takemoto, S. K. & Terasaki, P. I. Anti-HLA antibodies after solid organ transplantation. *Transplantation* **69**, 319-326 (2000).
32 Rock, K. L. *et al.* Inhibitors of the proteasome block the degradation of most cell proteins and the generation of peptides presented on MHC class I molecules. *Cell* **78**, 761-771 (1994).
33 Rock, K. L., York, I. A. & Goldberg, A. L. Post-proteasomal antigen processing for major histocompatibility complex class I presentation. *Nat Immunol* **5**, 670-677, doi:10.1038/ni1089 (2004).
34 Townsend, A. & Trowsdale, J. The transporters associated with antigen presentation. *Semin Cell Biol* **4**, 53-61 (1993).
35 Serwold, T., Gonzalez, F., Kim, J., Jacob, R. & Shastri, N. ERAAP customizes peptides for MHC class I molecules in the endoplasmic reticulum. *Nature* **419**, 480-483, doi:10.1038/nature01074 (2002).
36 York, I. A. *et al.* The ER aminopeptidase ERAP1 enhances or limits antigen presentation by trimming epitopes to 8-9 residues. *Nat Immunol* **3**, 1177-1184, doi:10.1038/ni860 (2002).
37 Neefjes, J., Jongsma, M. L. M., Paul, P. & Bakke, O. Towards a systems understanding of MHC class I and MHC class II antigen presentation. *Nature reviews. Immunology* **11**, 823-836, doi:10.1038/nri3084 (2011).
38 Wearsch, P. A., Peaper, D. R. & Cresswell, P. Essential glycan-dependent interactions optimize MHC class I peptide loading. *Proc Natl Acad Sci U S A* **108**, 4950-4955, doi:10.1073/pnas.1102524108 (2011).
39 Hebert, D. N., Garman, S. C. & Molinari, M. The glycan code of the endoplasmic reticulum: asparagine-linked carbohydrates as protein maturation and quality-control tags. *Trends Cell Biol* **15**, 364-370, doi:10.1016/j.tcb.2005.05.007 (2005).
40 Van Gool, S. W., Vandenberghe, P., de Boer, M. & Ceuppens, J. L. CD80, CD86 and CD40 provide accessory signals in a multiple-step T-cell activation model. *Immunol Rev* **153**, 47-83 (1996).
41 Rammensee, H. G., Friede, T. & Stevanoviic, S. MHC ligands and peptide motifs: first listing. *Immunogenetics* **41**, 178-228 (1995).

42 Nelson, C. A. & Fremont, D. H. Structural principles of MHC class II antigen presentation. *Rev Immunogenet* **1**, 47-59 (1999).
43 Yassai, M., Afsari, A., Garlie, J. & Gorski, J. C-terminal anchoring of a peptide to class II MHC via the P10 residue is compatible with a peptide bulge. *J Immunol* **168**, 1281-1285 (2002).
44 Muller, S., Dennemarker, J. & Reinheckel, T. Specific functions of lysosomal proteases in endocytic and autophagic pathways. *Biochim Biophys Acta* **1824**, 34-43, doi:10.1016/j.bbapap.2011.07.003 (2012).
45 Maric, M. *et al.* Defective antigen processing in GILT-free mice. *Science* **294**, 1361-1365, doi:10.1126/science.1065500 (2001).
46 Haque, M. A. *et al.* Absence of gamma-interferon-inducible lysosomal thiol reductase in melanomas disrupts T cell recognition of select immunodominant epitopes. *J Exp Med* **195**, 1267-1277 (2002).
47 Busch, R., Doebele, R. C., Patil, N. S., Pashine, A. & Mellins, E. D. Accessory molecules for MHC class II peptide loading. *Curr Opin Immunol* **12**, 99-106 (2000).
48 Landsverk, O. J., Bakke, O. & Gregers, T. F. MHC II and the endocytic pathway: regulation by invariant chain. *Scand J Immunol* **70**, 184-193, doi:10.1111/j.1365-3083.2009.02301.x (2009).
49 Hofmann, M. W. *et al.* The leucine-based sorting motifs in the cytoplasmic domain of the invariant chain are recognized by the clathrin adaptors AP1 and AP2 and their medium chains. *J Biol Chem* **274**, 36153-36158 (1999).
50 Kropshofer, H. *et al.* Editing of the HLA-DR-peptide repertoire by HLA-DM. *EMBO J* **15**, 6144-6154 (1996).
51 Paul, P. *et al.* A Genome-wide multidimensional RNAi screen reveals pathways controlling MHC class II antigen presentation. *Cell* **145**, 268-283, doi:10.1016/j.cell.2011.03.023 (2011).
52 Vascotto, F. *et al.* The actin-based motor protein myosin II regulates MHC class II trafficking and BCR-driven antigen presentation. *J Cell Biol* **176**, 1007-1019, doi:10.1083/jcb.200611147 (2007).
53 Abbas, A. K., Murphy, K. M. & Sher, A. Functional diversity of helper T lymphocytes. *Nature* **383**, 787-793, doi:10.1038/383787a0 (1996).
54 Casares, N. *et al.* Caspase-dependent immunogenicity of doxorubicin-induced tumor cell death. *J Exp Med* **202**, 1691-1701, doi:10.1084/jem.20050915 (2005).
55 Shimizu, K., Kurosawa, Y., Taniguchi, M., Steinman, R. M. & Fujii, S. Cross-presentation of glycolipid from tumor cells loaded with alpha-galactosylceramide leads to potent and long-lived T cell mediated immunity via dendritic cells. *J Exp Med* **204**, 2641-2653, doi:10.1084/jem.20070458 (2007).
56 Huang, A. *et al.* Role of bone marrow-derived cells in presenting MHC class I-restricted tumor antigens. *Science* **264**, 961-965, doi:10.1126/science.7513904 (1994).

57 Sigal, L. J., Crotty, S., Andino, R. & Rock, K. L. Cytotoxic T-cell immunity to virus-infected non-haematopoietic cells requires presentation of exogenous antigen. *Nature* **398**, 77-80, doi:10.1038/18038 (1999).
58 Iborra, S. *et al.* The DC receptor DNGR-1 mediates cross-priming of CTLs during vaccinia virus infection in mice. *J Clin Invest* **122**, 1628-1643, doi:10.1172/JCI60660 (2012).
59 Smed-Sorensen, A. *et al.* Influenza A virus infection of human primary dendritic cells impairs their ability to cross-present antigen to CD8 T cells. *PLoS Pathog* **8**, e1002572, doi:10.1371/journal.ppat.1002572 (2012).
60 Shen, L., Sigal, L. J., Boes, M. & Rock, K. L. Important role of cathepsin S in generating peptides for TAP-independent MHC class I crosspresentation in vivo. *Immunity* **21**, 155-165, doi:10.1016/j.immuni.2004.07.004 (2004).
61 Toubai, T. *et al.* Host-derived CD8+ dendritic cells are required for induction of optimal graft-versus-tumor responses after experimental allogeneic bone marrow transplantation. *Blood* **121**, 4231-4241, doi:10.1182/blood-2012-05-432872 (2013).
62 Toubai, T., Mathewson, N., Oravecz-Wilson, K. & Reddy, P. Host CD8alpha+ dendritic cells may be a key factor for separating graft-versus-host disease from graft-versus-leukemia. *Biol Blood Marrow Transplant* **21**, 775-776, doi:10.1016/j.bbmt.2015.01.005 (2015).
63 Toubai, T., Tawara, I., Malter, C., Matzinger, P. & Reddy, P. Crucial Role For Cross-Presentation In The Induction Of GVHD By T Cells Directed Against A Single Immunodominant Minor Histocompatibility Antigen Despite Lack Of Epitope Spreading. *Biology of Blood and Marrow Transplantation* **16**, S170-S170, doi:10.1016/j.bbmt.2009.12.058 (2010).
64 Reddy, P. *et al.* A crucial role for antigen-presenting cells and alloantigen expression in graft-versus-leukemia responses. *Nature medicine* **11**, 1244-1249, doi:10.1038/nm1309 (2005).
65 Ferris, S. T. *et al.* A minor subset of Batf3-dependent antigen-presenting cells in islets of Langerhans is essential for the development of autoimmune diabetes. *Immunity* **41**, 657-669, doi:10.1016/j.immuni.2014.09.012 (2014).
66 de Jersey, J. *et al.* Beta cells cannot directly prime diabetogenic CD8 T cells in nonobese diabetic mice. *Proc Natl Acad Sci U S A* **104**, 1295-1300, doi:10.1073/pnas.0610057104 (2007).
67 Calderon, B. & Unanue, E. R. Antigen presentation events in autoimmune diabetes. *Curr Opin Immunol* **24**, 119-128, doi:10.1016/j.coi.2011.11.005 (2012).
68 Esterhazy, D. *et al.* Classical dendritic cells are required for dietary antigen-mediated induction of peripheral T(reg) cells and tolerance. *Nat Immunol* **17**, 545-555, doi:10.1038/ni.3408 (2016).

69 Luckashenak, N. *et al.* Constitutive crosspresentation of tissue antigens by dendritic cells controls CD8+ T cell tolerance in vivo. *Immunity* **28**, 521-532, doi:10.1016/j.immuni.2008.02.018 (2008).
70 Kurts, C., Kosaka, H., Carbone, F. R., Miller, J. F. & Heath, W. R. Class I-restricted cross-presentation of exogenous self-antigens leads to deletion of autoreactive CD8(+) T cells. *J Exp Med* **186**, 239-245 (1997).
71 Gallegos, A. M. & Bevan, M. J. Central tolerance to tissue-specific antigens mediated by direct and indirect antigen presentation. *The Journal of experimental medicine* **200**, 1039-1049, doi:10.1084/jem.20041457 (2004).
72 Alloatti, A. *et al.* Toll-like Receptor 4 Engagement on Dendritic Cells Restrains Phago-Lysosome Fusion and Promotes Cross-Presentation of Antigens. *Immunity* **43**, 1087-1100, doi:10.1016/j.immuni.2015.11.006 (2015).
73 Chougnet, C. A. *et al.* Loss of Phagocytic and Antigen Cross-Presenting Capacity in Aging Dendritic Cells Is Associated with Mitochondrial Dysfunction. *J Immunol* **195**, 2624-2632, doi:10.4049/jimmunol.1501006 (2015).
74 Samie, M. & Cresswell, P. The transcription factor TFEB acts as a molecular switch that regulates exogenous antigen-presentation pathways. *Nat Immunol* **16**, 729-736, doi:10.1038/ni.3196 (2015).
75 Zehner, M. & Burgdorf, S. Sec61 in antigen cross-presentation. *Oncotarget* **6**, 19954-19955, doi:10.18632/oncotarget.4587 (2015).
76 Hari, A. *et al.* Redirecting soluble antigen for MHC class I cross-presentation during phagocytosis. *European journal of immunology* **45**, 383-395, doi:10.1002/eji.201445156 (2014).
77 Desch, A. N. *et al.* Dendritic cell subsets require cis-activation for cytotoxic CD8 T-cell induction. *Nat Commun* **5**, 4674, doi:10.1038/ncomms5674 (2014).
78 Nair-Gupta, P. *et al.* TLR signals induce phagosomal MHC-I delivery from the endosomal recycling compartment to allow cross-presentation. *Cell* **158**, 506-521, doi:10.1016/j.cell.2014.04.054 (2014).
79 Matheoud, D. *et al.* Cross-presentation by dendritic cells from live cells induces protective immune responses in vivo. *Blood* **115**, 4412-4420, doi:10.1182/blood-2009-11-255935 (2010).
80 Savina, A. *et al.* NOX2 controls phagosomal pH to regulate antigen processing during crosspresentation by dendritic cells. *Cell* **126**, 205-218, doi:10.1016/j.cell.2006.05.035 (2006).
81 Savina, A. *et al.* The small GTPase Rac2 controls phagosomal alkalinization and antigen crosspresentation selectively in CD8(+) dendritic cells. *Immunity* **30**, 544-555, doi:10.1016/j.immuni.2009.01.013 (2009).

82 Guermonprez, P. *et al.* ER-phagosome fusion defines an MHC class I cross-presentation compartment in dendritic cells. *Nature* **425**, 397-402, doi:10.1038/nature01911 (2003).
83 Houde, M. *et al.* Phagosomes are competent organelles for antigen cross-presentation. *Nature* **425**, 402-406, doi:10.1038/nature01912 (2003).
84 den Haan, J. M. M., Lehar, S. M. & Bevan, M. J. Cd8+ but Not Cd8- Dendritic Cells Cross-Prime Cytotoxic T Cells in Vivo. *Journal of Experimental Medicine* **192**, 1685-1696, doi:10.1084/jem.192.12.1685 (2000).
85 Bevan, M. J. Cross-priming for a secondary cytotoxic response to minor H antigens with H-2 congenic cells which do not cross-react in the cytotoxic assay. *The Journal of experimental medicine* **143**, 1283-1288 (1976).
86 Bevan, M. J. Minor H antigens introduced on H-2 different stimulating cells cross-react at the cytotoxic T cell level during in vivo priming. *J Immunol* **117**, 2233-2238 (1976).
87 Lin, M. L. *et al.* Selective suicide of cross-presenting CD8+ dendritic cells by cytochrome c injection shows functional heterogeneity within this subset. *Proc Natl Acad Sci U S A* **105**, 3029-3034, doi:10.1073/pnas.0712394105 (2008).
88 Norbury, C. C., Hewlett, L. J., Prescott, A. R., Shastri, N. & Watts, C. Class I MHC presentation of exogenous soluble antigen via macropinocytosis in bone marrow macrophages. *Immunity* **3**, 783-791 (1995).
89 Kovacsovics-Bankowski, M. & Rock, K. L. A phagosome-to-cytosol pathway for exogenous antigens presented on MHC class I molecules. *Science* **267**, 243-246 (1995).
90 Jung, S. *et al.* In Vivo Depletion of CD11c+ Dendritic Cells Abrogates Priming of CD8+ T Cells by Exogenous Cell-Associated Antigens. *Immunity* **17**, 211-220, doi:10.1016/S1074-7613(02)00365-5 (2002).
91 Cruz, F. M., Colbert, J. D., Merino, E., Kriegsman, B. A. & Rock, K. L. The Biology and Underlying Mechanisms of Cross-Presentation of Exogenous Antigens on MHC-I Molecules. *Annu Rev Immunol* **35**, 149-176, doi:10.1146/annurev-immunol-041015-055254 (2017).
92 Joffre, O. P., Segura, E., Savina, A. & Amigorena, S. Cross-presentation by dendritic cells. *Nature reviews. Immunology* **12**, 557-569, doi:10.1038/nri3254 (2012).
93 Ma, W. *et al.* Long-Peptide Cross-Presentation by Human Dendritic Cells Occurs in Vacuoles by Peptide Exchange on Nascent MHC Class I Molecules. *J Immunol* **196**, 1711-1720, doi:10.4049/jimmunol.1501574 (2016).
94 Song, R. & Harding, C. V. Roles of proteasomes, transporter for antigen presentation (TAP), and beta 2-microglobulin in the processing of

bacterial or particulate antigens via an alternate class I MHC processing pathway. *J Immunol* **156**, 4182-4190 (1996).

95 Tiwari, N. *et al.* A transporter associated with antigen-processing independent vacuolar pathway for the MHC class I-mediated presentation of endogenous transmembrane proteins. *J Immunol* **178**, 7932-7942 (2007).

96 Bertholet, S. *et al.* Leishmania Antigens Are Presented to CD8+ T Cells by a Transporter Associated with Antigen Processing-Independent Pathway In Vitro and In Vivo. *The Journal of Immunology* **177**, 3525-3533, doi:10.4049/jimmunol.177.6.3525 (2006).

97 Mant, A., Chinnery, F., Elliott, T. & Williams, A. P. The pathway of cross-presentation is influenced by the particle size of phagocytosed antigen. *Immunology* **136**, 163-175, doi:10.1111/j.1365-2567.2012.03558.x (2012).

98 Fonteneau, J. F. *et al.* Characterization of the MHC class I cross-presentation pathway for cell-associated antigens by human dendritic cells. *Blood* **102**, 4448-4455, doi:10.1182/blood-2003-06-1801 (2003).

99 Imai, T. *et al.* Heat shock protein 90 (HSP90) contributes to cytosolic translocation of extracellular antigen for cross-presentation by dendritic cells. *Proc Natl Acad Sci U S A* **108**, 16363-16368, doi:10.1073/pnas.1108372108 (2011).

100 Burgdorf, S., Schölz, C., Kautz, A., Tampé, R. & Kurts, C. Spatial and mechanistic separation of cross-presentation and endogenous antigen presentation. *Nature immunology* **9**, 558-566, doi:10.1038/ni.1601 (2008).

101 Merzougui, N., Kratzer, R., Saveanu, L. & van Endert, P. A proteasome-dependent, TAP-independent pathway for cross-presentation of phagocytosed antigen. *EMBO Rep* **12**, 1257-1264, doi:10.1038/embor.2011.203 (2011).

102 Belizaire, R. & Unanue, E. R. Targeting proteins to distinct subcellular compartments reveals unique requirements for MHC class I and II presentation. *Proc Natl Acad Sci U S A* **106**, 17463-17468, doi:10.1073/pnas.0908583106 (2009).

103 Rock, K. L., Gamble, S. & Rothstein, L. Presentation of exogenous antigen with class I major histocompatibility complex molecules. *Science* **249**, 918-921 (1990).

104 Kovacsovics-Bankowski, M., Clark, K., Benacerraf, B. & Rock, K. L. Efficient major histocompatibility complex class I presentation of exogenous antigen upon phagocytosis by macrophages. *Proc Natl Acad Sci U S A* **90**, 4942-4946 (1993).

105 van Montfoort, N. *et al.* Circulating specific antibodies enhance systemic cross-priming by delivery of complexed antigen to dendritic cells in vivo. *Eur J Immunol* **42**, 598-606, doi:10.1002/eji.201141613 (2012).

106 Burgdorf, S., Lukacs-Kornek, V. & Kurts, C. The mannose receptor mediates uptake of soluble but not of cell-associated antigen for cross-

presentation. *J Immunol* **176**, 6770-6776, doi:10.4049/jimmunol.176.11.6770 (2006).
107 Kamphorst, A. O., Guermonprez, P., Dudziak, D. & Nussenzweig, M. C. Route of antigen uptake differentially impacts presentation by dendritic cells and activated monocytes. *J Immunol* **185**, 3426-3435, doi:10.4049/jimmunol.1001205 (2010).
108 Pfeifer, J. D. *et al.* Phagocytic processing of bacterial antigens for class I MHC presentation to T cells. *Nature* **361**, 359-362, doi:10.1038/361359a0 (1993).
109 Smyth, L. A. *et al.* Acquisition of MHC:peptide complexes by dendritic cells contributes to the generation of antiviral CD8+ T cell immunity in vivo. *J Immunol* **189**, 2274-2282, doi:10.4049/jimmunol.1200664 (2012).
110 Li, L. *et al.* Cross-dressed CD8alpha+/CD103+ dendritic cells prime CD8+ T cells following vaccination. *Proc Natl Acad Sci U S A* **109**, 12716-12721, doi:10.1073/pnas.1203468109 (2012).
111 Dolan, B. P., Gibbs, K. D., Jr. & Ostrand-Rosenberg, S. Dendritic cells cross-dressed with peptide MHC class I complexes prime CD8+ T cells. *J Immunol* **177**, 6018-6024 (2006).
112 Ruggiano, A., Foresti, O. & Carvalho, P. Quality control: ER-associated degradation: protein quality control and beyond. *J Cell Biol* **204**, 869-879, doi:10.1083/jcb.201312042 (2014).
113 Ye, Y., Meyer, H. H. & Rapoport, T. A. The AAA ATPase Cdc48/p97 and its partners transport proteins from the ER into the cytosol. *Nature* **414**, 652-656, doi:10.1038/414652a (2001).
114 Ackerman, A. L., Giodini, A. & Cresswell, P. A role for the endoplasmic reticulum protein retrotranslocation machinery during crosspresentation by dendritic cells. *Immunity* **25**, 607-617, doi:10.1016/j.immuni.2006.08.017 (2006).
115 Zehner, M. *et al.* Mannose receptor polyubiquitination regulates endosomal recruitment of p97 and cytosolic antigen translocation for cross-presentation. *Proc Natl Acad Sci U S A* **108**, 9933-9938, doi:10.1073/pnas.1102397108 (2011).
116 Menager, J. *et al.* Cross-presentation of synthetic long peptides by human dendritic cells: a process dependent on ERAD component p97/VCP but Not sec61 and/or Derlin-1. *PLoS One* **9**, e89897, doi:10.1371/journal.pone.0089897 (2014).
117 Zehner, M. *et al.* The translocon protein Sec61 mediates antigen transport from endosomes in the cytosol for cross-presentation to CD8(+) T cells. *Immunity* **42**, 850-863, doi:10.1016/j.immuni.2015.04.008 (2015).
118 Wiertz, E. J. *et al.* Sec61-mediated transfer of a membrane protein from the endoplasmic reticulum to the proteasome for destruction. *Nature* **384**, 432-438, doi:10.1038/384432a0 (1996).

119 Mehnert, M., Sommer, T. & Jarosch, E. Der1 promotes movement of misfolded proteins through the endoplasmic reticulum membrane. *Nat Cell Biol* **16**, 77-86, doi:10.1038/ncb2882 (2014).
120 Carvalho, P., Stanley, A. M. & Rapoport, T. A. Retrotranslocation of a misfolded luminal ER protein by the ubiquitin-ligase Hrd1p. *Cell* **143**, 579-591, doi:10.1016/j.cell.2010.10.028 (2010).
121 Hornung, V. *et al.* Silica crystals and aluminum salts activate the NALP3 inflammasome through phagosomal destabilization. *Nat Immunol* **9**, 847-856, doi:10.1038/ni.1631 (2008).
122 Dingjan, I. *et al.* Lipid peroxidation causes endosomal antigen release for cross-presentation. *Sci Rep* **6**, 22064, doi:10.1038/srep22064 (2016).
123 Accapezzato, D. *et al.* Chloroquine enhances human CD8+ T cell responses against soluble antigens in vivo. *J Exp Med* **202**, 817-828, doi:10.1084/jem.20051106 (2005).
124 Jancic, C. *et al.* Rab27a regulates phagosomal pH and NADPH oxidase recruitment to dendritic cell phagosomes. *Nature cell biology* **9**, 367-378, doi:10.1038/ncb1552 (2007).
125 Graham, D. B. *et al.* An ITAM-signaling pathway controls cross-presentation of particulate but not soluble antigens in dendritic cells. *J Exp Med* **204**, 2889-2897, doi:10.1084/jem.20071283 (2007).
126 Ding, Y. *et al.* The lectin Siglec-G inhibits dendritic cell cross-presentation by impairing MHC class I-peptide complex formation. *Nat Immunol* **17**, 1167-1175, doi:10.1038/ni.3535 (2016).
127 Bougneres, L. *et al.* A role for lipid bodies in the cross-presentation of phagocytosed antigens by MHC class I in dendritic cells. *Immunity* **31**, 232-244, doi:10.1016/j.immuni.2009.06.022 (2009).
128 Rizzitelli, A. *et al.* Serpinb9 (Spi6)-deficient mice are impaired in dendritic cell-mediated antigen cross-presentation. *Immunol Cell Biol* **90**, 841-851, doi:10.1038/icb.2012.29 (2012).
129 Basha, G. *et al.* MHC class I endosomal and lysosomal trafficking coincides with exogenous antigen loading in dendritic cells. *PLoS One* **3**, e3247, doi:10.1371/journal.pone.0003247 (2008).
130 Ramachandra, L., Sramkoski, R. M., Canaday, D. H., Boom, W. H. & Harding, C. V. Flow analysis of MHC molecules and other membrane proteins in isolated phagosomes. *J Immunol Methods* **213**, 53-71 (1998).
131 Lizee, G. *et al.* Control of dendritic cell cross-presentation by the major histocompatibility complex class I cytoplasmic domain. *Nat Immunol* **4**, 1065-1073, doi:10.1038/ni989 (2003).
132 Crespo, M. I. *et al.* TLR7 triggering with polyuridylic acid promotes cross-presentation in CD8alpha+ conventional dendritic cells by enhancing antigen preservation and MHC class I antigen permanence on the dendritic cell surface. *J Immunol* **190**, 948-960, doi:10.4049/jimmunol.1102725 (2013).

133 Zelenay, S. *et al.* The dendritic cell receptor DNGR-1 controls endocytic handling of necrotic cell antigens to favor cross-priming of CTLs in virus-infected mice. *J Clin Invest* **122**, 1615-1627, doi:10.1172/JCI60644 (2012).
134 Burgdorf, S., Kautz, A., Böhnert, V., Knolle, P. A. & Kurts, C. Distinct pathways of antigen uptake and intracellular routing in CD4 and CD8 T cell activation. *Science (New York, N.Y.)* **316**, 612-616, doi:10.1126/science.1137971 (2007).
135 Saveanu, L. *et al.* IRAP identifies an endosomal compartment required for MHC class I cross-presentation. *Science* **325**, 213-217, doi:10.1126/science.1172845 (2009).
136 Chatterjee, B. *et al.* Internalization and endosomal degradation of receptor-bound antigens regulate the efficiency of cross presentation by human dendritic cells. *Blood* **120**, 2011-2020, doi:10.1182/blood-2012-01-402370 (2012).
137 Ackerman, A. L., Kyritsis, C., Tampé, R. & Cresswell, P. Early phagosomes in dendritic cells form a cellular compartment sufficient for cross presentation of exogenous antigens. *Proceedings of the National Academy of Sciences of the United States of America* **100**, 12889-12894, doi:10.1073/pnas.1735556100 (2003).
138 Sugita, M. & Brenner, M. B. Association of the invariant chain with major histocompatibility complex class I molecules directs trafficking to endocytic compartments. *J Biol Chem* **270**, 1443-1448 (1995).
139 Basha, G. *et al.* A CD74-dependent MHC class I endolysosomal cross-presentation pathway. *Nat Immunol* **13**, 237-245, doi:10.1038/ni.2225 (2012).
140 Harding, C. V. & Song, R. Phagocytic processing of exogenous particulate antigens by macrophages for presentation by class I MHC molecules. *J Immunol* **153**, 4925-4933 (1994).
141 Zou, L. *et al.* The GTPase Rab3b/3c-positive recycling vesicles are involved in cross-presentation in dendritic cells. *Proc Natl Acad Sci U S A* **106**, 15801-15806, doi:10.1073/pnas.0905684106 (2009).
142 Cebrian, I., Croce, C., Guerrero, N. A., Blanchard, N. & Mayorga, L. S. Rab22a controls MHC-I intracellular trafficking and antigen cross-presentation by dendritic cells. *EMBO Rep* **17**, 1753-1765, doi:10.15252/embr.201642358 (2016).
143 Weigert, R., Yeung, A. C., Li, J. & Donaldson, J. G. Rab22a regulates the recycling of membrane proteins internalized independently of clathrin. *Mol Biol Cell* **15**, 3758-3770, doi:10.1091/mbc.E04-04-0342 (2004).
144 Lee, H. K. *et al.* In vivo requirement for Atg5 in antigen presentation by dendritic cells. *Immunity* **32**, 227-239, doi:10.1016/j.immuni.2009.12.006 (2010).

145 Mintern, J. D. *et al.* Differential use of autophagy by primary dendritic cells specialized in cross-presentation. *Autophagy* **11**, 906-917, doi:10.1080/15548627.2015.1045178 (2015).
146 Martinez, J. *et al.* Molecular characterization of LC3-associated phagocytosis reveals distinct roles for Rubicon, NOX2 and autophagy proteins. *Nat Cell Biol* **17**, 893-906, doi:10.1038/ncb3192 (2015).
147 Sanjuan, M. A. *et al.* Toll-like receptor signalling in macrophages links the autophagy pathway to phagocytosis. *Nature* **450**, 1253-1257, doi:10.1038/nature06421 (2007).
148 Wagner, C. S., Grotzke, J. & Cresswell, P. Intracellular regulation of cross-presentation during dendritic cell maturation. *PloS one* **8**, e76801-e76801, doi:10.1371/journal.pone.0076801 (2013).
149 Wilson, N. S. *et al.* Systemic activation of dendritic cells by Toll-like receptor ligands or malaria infection impairs cross-presentation and antiviral immunity. *Nat Immunol* **7**, 165-172, doi:10.1038/ni1300 (2006).
150 Li, Y. *et al.* The Valpha14 invariant natural killer T cell TCR forces microbial glycolipids and CD1d into a conserved binding mode. *J Exp Med* **207**, 2383-2393, doi:10.1084/jem.20101335 (2010).
151 Nair-Gupta, P. *et al.* TLR Signals Induce Phagosomal MHC-I Delivery from the Endosomal Recycling Compartment to Allow Cross-Presentation. *Cell* **158**, 506-521, doi:10.1016/j.cell.2014.04.054 (2014).
152 Diamond, M. S. *et al.* Type I interferon is selectively required by dendritic cells for immune rejection of tumors. *J Exp Med* **208**, 1989-2003, doi:10.1084/jem.20101158 (2011).
153 Steinman, R. M., Kaplan, G., Witmer, M. D. & Cohn, Z. A. Identification of a novel cell type in peripheral lymphoid organs of mice. V. Purification of spleen dendritic cells, new surface markers, and maintenance in vitro. *J Exp Med* **149**, 1-16 (1979).
154 Metlay, J. P. *et al.* The distinct leukocyte integrins of mouse spleen dendritic cells as identified with new hamster monoclonal antibodies. *J Exp Med* **171**, 1753-1771 (1990).
155 Hildner, K. *et al.* Batf3 deficiency reveals a critical role for CD8alpha+ dendritic cells in cytotoxic T cell immunity. *Science (New York, N.Y.)* **322**, 1097-1100, doi:10.1126/science.1164206 (2008).
156 Thaikruea, L. & Siriariyaporn, P. The magnitude of severe box jellyfish cases on Koh Samui and Koh Pha-ngan in the Gulf of Thailand. *BMC Res Notes* **9**, 108, doi:10.1186/s13104-016-1931-8 (2016).
157 Tel, J. *et al.* Targeting uptake receptors on human plasmacytoid dendritic cells triggers antigen cross-presentation and robust type I IFN secretion. *J Immunol* **191**, 5005-5012, doi:10.4049/jimmunol.1300787 (2013).
158 Segura, E., Durand, M. & Amigorena, S. Similar antigen cross-presentation capacity and phagocytic functions in all freshly isolated human lymphoid organ-resident dendritic cells. *J Exp Med* **210**, 1035-1047, doi:10.1084/jem.20121103 (2013).

159 Rock, K. L., Rothstein, L., Gamble, S. & Fleischacker, C. Characterization of antigen-presenting cells that present exogenous antigens in association with class I MHC molecules. *J Immunol* **150**, 438-446 (1993).
160 Busche, A. *et al.* Priming of CD8+ T cells against cytomegalovirus-encoded antigens is dominated by cross-presentation. *J Immunol* **190**, 2767-2777, doi:10.4049/jimmunol.1200966 (2013).
161 Durai, V. & Murphy, K. M. Functions of Murine Dendritic Cells. *Immunity* **45**, 719-736, doi:10.1016/j.immuni.2016.10.010 (2016).
162 Crozat, K. *et al.* The XC chemokine receptor 1 is a conserved selective marker of mammalian cells homologous to mouse CD8alpha+ dendritic cells. *J Exp Med* **207**, 1283-1292, doi:10.1084/jem.20100223 (2010).
163 Crozat, K. *et al.* Cutting edge: expression of XCR1 defines mouse lymphoid-tissue resident and migratory dendritic cells of the CD8alpha+ type. *J Immunol* **187**, 4411-4415, doi:10.4049/jimmunol.1101717 (2011).
164 Guilliams, M. *et al.* Unsupervised High-Dimensional Analysis Aligns Dendritic Cells across Tissues and Species. *Immunity* **45**, 669-684, doi:10.1016/j.immuni.2016.08.015 (2016).
165 Chiang, M. C. *et al.* Differential uptake and cross-presentation of soluble and necrotic cell antigen by human DC subsets. *Eur J Immunol* **46**, 329-339, doi:10.1002/eji.201546023 (2016).
166 Cohn, L. *et al.* Antigen delivery to early endosomes eliminates the superiority of human blood BDCA3+ dendritic cells at cross presentation. *J Exp Med* **210**, 1049-1063, doi:10.1084/jem.20121251 (2013).
167 Haniffa, M. *et al.* Human tissues contain CD141hi cross-presenting dendritic cells with functional homology to mouse CD103+ nonlymphoid dendritic cells. *Immunity* **37**, 60-73, doi:10.1016/j.immuni.2012.04.012 (2012).
168 Desch, A. N. *et al.* CD103+ pulmonary dendritic cells preferentially acquire and present apoptotic cell-associated antigen. *J Exp Med* **208**, 1789-1797, doi:10.1084/jem.20110538 (2011).
169 Porgador, A., Yewdell, J. W., Deng, Y., Bennink, J. R. & Germain, R. N. Localization, quantitation, and in situ detection of specific peptide-MHC class I complexes using a monoclonal antibody. *Immunity* **6**, 715-726 (1997).
170 Hogquist, K. A. *et al.* T cell receptor antagonist peptides induce positive selection. *Cell* **76**, 17-27 (1994).
171 Shastri, N. & Gonzalez, F. Endogenous generation and presentation of the ovalbumin peptide/Kb complex to T cells. *J Immunol* **150**, 2724-2736 (1993).
172 Brandle, D. *et al.* T cell development and repertoire of mice expressing a single T cell receptor alpha chain. *Eur J Immunol* **25**, 2650-2655, doi:10.1002/eji.1830250937 (1995).

173 Muul, L. M. *et al.* Measurement of proliferative responses of cultured lymphocytes. *Curr Protoc Immunol* **Chapter 7**, Unit7 10, doi:10.1002/0471142735.im0710s94 (2011).
174 Lalor, P. A., Mapp, P. I., Hall, P. A. & Revell, P. A. Proliferative activity of cells in the synovium as demonstrated by a monoclonal antibody, Ki67. *Rheumatol Int* **7**, 183-186 (1987).
175 Smith-Garvin, J. E., Koretzky, G. A. & Jordan, M. S. T cell activation. *Annu Rev Immunol* **27**, 591-619, doi:10.1146/annurev.immunol.021908.132706 (2009).
176 Chen, Y. A. & Scheller, R. H. SNARE-mediated membrane fusion. *Nat Rev Mol Cell Biol* **2**, 98-106, doi:10.1038/35052017 (2001).
177 Zhang, T., Wong, S. H., Tang, B. L., Xu, Y. & Hong, W. Morphological and functional association of Sec22b/ERS-24 with the pre-Golgi intermediate compartment. *Mol Biol Cell* **10**, 435-453, doi:10.1091/mbc.10.2.435 (1999).
178 Arasaki, K. & Roy, C. R. Legionella pneumophila promotes functional interactions between plasma membrane syntaxins and Sec22b. *Traffic* **11**, 587-600, doi:10.1111/j.1600-0854.2010.01050.x (2010).
179 Arasaki, K., Toomre, D. K. & Roy, C. R. The Legionella pneumophila effector DrrA is sufficient to stimulate SNARE-dependent membrane fusion. *Cell Host Microbe* **11**, 46-57, doi:10.1016/j.chom.2011.11.009 (2012).
180 Renna, M. *et al.* Autophagic substrate clearance requires activity of the syntaxin-5 SNARE complex. *J Cell Sci* **124**, 469-482, doi:10.1242/jcs.076489 (2011).
181 Maguire, S. *et al.* Targeting of Slc25a21 is associated with orofacial defects and otitis media due to disrupted expression of a neighbouring gene. *PLoS One* **9**, e91807, doi:10.1371/journal.pone.0091807 (2014).
182 Keller, G., Kennedy, M., Papayannopoulou, T. & Wiles, M. V. Hematopoietic commitment during embryonic stem cell differentiation in culture. *Mol Cell Biol* **13**, 473-486 (1993).
183 Zmuidzinas, A. *et al.* The vav proto-oncogene is required early in embryogenesis but not for hematopoietic development in vitro. *EMBO J* **14**, 1-11 (1995).
184 Bustelo, X. R., Rubin, S. D., Suen, K. L., Carrasco, D. & Barbacid, M. Developmental expression of the vav protooncogene. *Cell Growth Differ* **4**, 297-308 (1993).
185 Banchereau, J. & Steinman, R. M. Dendritic cells and the control of immunity. *Nature* **392**, 245-252, doi:10.1038/32588 (1998).
186 Gutierrez-Martinez, E. *et al.* Cross-Presentation of Cell-Associated Antigens by MHC Class I in Dendritic Cell Subsets. *Front Immunol* **6**, 363, doi:10.3389/fimmu.2015.00363 (2015).

187 Mintern, J. D., Macri, C. & Villadangos, J. A. Modulation of antigen presentation by intracellular trafficking. *Current opinion in immunology* **34C**, 16-21, doi:10.1016/j.coi.2014.12.006 (2015).
188 Savina, A. *et al.* NOX2 controls phagosomal pH to regulate antigen processing during crosspresentation by dendritic cells. *Cell* **126**, 205-218, doi:10.1016/j.cell.2006.05.035 (2006).
189 Palmowski, M. J. *et al.* Role of immunoproteasomes in cross-presentation. *J Immunol* **177**, 983-990, doi:10.4049/jimmunol.177.2.983 (2006).
190 Firat, E. *et al.* The role of endoplasmic reticulum-associated aminopeptidase 1 in immunity to infection and in cross-presentation. *J Immunol* **178**, 2241-2248, doi:10.4049/jimmunol.178.4.2241 (2007).
191 Adiko, A. C., Babdor, J., Gutierrez-Martinez, E., Guermonprez, P. & Saveanu, L. Intracellular Transport Routes for MHC I and Their Relevance for Antigen Cross-Presentation. *Front Immunol* **6**, 335, doi:10.3389/fimmu.2015.00335 (2015).
192 Segura, E. & Amigorena, S. Cross-Presentation in Mouse and Human Dendritic Cells. *Adv Immunol* **127**, 1-31, doi:10.1016/bs.ai.2015.03.002 (2015).
193 Blander, J. M. The comings and goings of MHC class I molecules herald a new dawn in cross-presentation. *Immunol Rev* **272**, 65-79, doi:10.1111/imr.12428 (2016).
194 Nair-Gupta, P. & Blander, J. M. An Updated View of the Intracellular Mechanisms Regulating Cross-Presentation. *Frontiers in immunology* **4**, 401-401, doi:10.3389/fimmu.2013.00401 (2013).
195 Mantegazza, A. R., Magalhaes, J. G., Amigorena, S. & Marks, M. S. Presentation of phagocytosed antigens by MHC class I and II. *Traffic (Copenhagen, Denmark)* **14**, 135-152, doi:10.1111/tra.12026 (2013).
196 Schuette, V. & Burgdorf, S. The ins-and-outs of endosomal antigens for cross-presentation. *Current Opinion in Immunology* **26**, 63-68, doi:10.1016/j.coi.2013.11.001 (2014).
197 Kool, M. *et al.* Alum adjuvant boosts adaptive immunity by inducing uric acid and activating inflammatory dendritic cells. *The Journal of experimental medicine* **205**, 869-882, doi:10.1084/jem.20071087 (2008).
198 Rossi, A. *et al.* Genetic compensation induced by deleterious mutations but not gene knockdowns. *Nature* **524**, 230-233, doi:10.1038/nature14580 (2015).
199 Jackson, A. L. *et al.* Expression profiling reveals off-target gene regulation by RNAi. *Nat Biotechnol* **21**, 635-637, doi:10.1038/nbt831 (2003).
200 Scacheri, P. C. *et al.* Short interfering RNAs can induce unexpected and divergent changes in the levels of untargeted proteins in mammalian cells. *Proc Natl Acad Sci U S A* **101**, 1892-1897, doi:10.1073/pnas.0308698100 (2004).

201 Snove, O., Jr. & Holen, T. Many commonly used siRNAs risk off-target activity. *Biochem Biophys Res Commun* **319**, 256-263, doi:10.1016/j.bbrc.2004.04.175 (2004).
202 Jackson, A. L. & Linsley, P. S. Noise amidst the silence: off-target effects of siRNAs? *Trends Genet* **20**, 521-524, doi:10.1016/j.tig.2004.08.006 (2004).
203 Hendel, A., Fine, E. J., Bao, G. & Porteus, M. H. Quantifying on- and off-target genome editing. *Trends Biotechnol* **33**, 132-140, doi:10.1016/j.tibtech.2014.12.001 (2015).
204 Koo, T., Lee, J. & Kim, J. S. Measuring and Reducing Off-Target Activities of Programmable Nucleases Including CRISPR-Cas9. *Mol Cells* **38**, 475-481, doi:10.14348/molcells.2015.0103 (2015).
205 Fu, Y. *et al.* High-frequency off-target mutagenesis induced by CRISPR-Cas nucleases in human cells. *Nat Biotechnol* **31**, 822-826, doi:10.1038/nbt.2623 (2013).
206 Hsu, P. D. *et al.* DNA targeting specificity of RNA-guided Cas9 nucleases. *Nat Biotechnol* **31**, 827-832, doi:10.1038/nbt.2647 (2013).
207 Pattanayak, V. *et al.* High-throughput profiling of off-target DNA cleavage reveals RNA-programmed Cas9 nuclease specificity. *Nat Biotechnol* **31**, 839-843, doi:10.1038/nbt.2673 (2013).
208 Kok, F. O. *et al.* Reverse genetic screening reveals poor correlation between morpholino-induced and mutant phenotypes in zebrafish. *Dev Cell* **32**, 97-108, doi:10.1016/j.devcel.2014.11.018 (2015).
209 Bray, N. L., Pimentel, H., Melsted, P. & Pachter, L. Near-optimal probabilistic RNA-seq quantification. *Nat Biotechnol* **34**, 525-527, doi:10.1038/nbt.3519 (2016).
210 Li, B. & Dewey, C. N. RSEM: accurate transcript quantification from RNA-Seq data with or without a reference genome. *BMC Bioinformatics* **12**, 323, doi:10.1186/1471-2105-12-323 (2011).
211 Love, M. I., Huber, W. & Anders, S. Moderated estimation of fold change and dispersion for RNA-seq data with DESeq2. *Genome Biol* **15**, 550, doi:10.1186/s13059-014-0550-8 (2014).
212 Buaillon, C. *et al.* MHC I presentation of Toxoplasma gondii immunodominant antigen does not require Sec22b and is regulated by antigen orientation at the vacuole membrane. *Eur J Immunol*, doi:10.1002/eji.201646859 (2017).
213 Cecconi, F. & Levine, B. The role of autophagy in mammalian development: cell makeover rather than cell death. *Dev Cell* **15**, 344-357, doi:10.1016/j.devcel.2008.08.012 (2008).
214 Chamberland, J. P., Antonow, L. T., Dias Santos, M. & Ritter, B. NECAP2 controls clathrin coat recruitment to early endosomes for fast endocytic recycling. *J Cell Sci* **129**, 2625-2637, doi:10.1242/jcs.173708 (2016).

215 Parnas, O. *et al.* A Genome-wide CRISPR Screen in Primary Immune Cells to Dissect Regulatory Networks. *Cell* **162**, 675-686, doi:10.1016/j.cell.2015.06.059 (2015).
216 Brandizzi, F. & Barlowe, C. Organization of the ER-Golgi interface for membrane traffic control. *Nature reviews. Molecular cell biology* **14**, 382-392, doi:10.1038/nrm3588 (2013).
217 Ayres, J. S. & Schneider, D. S. Tolerance of infections. *Annu Rev Immunol* **30**, 271-294, doi:10.1146/annurev-immunol-020711-075030 (2012).
218 Medzhitov, R., Schneider, D. S. & Soares, M. P. Disease tolerance as a defense strategy. *Science* **335**, 936-941, doi:10.1126/science.1214935 (2012).
219 Soares, M. P., Gozzelino, R. & Weis, S. Tissue damage control in disease tolerance. *Trends Immunol* **35**, 483-494, doi:10.1016/j.it.2014.08.001 (2014).
220 Ratanatharathorn, V. *et al.* Phase III study comparing methotrexate and tacrolimus (prograf, FK506) with methotrexate and cyclosporine for graft-versus-host disease prophylaxis after HLA-identical sibling bone marrow transplantation. *Blood* **92**, 2303-2314 (1998).
221 Mathieu, A. L. *et al.* PRKDC mutations associated with immunodeficiency, granuloma, and autoimmune regulator-dependent autoimmunity. *J Allergy Clin Immunol* **135**, 1578-1588 e1575, doi:10.1016/j.jaci.2015.01.040 (2015).
222 Rakoff-Nahoum, S., Paglino, J., Eslami-Varzaneh, F., Edberg, S. & Medzhitov, R. Recognition of commensal microflora by toll-like receptors is required for intestinal homeostasis. *Cell* **118**, 229-241, doi:10.1016/j.cell.2004.07.002 (2004).
223 Mathewson, N. D. *et al.* Gut microbiome-derived metabolites modulate intestinal epithelial cell damage and mitigate graft-versus-host disease. *Nat Immunol*, doi:10.1038/ni.3400 (2016).
224 Hanash, A. M. *et al.* Interleukin-22 protects intestinal stem cells from immune-mediated tissue damage and regulates sensitivity to graft versus host disease. *Immunity* **37**, 339-350, doi:10.1016/j.immuni.2012.05.028 (2012).
225 Takashima, S. *et al.* The Wnt agonist R-spondin1 regulates systemic graft-versus-host disease by protecting intestinal stem cells. *J Exp Med* **208**, 285-294, doi:10.1084/jem.20101559 (2011).
226 Lynch, R. J. & Platt, J. L. Accommodation in organ transplantation. *Curr Opin Organ Transplant* **13**, 165-170, doi:10.1097/MOT.0b013e3282f6391e (2008).
227 Ramsey, H. E. *et al.* A20 protects mice from lethal liver ischemia/reperfusion injury by increasing peroxisome proliferator-activated receptor-alpha expression. *Liver Transpl* **15**, 1613-1621, doi:10.1002/lt.21879 (2009).

228 Lynch, R. J. & Platt, J. L. Accommodation in renal transplantation: unanswered questions. *Curr Opin Organ Transplant* **15**, 481-485, doi:10.1097/MOT.0b013e32833b9c25 (2010).
229 Blazar, B. R., Murphy, W. J. & Abedi, M. Advances in graft-versus-host disease biology and therapy. *Nat Rev Immunol* **12**, 443-458, doi:10.1038/nri3212 (2012).
230 Schneider, D. S. & Ayres, J. S. Two ways to survive infection: what resistance and tolerance can teach us about treating infectious diseases. *Nat Rev Immunol* **8**, 889-895, doi:10.1038/nri2432 (2008).
231 Wang, A. *et al.* Opposing Effects of Fasting Metabolism on Tissue Tolerance in Bacterial and Viral Inflammation. *Cell* **166**, 1512-1525 e1512, doi:10.1016/j.cell.2016.07.026 (2016).
232 Matzinger, P. Friendly and dangerous signals: is the tissue in control? *Nat Immunol* **8**, 11-13, doi:10.1038/ni0107-11 (2007).
233 Matzinger, P. & Kamala, T. Tissue-based class control: the other side of tolerance. *Nat Rev Immunol* **11**, 221-230, doi:10.1038/nri2940 (2011).
234 Ramsay, N. K. *et al.* A randomized study of the prevention of acute graft-versus-host disease. *N Engl J Med* **306**, 392-397, doi:10.1056/NEJM198202183060703 (1982).
235 Weisdorf, D. *et al.* Treatment of moderate/severe acute graft-versus-host disease after allogeneic bone marrow transplantation: an analysis of clinical risk features and outcome. *Blood* **75**, 1024-1030 (1990).
236 Martin, P. J. *et al.* A retrospective analysis of therapy for acute graft-versus-host disease: secondary treatment. *Blood* **77**, 1821-1828 (1991).
237 Chao, N. J. *et al.* Cyclosporine, methotrexate, and prednisone compared with cyclosporine and prednisone for prophylaxis of acute graft-versus-host disease. *N Engl J Med* **329**, 1225-1230, doi:10.1056/NEJM199310213291703 (1993).
238 Hings, I. M. *et al.* Treatment of moderate and severe acute GVHD after allogeneic bone marrow transplantation. *Transplantation* **58**, 437-442 (1994).
239 Przepiorka, D. *et al.* Tacrolimus and minidose methotrexate for prevention of acute graft-versus-host disease after matched unrelated donor marrow transplantation. *Blood* **88**, 4383-4389 (1996).
240 MacMillan, M. L. *et al.* Response of 443 patients to steroids as primary therapy for acute graft-versus-host disease: comparison of grading systems. *Biol Blood Marrow Transplant* **8**, 387-394 (2002).
241 Lee, S. J. *et al.* Effect of up-front daclizumab when combined with steroids for the treatment of acute graft-versus-host disease: results of a randomized trial. *Blood* **104**, 1559-1564, doi:10.1182/blood-2004-03-0854 (2004).
242 Levine, J. E. *et al.* Etanercept plus methylprednisolone as initial therapy for acute graft-versus-host disease. *Blood* **111**, 2470-2475, doi:10.1182/blood-2007-09-112987 (2008).

243 Chang, Y. J. *et al.* Controlled, Randomized, Open-Label Trial of Risk-Stratified Corticosteroid Prevention of Acute Graft-Versus-Host Disease After Haploidentical Transplantation. *J Clin Oncol* **34**, 1855-1863, doi:10.1200/JCO.2015.63.8817 (2016).
244 Gooley, T. A. *et al.* Reduced mortality after allogeneic hematopoietic-cell transplantation. *N Engl J Med* **363**, 2091-2101, doi:10.1056/NEJMoa1004383 (2010).
245 van Bekkum, D. W., Roodenburg, J., Heidt, P. J. & van der Waaij, D. Mitigation of secondary disease of allogeneic mouse radiation chimeras by modification of the intestinal microflora. *J Natl Cancer Inst* **52**, 401-404 (1974).
246 Eriguchi, Y. *et al.* Graft-versus-host disease disrupts intestinal microbial ecology by inhibiting Paneth cell production of alpha-defensins. *Blood* **120**, 223-231, doi:10.1182/blood-2011-12-401166 (2012).
247 Jenq, R. R. *et al.* Regulation of intestinal inflammation by microbiota following allogeneic bone marrow transplantation. *J Exp Med* **209**, 903-911, doi:10.1084/jem.20112408 (2012).
248 Shono, Y. *et al.* Increased GVHD-related mortality with broad-spectrum antibiotic use after allogeneic hematopoietic stem cell transplantation in human patients and mice. *Sci Transl Med* **8**, 339ra371, doi:10.1126/scitranslmed.aaf2311 (2016).
249 Maloy, K. J. & Powrie, F. Intestinal homeostasis and its breakdown in inflammatory bowel disease. *Nature* **474**, 298-306, doi:10.1038/nature10208 (2011).
250 Kabat, A. M., Srinivasan, N. & Maloy, K. J. Modulation of immune development and function by intestinal microbiota. *Trends Immunol* **35**, 507-517, doi:10.1016/j.it.2014.07.010 (2014).
251 Rooks, M. G. & Garrett, W. S. Gut microbiota, metabolites and host immunity. *Nat Rev Immunol* **16**, 341-352, doi:10.1038/nri.2016.42 (2016).
252 Furusawa, Y. *et al.* Commensal microbe-derived butyrate induces the differentiation of colonic regulatory T cells. *Nature* **504**, 446-450, doi:10.1038/nature12721 (2013).
253 Toubai, T. *et al.* NLRP6 in Host Target Tissues Exacerbates Graft-Versus-Host Disease. *Blood* **126**, 148-148 (2015).
254 Yang, H., Antony, P. A., Wildhaber, B. E. & Teitelbaum, D. H. Intestinal intraepithelial lymphocyte gamma delta-T cell-derived keratinocyte growth factor modulates epithelial growth in the mouse. *J Immunol* **172**, 4151-4158 (2004).
255 Panoskaltsis-Mortari, A., Lacey, D. L., Vallera, D. A. & Blazar, B. R. Keratinocyte growth factor administered before conditioning ameliorates graft-versus-host disease after allogeneic bone marrow transplantation in mice. *Blood* **92**, 3960-3967 (1998).

256 Krijanovski, O. I. *et al.* Keratinocyte growth factor separates graft-versus-leukemia effects from graft-versus-host disease. *Blood* **94**, 825-831 (1999).
257 Vanclee, A. *et al.* Keratinocyte growth factor ameliorates acute graft-versus-host disease in a novel nonmyeloablative haploidentical transplantation model. *Bone Marrow Transplant* **36**, 907-915, doi:10.1038/sj.bmt.1705157 (2005).
258 Little, T. J., Shuker, D. M., Colegrave, N., Day, T. & Graham, A. L. The coevolution of virulence: tolerance in perspective. *PLoS Pathog* **6**, e1001006, doi:10.1371/journal.ppat.1001006 (2010).